RHEINISCH-
WESTFÄLISCHE
TECHNISCHE
HOCHSCHULE
AACHEN

Institut für Werkstoffanwendungen im Maschinenbau

Univ.-Prof. Dr.-Ing. Christoph Broeckmann

DETERMINE CREEP AND RHEOLOGICAL PARAMETERS FOR HOT ISOSTATIC PRESSING (HIP) MODEL OF 316L

Master Thesis

Daniel Ruiz Sanz

Supervisor: M. Sc. Chung Van Nguyen

Contents

page 2

Abstract 4

1. Introduction 5

Problem description and scope of the thesis 6

2. Theorical basis 7

3. Creep laws 14

3.1. Secondary creep laws 14

3.2. Primary creep laws 18

4. Experiments 19

4.1. Uniaxial compression test on dense material 19

4.2. Hot Isostatic Pressing test 20

4.3. Uniaxial compression test on porous material 21

4.4. Experiments using ZWICK/ROELL Z020 23

4.5. Experiments using INSTRON/ZWICK 1362 38

5. Data analysis 50

5.1. Data collected 50

5.2. Data processing 52

5.3. Secondary creep analysis 54

5.3.1. Full dense material 54

5.3.2. Porous material 55

5.4. Primary creep analysis 56

6. Results 58

6.1. Secondary creep 58

6.1.1. 304 stainless steel 59
6.1.2. 316L stainless steel 64
6.1.3. Porous material 69
6.2. Primary creep 75
6.2.1. 304 stainless steel 76
6.2.2. 316L stainless steel 95
7. Problems 115
8. Conclusion and further works 118
9. References 119

Abstract

In this thesis, experiments which are needed to obtain initial and secondary creep parameters of full dense 316L and rheological parameters of porous 316L are presented.

After completing these experiments, parameters needed for HIP simulation model will be determined. Subsequently densification process of different geometries during HIP will be simulated with the determined parameters in order to check the numerical problems and verify the quality of HIP simulation results.

1 Introduction

Creep and rheological parameters are very needed for an appropriate simulation of materials behavior, being the object of study in this case stainless steel.

Studies on dimensional changes in materials exposed to different situations of tension and temperature are carried out in IWM. It is for this reason that it is necessary and will be useful for other future work to obtain these parameters.

In summary, this thesis aims at obtaining some experimental parameters (rheological and yield) to serve for a better understanding of the nature of these materials and provide greater quality in the subsequent simulations IWM

The aim of this thesis is to analyze the creep behavior of two given materials (stainless steel type 304 and 316L).

The study of the parameters of creep is carried out from the analysis of the full dense material. In the case of 316L stainless steel, porous material samples were also studied with different densities to determine their rheology's parameters.

The determination of these parameters will be preceded by various mechanical tests. These experimental determined parameters are important for HIP simulation.

Creep (sometimes called cold flow) is the tendency of a solid material to move slowly or deform permanently under the influence of mechanical stresses. It can occur as a result of long-term exposure to high levels of stress that are still below the yield strength of the material. Creep is more severe in materials that are subjected to heat for long periods, and generally increases as they near their melting point. Creep always increases with temperature [1].

The rate of deformation is a function of the material properties, exposure time, exposure temperature and the applied structural load. Depending on the magnitude of the applied stress and its duration, the deformation may become so large that a component can no longer perform its function. Creep is usually of concern to engineers and metallurgists when evaluating components that operate under high stresses or high temperatures. Creep is a deformation mechanism that may or may not constitute a failure mode. For example, moderate creep in concrete is sometimes welcomed because it relieves tensile stresses that might otherwise lead to cracking.

Unlike brittle fracture, creep deformation does not occur suddenly upon the application of stress. Instead, strain accumulates as a result of long-term stress. Therefore, creep is a "time-dependent" deformation.

Rheology is the part of physics that studies the relationship between stress and strain in materials that are able to flow. Rheology is a part of continuum mechanics. One of the most important goals is to find rheology constitutive equations to model the behavior of materials. These equations are generally tensorial character.

An ideal solid is elastically deformed and the energy required for deformation is totally recovered when the applied stress is removed. While the ideal fluids irreversibly deform, flow, and the energy required for deformation is dissipated into the fluid as heat and can not be recovered by removing the stress. But only a few liquids behave as ideal fluids, the vast majority of the liquid shows a rheological behavior that is classified in an intermediate region between the liquid and solid: they are both elastic and viscous time, which are called viscoelastic . Moreover, the actual solid can deform irreversibly under the influence of forces of sufficient magnitude, in short, may flow. [2]

2 Theoretical basis

So far two approaches, microscopic and macroscopic models are the ways to describe an appropriate behavior of the HIP process.

Microscopic models provide a means to derive macroscopic model parameters from information on a smaller length scale, particle level. These methods offer a rigorous approach to describing the behavior of porous materials, but their predictive capability can be limited.

The microscopic approach unites the material properties and processing parameters into an analytical-rate equation; it is therefore, relatively easy to estimate their roles in the hipping process and the effect on hipped products. Since the microscopic approach describes the densification and deformation behavior by analyzing the microdensification mechanism, it is physical, rational, and can be conveniently modified to take account of new densification rate. This makes it difficult to predict shape change, particularly when the stresses contain a deviatoric component.[3]

In contrast to the microscopic approach, the macroscopic approach treats the powder compact as a continuous medium. Constitutive equations describing the macroscale deformation of porous material are obtained by modification of plastic theory for solid materials.

In the macroscopic approach, i.e., a continuum mechanical model, the general plasticity theory for solids is modified for a porous continuum, and a constitutive equation is constructed that relates the strain increment and the stress. In the equation, there are some important coefficients that have to be determined experimentally. The values of these coefficients obtained under certain experimental conditions may not be extrapolated to other conditions. [4]

It is difficult to conclude which approach, microscopic or macroscopic, is better for describing the behavior of the powder densification process during HIP. The microscopic approach unites the material properties and processing parameters into an analytical rate equation related to the microphysical mechanisms. Subsequently it is relatively easy to estimate their roles in the HIP process which can conveniently be modified to take into account new densification mechanisms. However, the micromechanical analysis is based on many assumptions to reduce the complexity of the problem, such as the assumption of homogeneity of particle size, assumption of steady stage of temperature and pressure etc. Additionally, the microscopic approach does not relate strain and strain rate to density and density rate. This feature of the model makes it difficult to predict the shape change, especially when the stresses contain a deviatory component [4, 5]. Furthermore results from [6] show that micromechanical analysis based microscopic approaches usually amounts to numerical problems and less accuracy. On the other hand the macroscopic approach can predict the shape changes and is convenient to use for complex geometrical components, as it has a more concise formulation and fewer parameters compared to the microscopic approach. As the main focus of this study is to predict the shape changes of components produced by PM HIP process, the macroscopic approach is chosen for further study.

The viscoplastic model has been used in IWM in order to simulate the densification during HIP, as it is the model that fits the behavior of materials under conditions subject to which the experiments are performed.

Viscoplasticity can be explained as a theory included within the continuum mechanics that aims to explain the inelastic behavior of solids depending on the load on these solids.

The elastic behavior of the material refers to the deformation experienced by the material undergoing unrecoverable when it reaches certain levels of loading. [7]

In the case where deformation is primarily controlled by plasticity or creep of each individual powder particle, the basic relevant concept is the equivalent stress σ_{eq}, defined by [8] :

$$\boldsymbol{\sigma}_{eq}^2 = 3cJ_2 + fI_1^2 \tag{2.1}$$

Where:

- J2 is the second deviatoric stress invariant.

$$J_2 = \frac{1}{2} S_{ij} : S_{ij} = \|dev(\boldsymbol{\sigma})\| \tag{2.2}$$

  - S is the deviatoric Cauchy stress tensor.
  - *dev* denoting respectively the deviator operator.

- I1 is the first stress invariant.

$$I_1 = \sigma_{ii} = tr(\sigma) \tag{2.3}$$

  - σ is Cauchy stress tensor

$$\sigma_{ij} = S_{ij} + \frac{1}{3}\sigma_{kk}\delta_{ij} \tag{2.4}$$

  - δ_{ij} is the Kronecker delta, $\boldsymbol{\delta}_{ij} = \begin{cases} = 1 \ if \ i = i \\ = 0 \ if \ i \neq j \end{cases}$ (2.5)
  - *tr* denoting the trace operator.

- *c* and *f* are functions of the relative density ρ which can be experimentally determined.

And consider a viscoplastic potential $\Omega(\sigma_{eq}, \theta)$ such that [8] :

$$\dot{\varepsilon} = \frac{\partial \Omega}{\partial \sigma} = \frac{\partial \Omega}{\partial \sigma_{eq}} \frac{1}{\sigma_{eq}} \left(\frac{3c}{2} s + f I_1 1 \right) = F(\sigma, \rho, \theta) \tag{2.6}$$

Where:

- θ is the temperature.
- 1 denotes the unity second-order tensor in R^3.

Density variations are then related to $\dot{\varepsilon}^v$ through mass conservation:

$$\frac{\dot{\rho}}{\rho} = -tr(\dot{\varepsilon}^v) = -\frac{\partial \Omega}{\partial \sigma_{eq}} \frac{3fI_1}{\partial_{eq}} \qquad (2.7)$$

The coefficients c (ρ), f (ρ) and the creep law $\partial\Omega/\partial\sigma_{eq}$ have been experimentally determined from various compression tests. These experiments will be explained later.

Flow rule is normality rule between viscoplastic strain rate tensor $\dot{\varepsilon}_{ij}^{vp}$ and the viscoplastic potential Ω=F(σ_{eq},T) where T is the absolute temperature [8].

$$\dot{\varepsilon}_{ij}^{vp} = \frac{\partial \Omega}{\partial \sigma_{ij}} = \frac{\partial \Omega}{\partial \sigma_{eq}} . \frac{\partial \sigma_{eq}}{\partial \sigma_{ij}} \qquad (2.8)$$

Taking the derivative equation (2.1) and using (2.2) and (2.3)

$$2\sigma_{eq} \frac{\partial \sigma_{eq}}{\partial \sigma_{ij}} = 3c \frac{\partial J_2}{\partial \sigma_{ij}} + f \frac{\partial I_1^2}{\partial \sigma_{ij}} \qquad (2.9)$$

$$\frac{\partial \sigma_{eq}}{\partial \sigma_{ij}} = \frac{1}{\sigma_{eq}} \left(\frac{3}{2} cS_{ij} + fI_1 \delta_{ij} \right) \qquad (2.10)$$

By substituting (2.2) into (2.3), we have

$$\dot{\varepsilon}_{ij}^{vp} = \frac{\partial \Omega}{\partial \sigma_{eq}} . \frac{1}{\sigma_{eq}} \left(\frac{3}{2} c S_{ij} + f I_1 \delta_{ij} \right) \qquad (2.11)$$

- *Equivalent strain rate* can be defined by assuming that the macroscopic plastic work rate W must be equal to the average plastic work done by powder particle per unit volume of the porous body [9]

$$\dot{W} = \sigma_{ij} : \dot{\varepsilon}_{ij}^{vp} = \sigma_{eq} \dot{\varepsilon}_{eq}^{vp} \qquad (2.12)$$

By substituting (2.6) and (2.13) into (2.14), with the notes that [8]:

- $Tr(S_{ij}) = 0$
- $\delta_{ij} : \delta_{ij} = tr(\delta_{ij}) = 3$

We have [9]:

$$\sigma_{eq} \dot{\varepsilon}_{eq}^{vp} = \sigma_{ij} : \dot{\varepsilon}_{j}^{vp} = \left(S_{ij} + \frac{1}{3} \sigma_{kk} \delta_{ij} \right) : \left(\frac{\partial \Omega}{\partial \sigma_{eq}} . \frac{1}{\sigma_{eq}} \frac{3}{2} c S_{ij} + \frac{\partial \Omega}{\partial \sigma_{eq}} . \frac{1}{\sigma_{eq}} f I_1 \delta_{ij} \right)$$
$$= \frac{\partial \Omega}{\partial \sigma_{eq}} . \frac{1}{\sigma_{eq}} \frac{3}{2} c \, (S_{ij} : S_{ij}) + \frac{1}{3} \sigma_{kk} \frac{\partial \Omega}{\partial \sigma_{eq}} . \frac{1}{\sigma_{eq}} f I_1 (\delta_{ij} : \delta_{ij}) = \frac{\partial \Omega}{\partial \sigma_{eq}} . \frac{1}{\sigma_{eq}} (3 c J_2 + f I_1^2) \qquad (2.13)$$

Therefore

$$\dot{\varepsilon}_{eq}^{vp} = \frac{\partial \Omega}{\partial \sigma_{eq}} \qquad (2.14)$$

$$\dot{\varepsilon}_{eq}^{vp} = F(\sigma_{eq}) \qquad (2.15)$$

In conclusion, the relationship between stress and strain rate is what will define the behavior of the material when it is subjected to a creep state.

In this model, the creep parameters (A, n) and rheological parameter (c, f) are important. They should be experimentaly determined by three experiments: uniaxial compression test on dense material, hot isostatic pressing test and Uniaxial compression test on porous material

2.3 Creep mechanics

Creep tests are performed loading the sample inside a furnace which is maintained at isothermal conditions at different levels temperature T. The sample length is measured as a function of time. A typical curve which describes creep behavior for metals, polymers and ceramics is represented in Figure 1 [10]. The temperature at which the material begins its creep behavior depends on the melting point Tm, for example, T> 0.4 Tm for metals and T> 0.5 Tm for ceramics.

The response of specimen loaded by σ_0 at time *t = 0* can be divided into an elastic and plastic part as [10] [11]:

$$\varepsilon_0 = \frac{\sigma_0}{E(T)} + \varepsilon_p(\sigma_0, T) \qquad (2.16)$$

Where:

- ε_0 is the initial strain, at time t = 0.
- σ_0 is the load applied on the specimen.
- E(T) is the modulus of Elasticity.
- ε_p is the plastic strain.
- T is the temperature.

The creep strain in *Fig.1* can then be expressed according to [10]:

$$\varepsilon_c = \varepsilon(t) - \varepsilon_0\, \alpha\, t^k \qquad (2.17)$$

Where:

- ε_c is the creep strain
- $\varepsilon(t)$ is the time-dependent strain.
- ε_0 is the initial strain, at time t = 0.
- α is a coefficient, determined experimentally.
- t is the time.
- k is an exponent, it depends on the creep phase.

Where “k” takes different values depending on the stage of creep [10].

- k < 1 in the primary stage.
- k = 1 in the secondary stage.
- k > 1 in the tertiary stage.

These terms correspond to a decreasing, constant, and increasing strain rate, respectively.

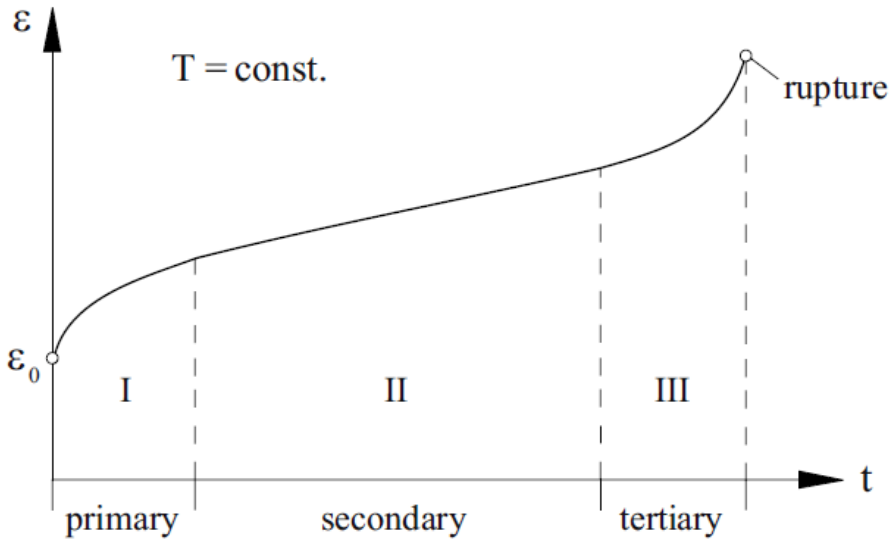

Fig.2. Typical creep curve.

The results (2.1) and (2.2) from creep test justify a classification of material behavior in three disciplines: *elasticity, plasticity*, and *creep mechanics*.

One can also distinguish four theories of material behavior as follows:

- The theory of *elasticity* is concerned with the *rate-independent* behavior *without hysteresis*.
- The theory of *plasticity* specifies the *rate-independent* behavior with *hysteresis.*
- The theory of *viscoelasticity* describes the *rate-dependent* behavior without *equilibrium hysteresis.*
- The theory of *viscoplasticity* is devoted to the *rate-dependent* behavior with *equilibrium hysteresis*.

The creep behavior exists in the theories of *viscoelasticity* and *viscoplasticity.*[10]

The theory of viscoelasticity refers to materials that exhibit features of elastic solids and characteristics of viscous fluids. One of the main features of elastic behavior is the capacity for materials to store mechanical energy when deformed by loading, and to set free this energy completely after removing the load.

In contrast, viscoplastic materials can sustain a shear stress even the rest. They begin to flow with viscous stresses after a yield condition has been satisfied. Materials studied in this thesis can be included on this category.

3.- Creep laws.

In this chapter different relationships for creep behavior in primary and secondary creep are proposed.

3.1. Secondary creep laws

Secondary or stationary creep is for many applications the most important creep model. After a relatively short transient period the material creeps in such a manner that an approximate equilibrium between hardening and softening processes can be assumed. This equilibrium exists for a long time and the long-term behavior of a structure can be analyzed assuming stationary creep processes. In this section several models of secondary creep are introduced. The secondary or stationary creep assumes constant or slowly varying loading and temperature conditions. [12]

Creep potential or equivalent creep rate must be specified as functions of equivalent stress and temperature, i.e.

Many empirical functions of stress and temperature which allow fit experimental data have been proposed in the literature, e.g. [13], [14],[15], [16].

The starting point is the assumption that the creep rate may be described as a product of two separate functions of stress and temperature. [13]

$$\dot{\varepsilon}_{eq} = f_{\sigma}(\sigma_{eq}) f_{T}(T) \tag{3.1}$$

The dependence on the temperature is usually expressed by the Arrhenius law [nuev]

$$f_{T}(T) = exp\left[-\frac{Q}{RT}\right] \tag{3.2}$$

where Q and R denote the activation energy and the Boltzmann's constant, respectively.

The widely used functions of stress are: [19] [10]

- **Power creep law :**

$$f_\sigma(\sigma_{eq}) = A^* \sigma^n \tag{3.3}$$

- **Unified creep law:**

$$f_\sigma(\sigma_{eq}) = A^* \left[\sinh(k\sigma)\right]^n \tag{3.4}$$

- **Exponential creep law:**

$$f_\sigma(\sigma_{eq}) = A^* \exp(n\sigma) \tag{3.5}$$

To calculate secondary creep parameters the following transformation is performed: [9]

$$A = A^* f_T(T) \tag{3.6}$$

Thus secondary creep laws used in this thesis are the following: [14] [15]

- **Power creep law :**

$$\dot{\varepsilon}_{eq} = A\sigma^n \tag{3.7}$$

- **Unified creep law:**

$$\dot{\varepsilon}_{eq} = A \left[\sinh(k\sigma)\right]^n \tag{3.8}$$

- **Exponential creep law:**

$$\dot{\varepsilon}_{eq} = A \exp(n\sigma) \tag{3.9}$$

Where:

- $\dot{\varepsilon}_{eq}$ is the reference strain rate.
- σ is the reference stress.
- *A* is Dorn's constant, temperature dependent. Experimentally determined later.
- *n* is the creep exponent, temperature dependent. Experimentally determined later.

- *Creep law* is given by the relationship between $\dot{\varepsilon}_{eq}^{vp}$ *and* σ_{eq}:

Porous material laws

In order to determine c and f in the equation (2.13) experimentally, we need at least two independent equations representing the relationship between c and f. These can be derived from the following notices:

1. It is proved that the creep law of porous material has the same type as that of its dense material in the whole strain rate range [4]. Therefore, the creep behavior of porous material can be determined from that of the dense material by using a modification factor which is proved to be $\sqrt{c+f}$ [15]. This factor is therefore dependent on the relative density. To get the function $\sqrt{c+f} = F(\rho)$, uniaxial compression test on porous material is usually used.

2. The second equation can be obtained from observing densification behavior of powder during HIP process. To do this task, there are two available experimental approaches, which are experiments with HIP test and experiments without HIP test.

From the equation (2.3), we can see the physical meaning of coefficients c and f that they reflect the impact level of the deviatoric stress causing distortion and of the hydrostatic stress causing volumetric change, respectively.

- In case of the experiments with HIP test approach, it is assumed that the applied force and the densification are homogeneous. That means only hydrostatic stress influences the deformation (i.e. c=0). By observing the densification behavior during HIP test, we can directly get the function f. However, a HIP test is usually expensive and difficult to setup.

The equivalent Misses stress σ_{eq} for a porous material can be written as, [17]

$$\sigma_{eq}^2 = 3cJ_2 + fI_1^2 \quad (3.10)$$

When c=1 and f=0, σ_{eq} in Eq. (2.20) reduces to the usual Misses stress. The parameters c and f in Eq. (2.20) can be determined from experiments as functions of relative density ρ [18]. Thus, [17]

$$f(\rho) = \frac{1}{9}\left[\frac{\exp(\dot{\rho}/\rho)}{A * P}\right]^{2/(n+1)} \quad (3.11)$$

$$c(\rho) = s(\rho)^{-2n/(n+1)} - f(\rho) \quad (3.12)$$

Where:

- P denotes the external pressure subjected to the container of a sample.
- A and n coefficients are calculated by the uniaxial compression test on dense materials. It will be explain later.
- exp($\dot{\rho}/\rho$) can be obtained from experimental data ρ = ρ$(t)_{exp}$ under Hip. It will be explain later.
- *s*(*ρ*) can be obtained from uniaxial compression creep data of porous powder compacts under high temperatures [*las dos ultimas antes del ultimo thus*]. It will be explain later.

Three tests are needed as shown in the flowchart below:

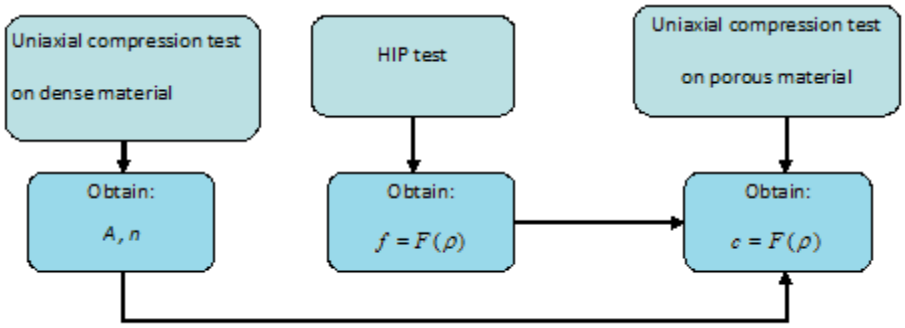

Fig.3: Flowchart of experiments

3.2. Primary creep laws.

The primary or transient creep is characterized by a monotonic decrease in the rate of creep (*Fig 1.)*, and the creep strain can be described by the formula: [10] [18]

$$\varepsilon_c = A\,\sigma^n\,t^m \tag{3.13}$$

Where the parameters A, n and m depend on the temperature

Starting from this equation, this section will present the approaches chosen to model the primary creep. These models are classified according to the mechanism by which hardening occurs, counting time hardening and strain hardening. [10] [13] [18][19]

- **Time hardening:**

$$\dot{\varepsilon}_{eq} = A\,\sigma^n\,m\,t^{m-1} \tag{3.14}$$

- **Strain hardening:**

$$\dot{\varepsilon}_{eq} = A\,\sigma^n\,\varepsilon^m \tag{3.15}$$

- **Modified strain hardening:**

$$\dot{\varepsilon}_{eq} = A\,\sigma^n\,[\,1 + (m - \exp(-k\varepsilon)]^n \tag{3.16}$$

Once the values of A and n after the analysis of the secondary creep are known, the different values of m and k for different models of primary creep is analyzed.

4. Experiments

4.1. Uniaxial compression test on dense material: to get A, n

Uniaxial free compression is carried on dense material at various constant strain rates and temperatures. The aim of this test is to find the relationship between equivalent stress, equivalent strain rate and temperature. This test is also done for capsule material, stainless 304.

In this case of compression for the dense material, we have:

$\sigma_2=\sigma_3=0$;

$\sigma_1=\sigma_z$

c=1; f=0

By substituting these into (3.10), we get the Von Mises stress:

$$\sqrt{3J_2} = |\sigma_z| \tag{4.1}$$

Test conditions:

- Length (L) = ~ 6mm
- Diameter (D) = ~ 4mm
- Strain rate $(\dot{\varepsilon}) = constant$

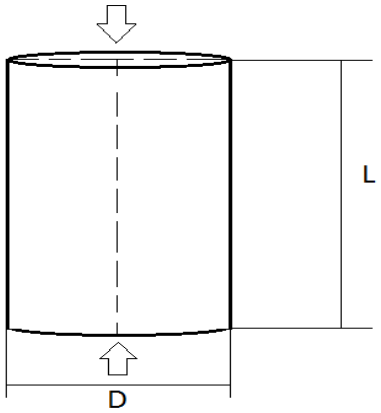

Fig.4: Compression test on dense material.

- Temperature (T°):

- 600°C: approximately temperature at which exists mainly first creep. This is known after performing the experiments.

- 700°C: approximately temperature at which secondary creep starts to can be considered. This is known after performing the experiments.

- 800°C: temperature sufficient to consider as essentially viscoplastic behavior for 316L

- 980°C: temperature just below carbide solubility in stainless steel.

- 1125°C: optimized temperature for the hot isostatic pressing of austenitic stainless steel.

- Strain rates: 10^{-4}; $5 * 10^{-5}$; 10^{-5} ; $5 * 10^{-6}\ s^{-1}$. Strain rates values have to be enough slow so that creep exists.

Number of samples: 5(T°) * 4(strain rates) * 2(materials) = 40 samples.

4.2. Hot Isostatic Pressing test: to get f(ρ)

Hot isostatic compression on metal powder. The aim of this test is to find the rate of volume change of the metal powder 316L during hot isostatic pressing process in the temperature range from room temperature to 1125°C.

It is assumed that the densification is homogenous. In fact, the shape and dimensions of the capsule much influence the homogeneity of the metal powder densification because of different stiffness distribution of the capsule. Therefore geometry of capsule is chosen, so that it gives as uniform stiffness as possible and it is easy to measure the densification during the HIP process. It is recommended that the capsule shape is a thin-walled cylinder with flat end-faces and the ratio between height and diameter is about one. [20]

There are two methods to measure the rate of densification of the specimens during the HIP cycle. The first one is interrupting the HIP process at selected points and rapid cooling down then measures the specimens. It is assumed there is no densification during the cooling stage. With this method, the elastic deformation is excluded but we have only “exact” values at several selected points; other points are interpolated.

The second method is continuously measuring the density of the specimen during the HIP cycle with a dilatometer. For this method, the elastic deformation is assumed to be negligible in comparison with viscoplastic deformation. The measured values of the volume change have to be corrected considering the different thermal expansion and flexibility of components of specimens and the HIP equipment.

For both methods, the deformation due to diffusion is negligible because most shape change of specimen is at the first stages while diffusion mechanism acts during final stage of spherical pore closure [1], [20]

4.3 Uniaxial compression test on porous material: to get c(ρ)

Uniaxial free compression on porous material at various constant strain rates and temperatures. This test need to be carried out at the strain rate and the temperatures as selected for the uniaxial compression test on the dense material. The aim of this test is to find the ratio between dilatation and distortion during compaction through the modification factor $\sqrt{c+f}$.

Test conditions:

- Length (L) = ~ 6mm
- Diameter (D) = ~ 4mm
- Strain rate $(\dot{\varepsilon}) = constant$

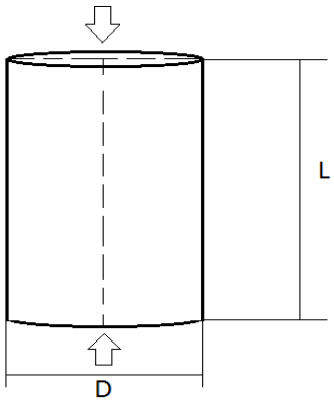

Fig.5: Compression test on porous material.

- Initial relative densities (ρ_0): 67%; 93%.
- Temperature (T°):

- 600°C: temperature at which exists mainly first creep.

- 700°C: temperature at which secondary creep starts to can be considered.

- 800°C: temperature sufficient to consider as essentially viscoplastic behavior for 316L

- 980°C: temperature just below carbide solubility in stainless steel.

- 1125°C: optimized temperature for the hot isostatic pressing of austenitic stainless steel.

- Strain rates: 10^{-4}; $5 * 10^{-5}$; 10^{-5} ; $5 * 10^{-6}\ s^{-1}$. Strain rates values have to be enough slow so that creep exists

Number of samples: 2(ρ_0) * 5(T°) * 4(strain rates) = 40 samples.

4.4. Experiments using ZWICK/ROELL Z020

In this machine have been performed the experiments at 600, 700 and 800 degrees. Experiments at 980 and 1125 degrees cannot be done in this machine because the limit temperature of the furnace is about 950°C.

The first step is to measure the sample test. The length and diameter of the cylinder are required for the inputs.

For the proper carrying out of the test, it is necessary to cover the surface contact of the samples with a lubricant made of graphite powder and oil. The aim is to reduce the friction between the sample and the punch.

The sample is positioned in the top of the lower punch, which is the fixed part (Fig.6).

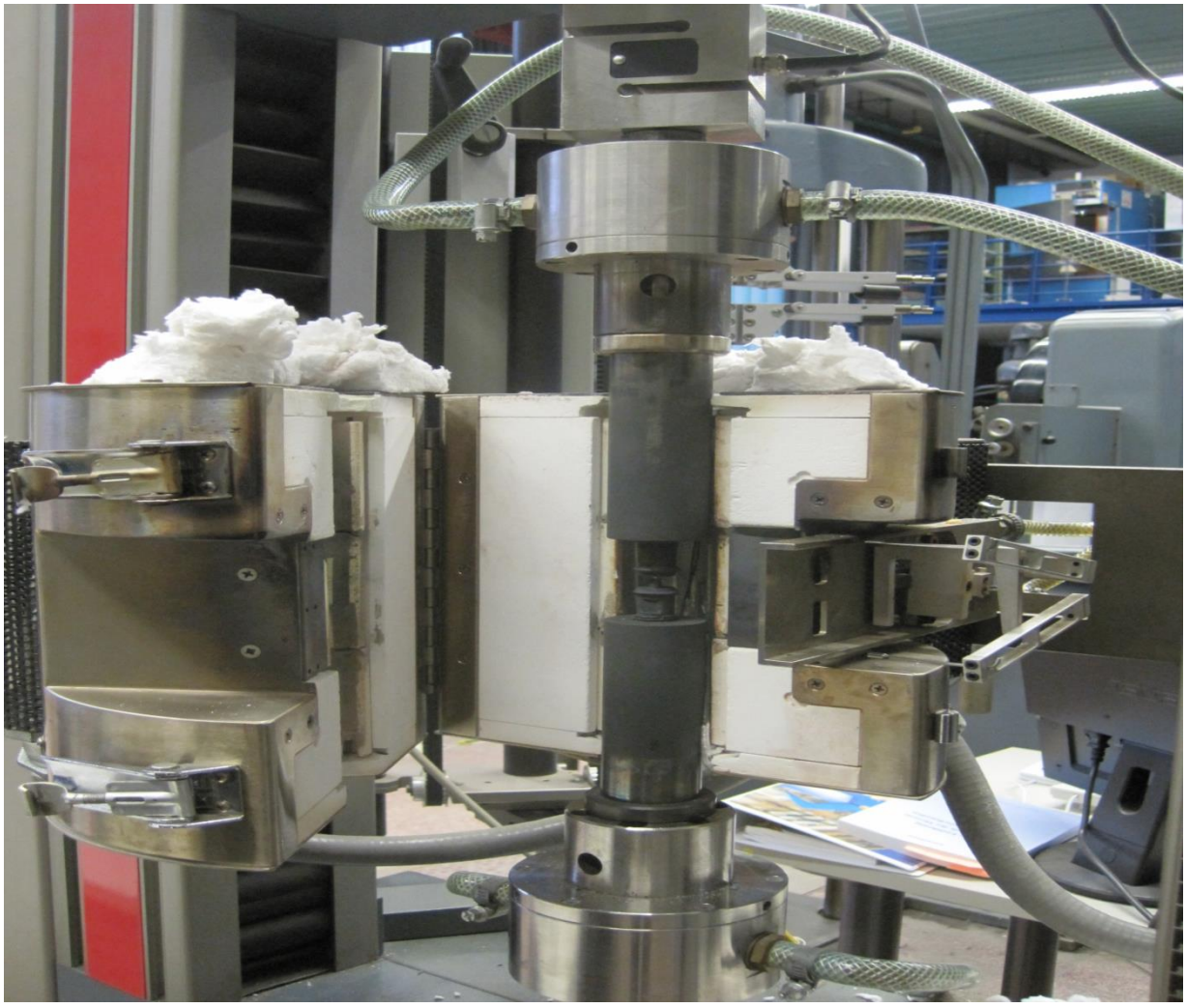

Fig.6: Placing sample in ZWICK/ROELL Z020

The upper punch is moved downward until it has contact with the sample. The distant movement of the punch and the force applied to the punches can be seen on the controlling interface of TestExpert V10 software as shown in the Fig.6. The initial preload value should be set to zero.

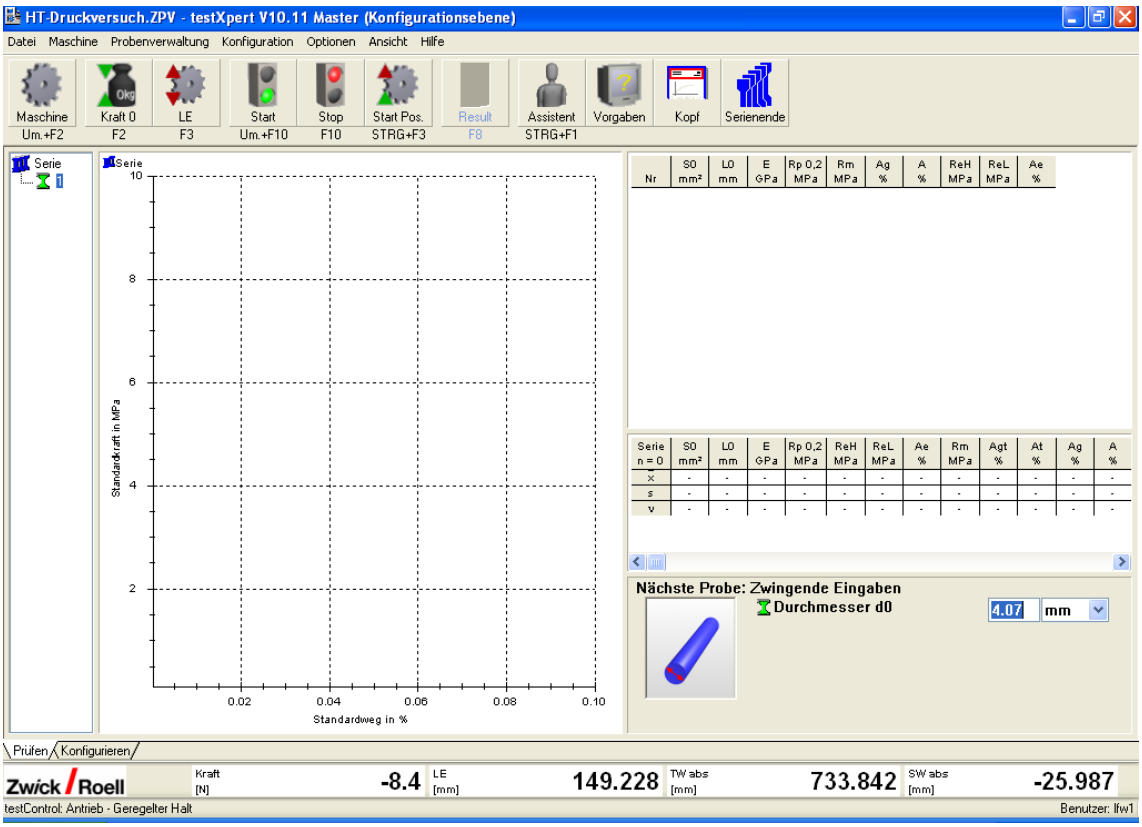

Fig.8: Interface of TextExpert V10 software

After that, extensometer type MTS 632-02 is placed to measure the relative distant movement of the punched.

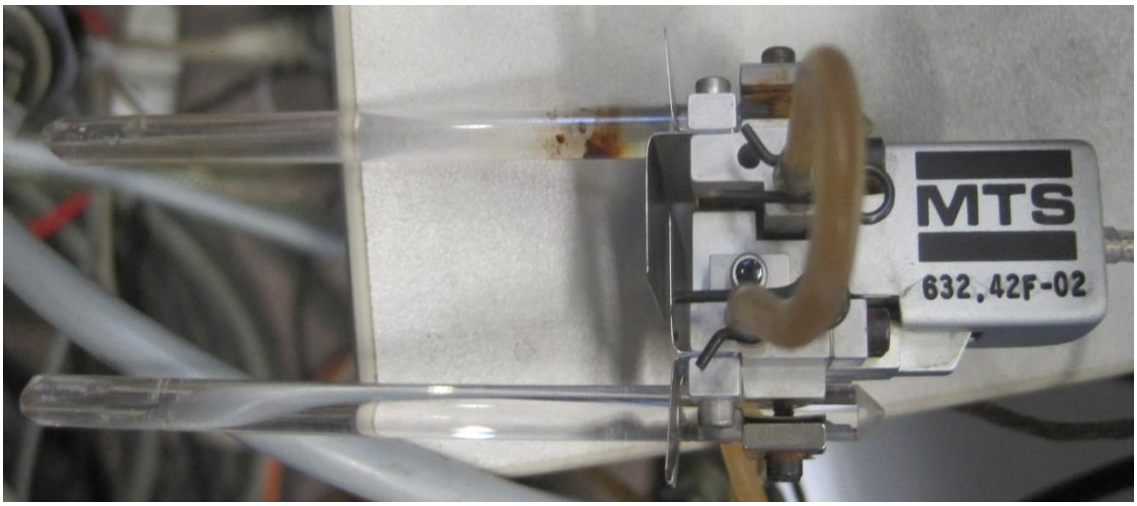

Fig.9: Extensometer MTS.

Before placing the extensometer, is very important to check that the measure shown on screen is what truly exists between the two legs of the extensometer, as it is very easy to be misadjusted. For this, there is a tool in which has an exact distance of 25 millimeters between two distinct points to calibrate the extensometer.The calibration process should be done as follows:

Press the Maschine button on the top of the screen and access the following menu:

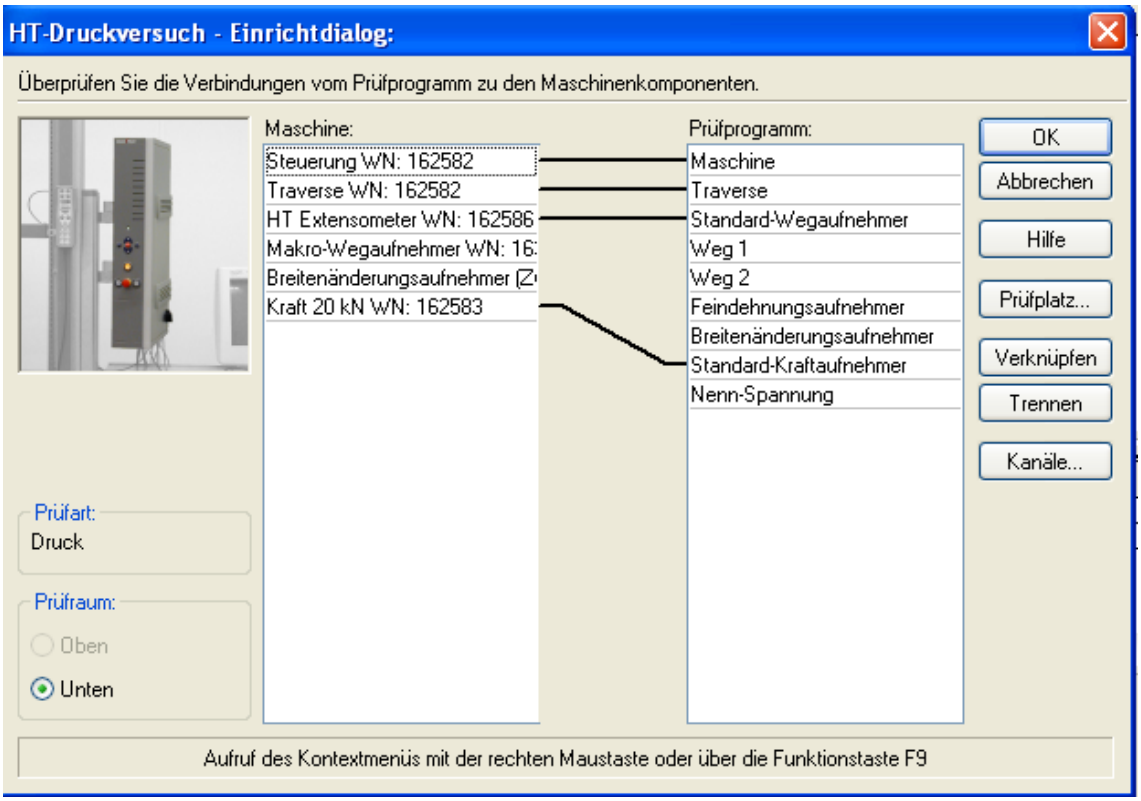

Fig.10: Setup menu

The relationship between measuring devices and their functions is shown in this menu. Double click on HT Extensometer button to open it.

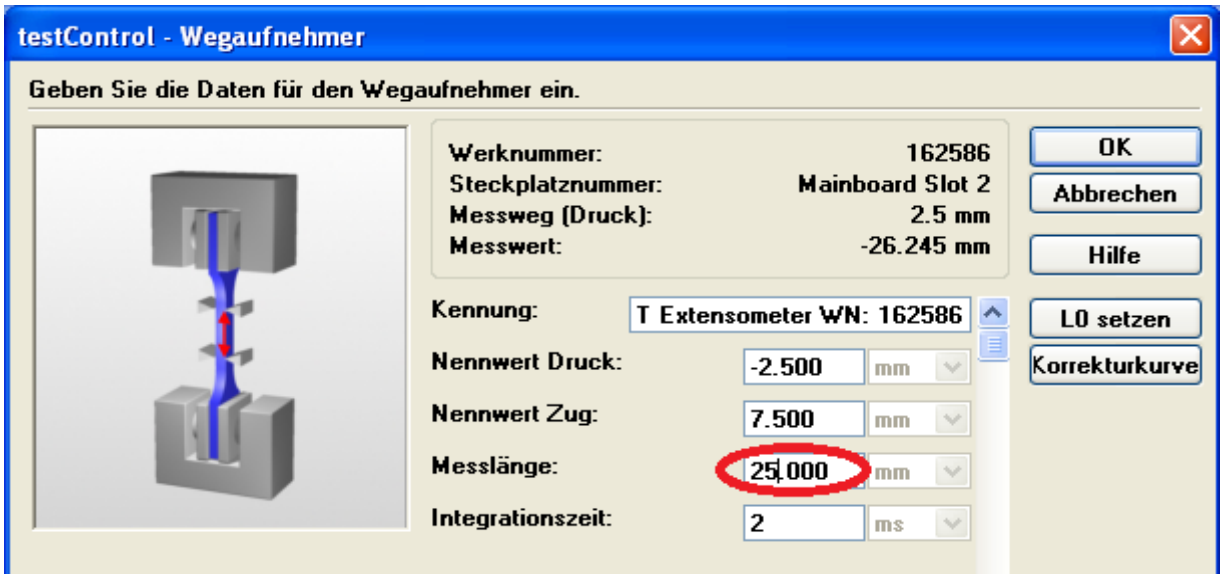

Fig.11: Setting of extensometer

The dimension of 25 millimeters is given, and then click on L0 setzen. The two legs of the extensometer are placed in side-contact with each punch as shown in Fig.12. It is very important to be sure that their contact is stable. Especially with the lower leg of the extensometer, since this one is more worn and more difficult to find this stable situation. Whenever a test is started, it is necessary to verify that the extensometer has been well calibrated.

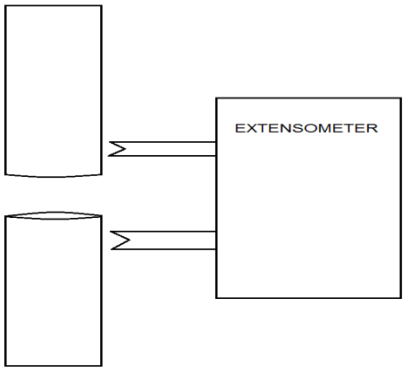

Fig.12: Position of extensometer.

Once the specimen and extensometer is positioned the furnace can be closed. During closing value of position value of the punch (from the strain gauge measuring) should not much changed.

Fig.13: ZWICK/ROELL Z020 closed and prepared

Regarding the preparation of software, to determine experiments parameter, *Assistent* menu is accessed. In each test should be specified:

- The speed at which the test is performed, the speed is determined by the product of strain rate and the initial length of the specimen. The speed is determined in several submenus:

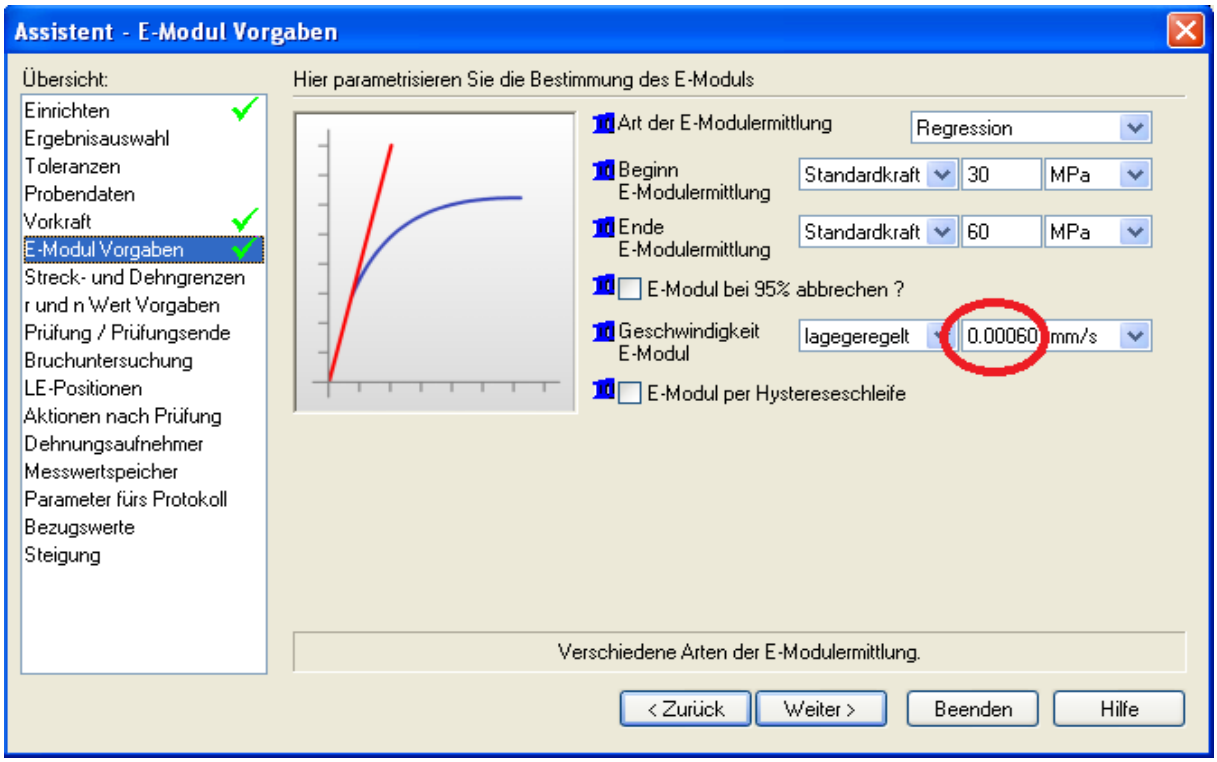

Fig.14: E-Modul Vorgaben Menu

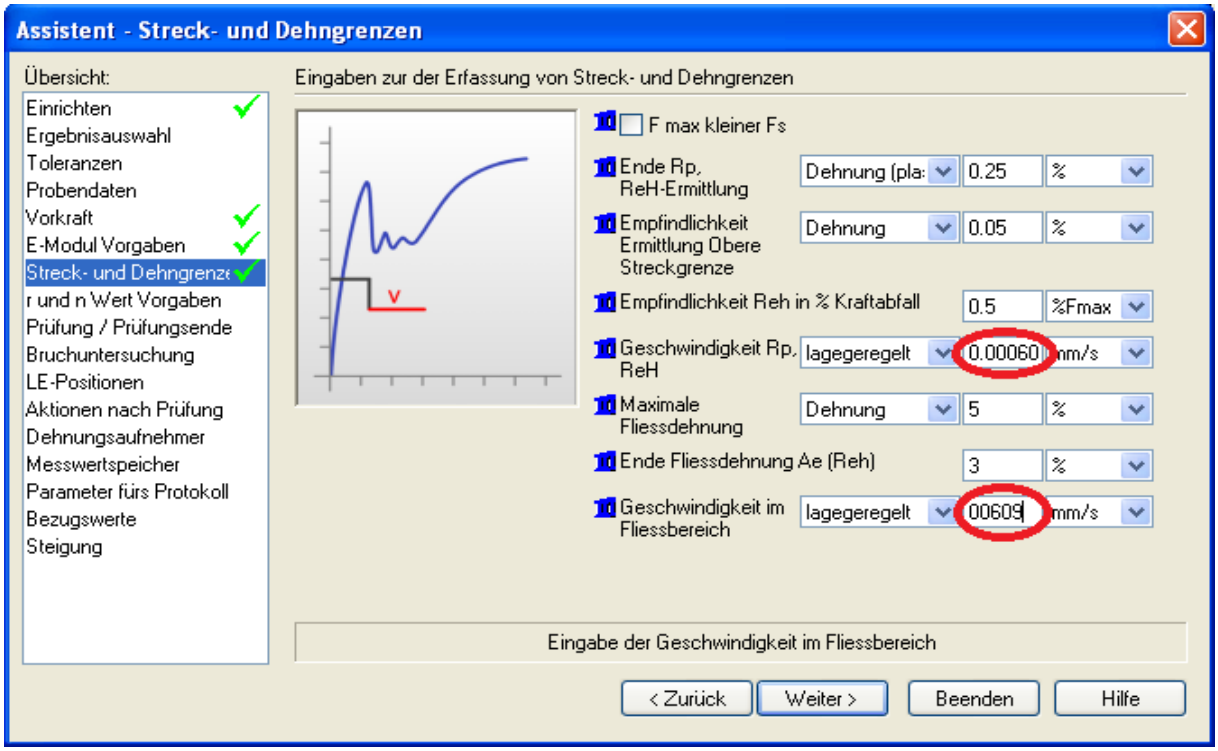

Fig.15: Streck- und Dehngrenzen Menu

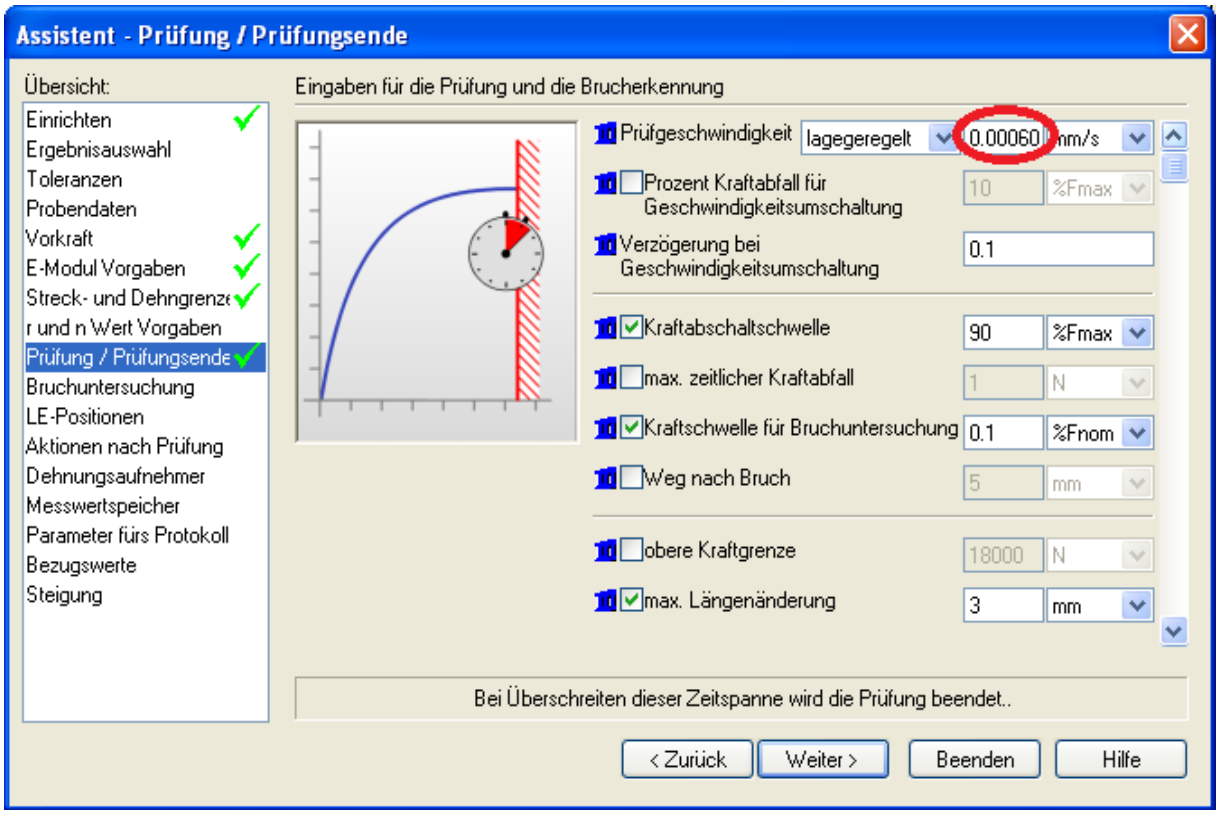

Fig.16: Prüfung / Prüfungsende Menu

- The time limit of the test, it depends on the speed, type of material and the relative density of the specimen this can vary from four hours to even values close to 20 hours

- The specimen deformation limit, the maximum length that can be shortened sample. This length ranges from 2.8 to 3 mm.

- The limit force applied on the specimen. This particular machine can apply a maximum force of 18000 N. Still, the chosen value is determined by the type of material, its relative density and the speed at which the test is performed.

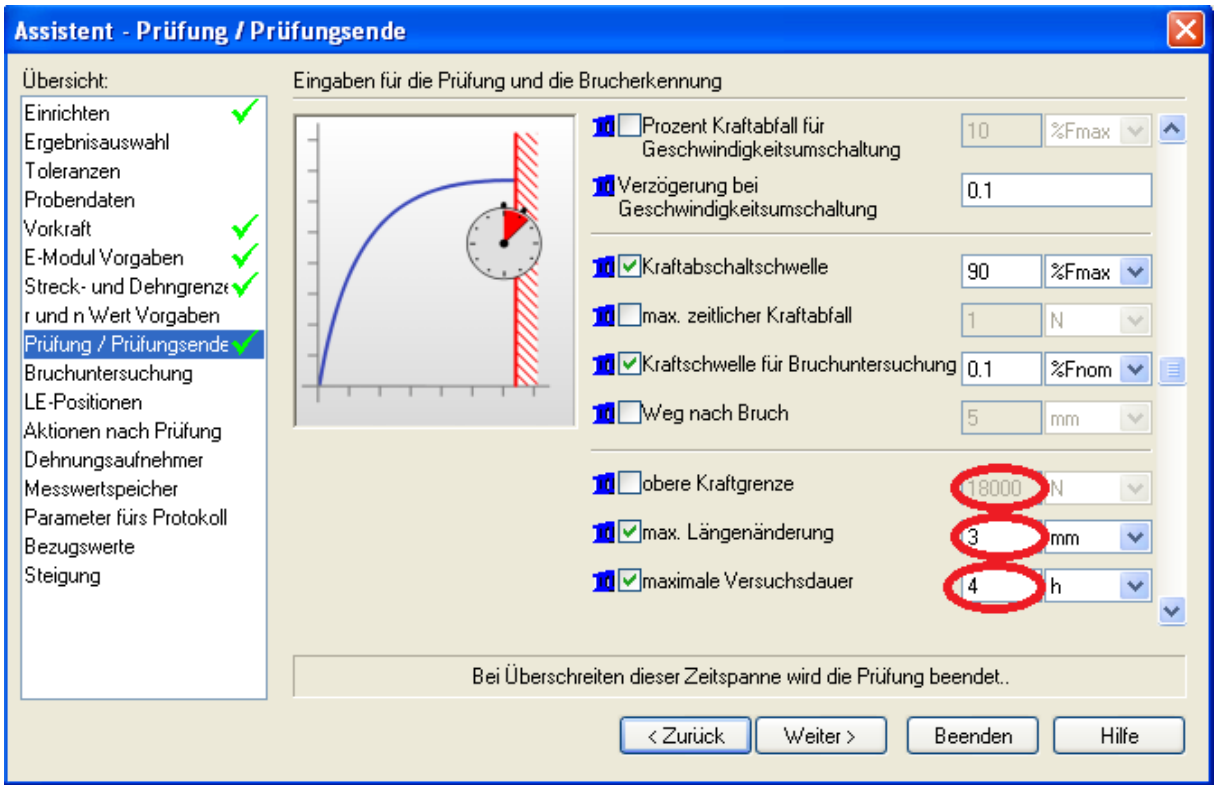

Fig.17: Experiments limits

After specifying all these parameters, *Start* button should be pressed. But before the test is started, the software requires determining:

- The name of the experiment is doing. The manner of appointing the tests is as follows:

CN-*material-temperature-relative density-strain rate-*

In case that a testis should be repeated more than once, the manner of appointing the successive experiments is with an S and the number of repeating them which is.

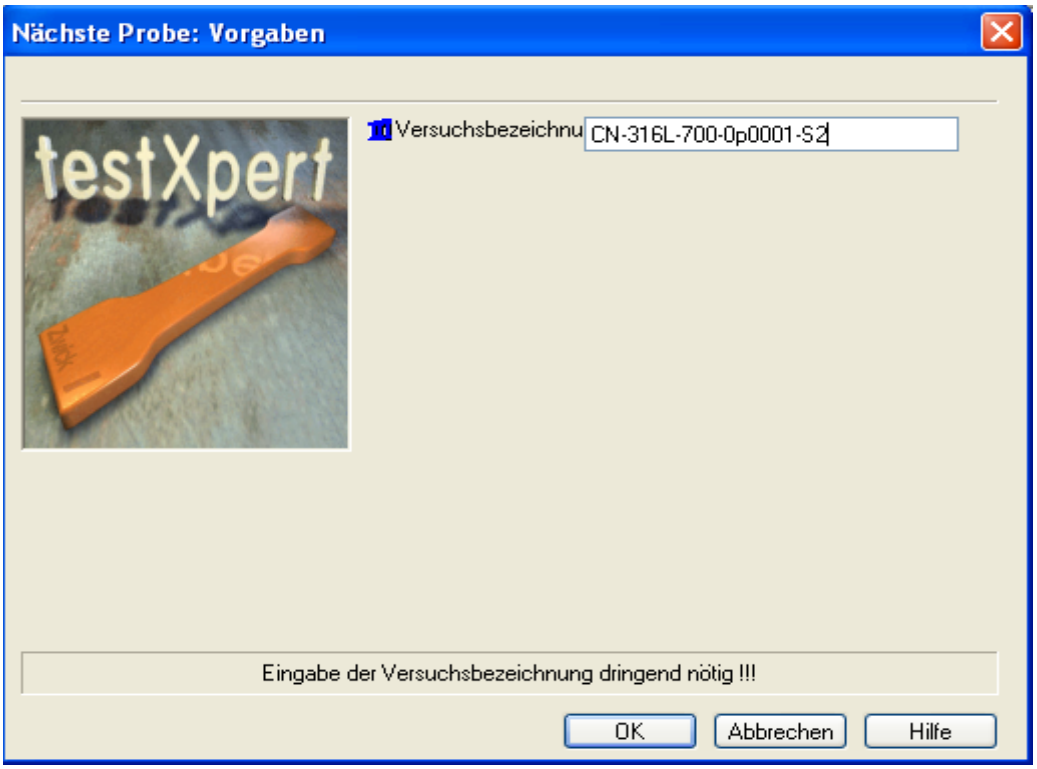

Fig.18: Test name

- The diameter of the sample. It needs to know the contact area of the sample.

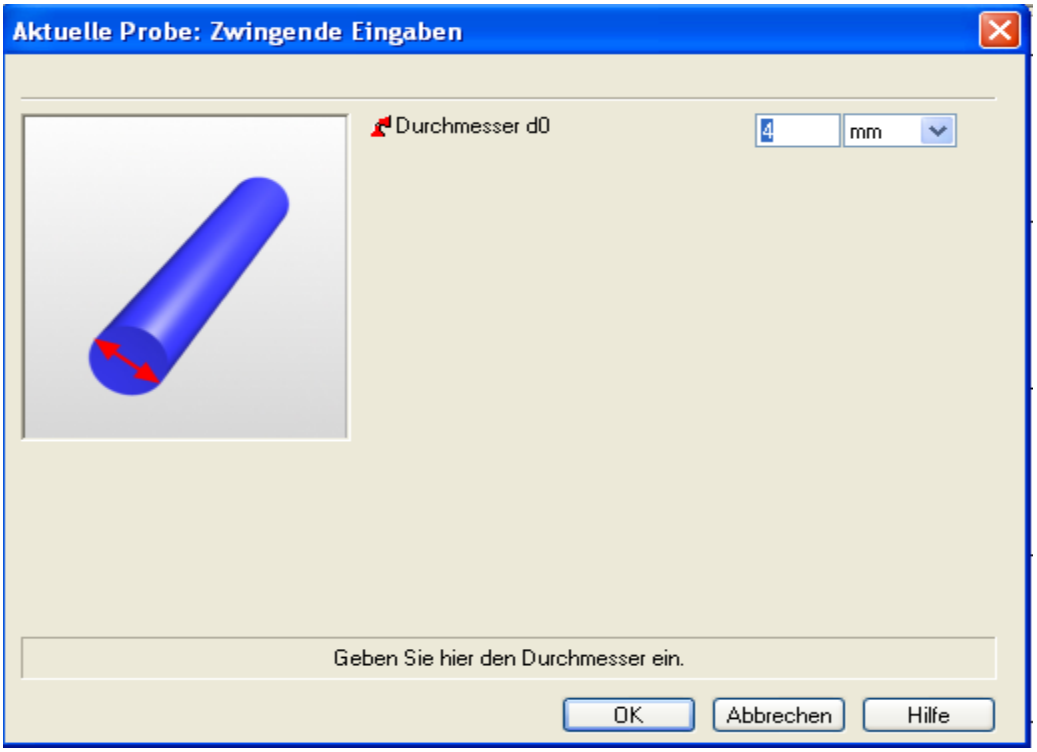

Fig.19: Sample diameter

When everything is setup, the test could start. Firstly, is necessary to preload with a force of 20N. For this, the upper punch comes down into contact with the sample and increasing the force on this, until it reaches 20 Newton, defined as preload. When this point is reached, the following message is displayed.

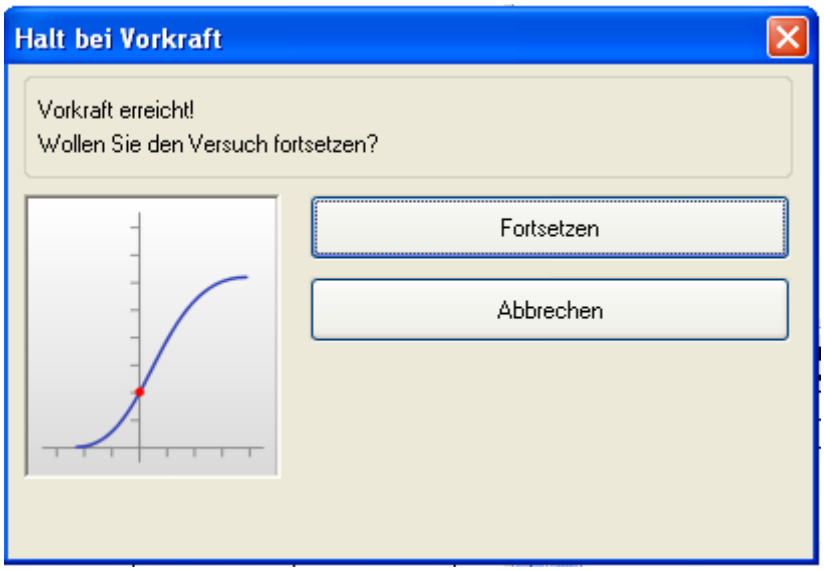

Fig.20: Stop at pre-load

At this moment, the furnace is turned on. It is necessary to adjust the ramp point with the room temperature, so is required to restart the furnace.

Once the desired temperature is reached is necessary to wait until the temperature is homogeneous and stabilized. In this way only the applied load influences on the deformation. Afterwards, click the button *Fortsetzen* to start the test. The choice of test limits is important because with a bad choice the desired creep stages cannot be obtained

This is the appearance of the software while the test is being performed:

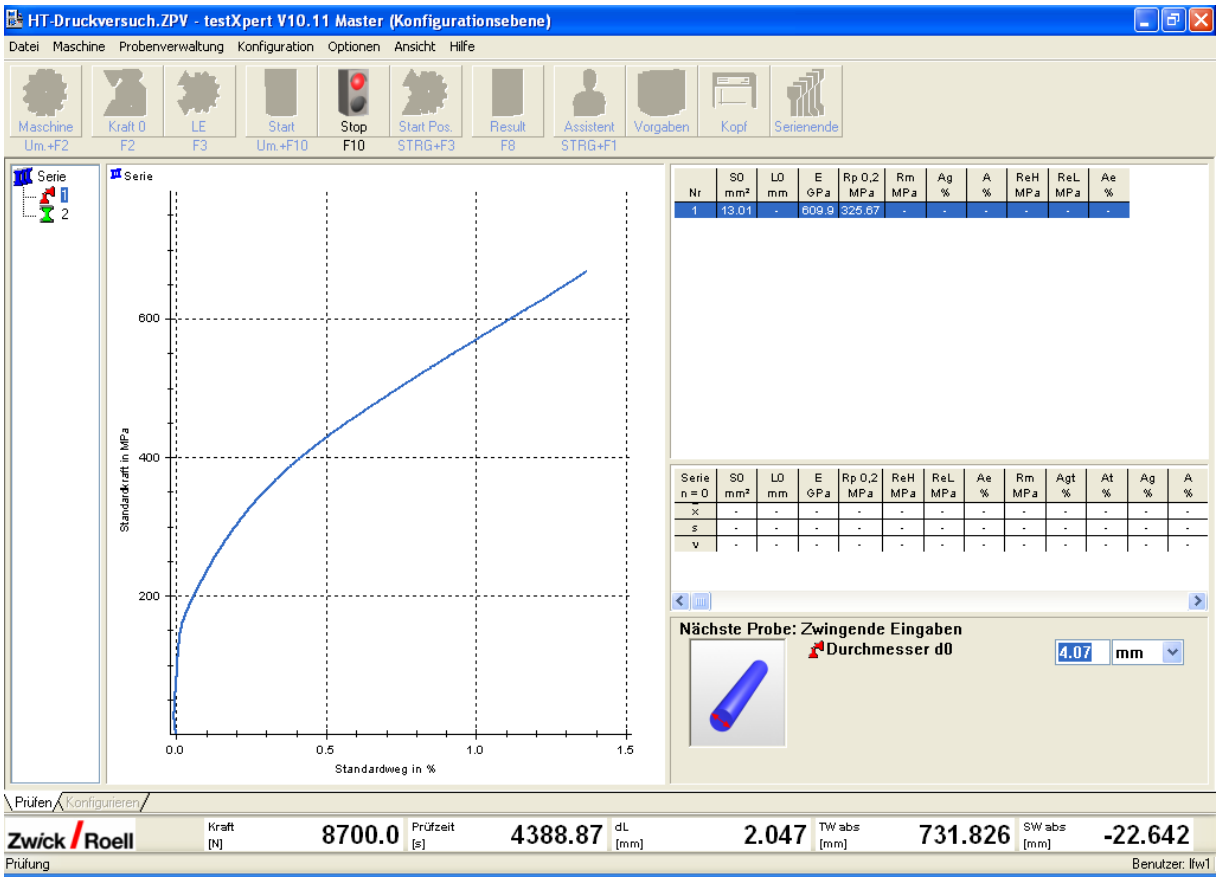

Fig.21: Test running

In the lower part of the screen from left to right, is displayed:

- Force applied on the sample.
- Test time.
- Shortening of the sample, the difference between the initial value measured by the strain gauge and the present.
- Position of the mobile punch, the higher punch in our case.
- Distance measured between pins of extensometer.

When one of the three limits is reached, the test will finished. Following message is displayed on screen. The extensometer should be removed before click OK button.

Fig.22: Remove the extensometer

After that, the *Serienende* button should be pressed to save the data. The display shows the following:

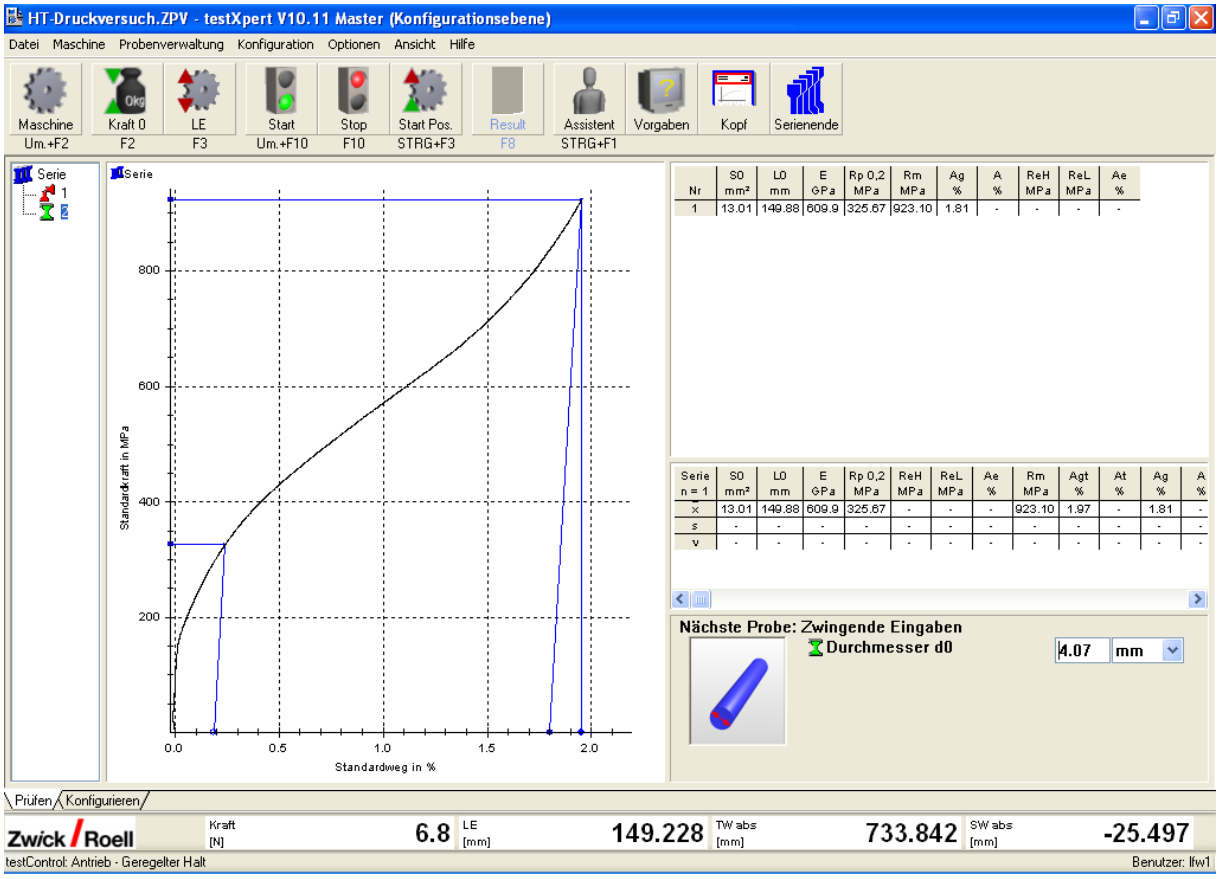

Fig.23: Test ended

Three files were generated, with formats: (.TRA, .ERG, .ZSE). The useful file for analyze the data is the .TRA file. This file contains table with data that are

progressively obtaining during the test such as : testing time, position of the machine´s moving part, applied force, absolute position of the punch measured by the extensometer, and relative distance between the two legs of the extensometer. The data in this table was later converted to an excel file to analyze.

After saving the data, the oven is turned off. The furnace should not be opened until it is cooled to room temperature. The specimen after the test is stored.

4.5. Experiments using INSTRON/ZWICK 1362

All the tests at higher temperatures, 980 and 1125 °C, are performed in this machine. The punches are made of a ceramic material (Al_2O_3), rather than metal as happened with the Zwick/Roell Z020due to its higher strength at higher temperature comparing to metal. At the end of the Al_20_3 punch, a press reception made of *SiO* is placed. It is the same as the test conducted with ZWICK/ROELL Z020, The length and diameter of the cylinder are required parameter inputs .

In this machine, opposite to the other one, the upper part is fixed and the lower part is moved, being able to control the movement of the lower one. In this case when the sample is placed, there is contact with both ends of the punches. This is because the press reception at the top does not stay attached to the punch and falls by gravity. Even so the drills are placed at a sufficient distance to this well positioned and that the applied force is zero.

In this case, the end of the upper plunger is not enough fixed to the plunger, so is necessary a special care in the placement of the piece. At placing the initial position for the sample and plungers is very important to be sure that the initial supported force by the sample is set to zero

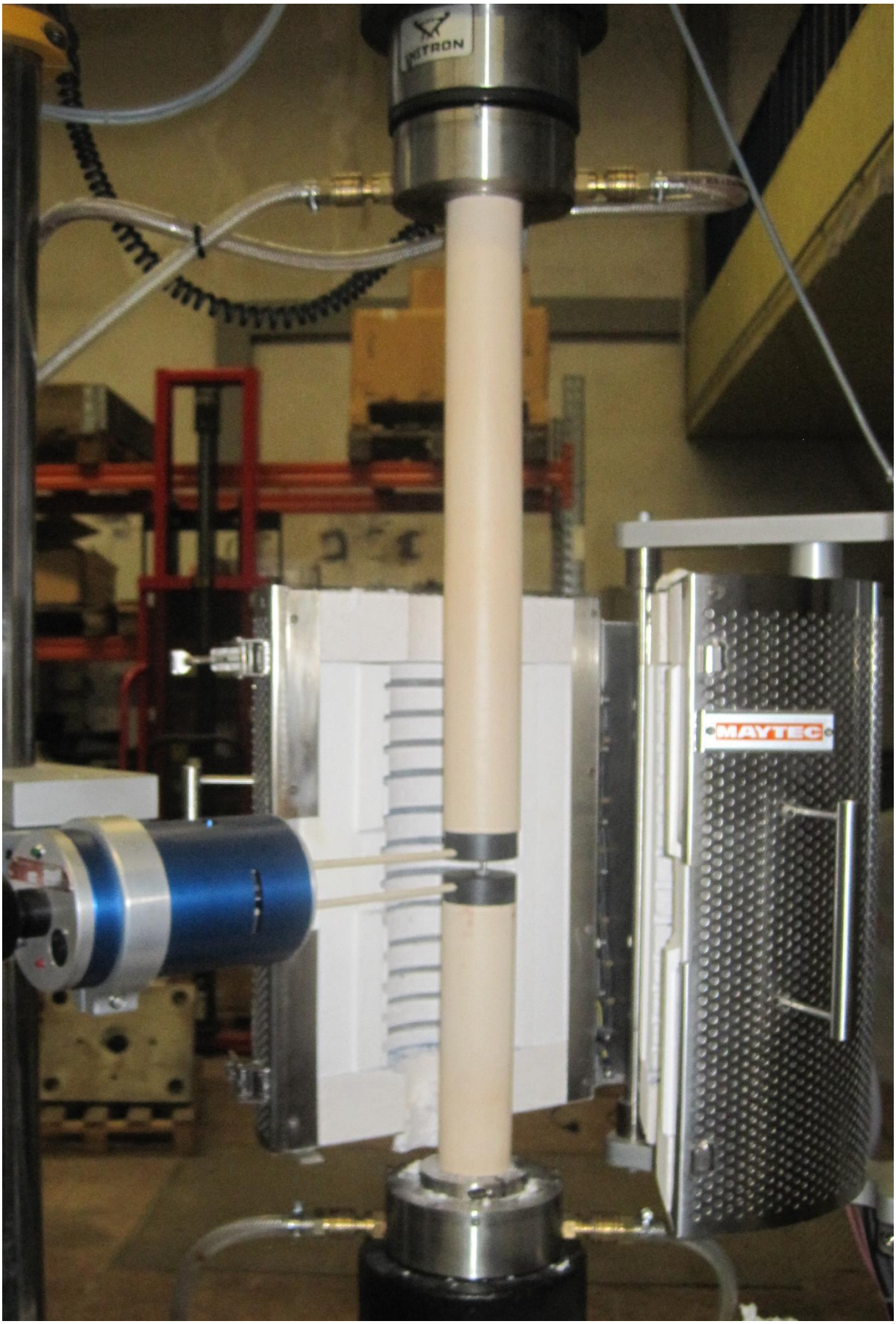

Fig.24: Placing sample in INSTRON/ZWICK 1362

Fig.25: INSTRON/ZWICK 1362 closed and prepared

There is little difference between the size of the diameter of the pistons relative to available in center of oven space. To leave no free space and thus prevent heat loss to the outside this space is filled with insulation.. In order to avoid heat loss due temperature dissipation, additional glass cloud is used for insulation.

Once the oven is properly closed and isolated, the software programming (testXpert II) can be startedThissoftware has some differences comparing to to

testXpert. The first one that concerns this case is the file. In this case an Excel document is generated directly. For that, to program a new experiment must determine where we are going to save and with which name. To define this, accessed by the menu:

Datei -> Exportschnittstellen -> Bearbeiten

This is the aspect of testXpert II software without having any ongoing experiment:

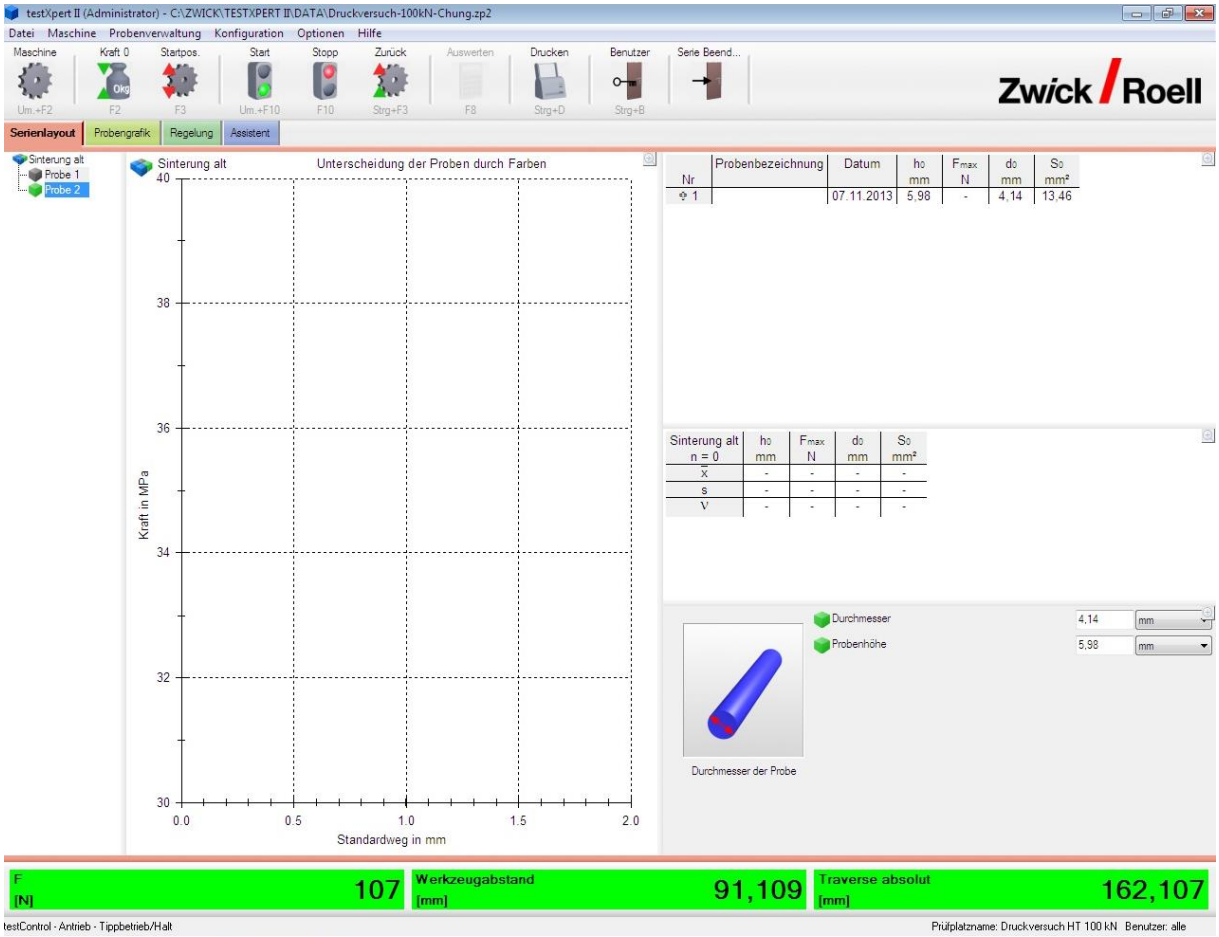

Fig.26: Interface of TextExpert II

At the bottom of the screen can be seen:

• The force applied between the two punches

• The distance between the two legs of the extensometer

• The position of the mobile punch (on this machine the below part).

When these numbers are on green background, as in this case, this means that control movement of machine´s moving part is enabled.

For defining the settings of the test, the *Assistent* tab at the top of the screen is pressed. In this new menu four parts are:

- **Vorkraft:** define the preload force value. The force applied to the sample during the time it is heated. In this case, this force is 40 Newtons.

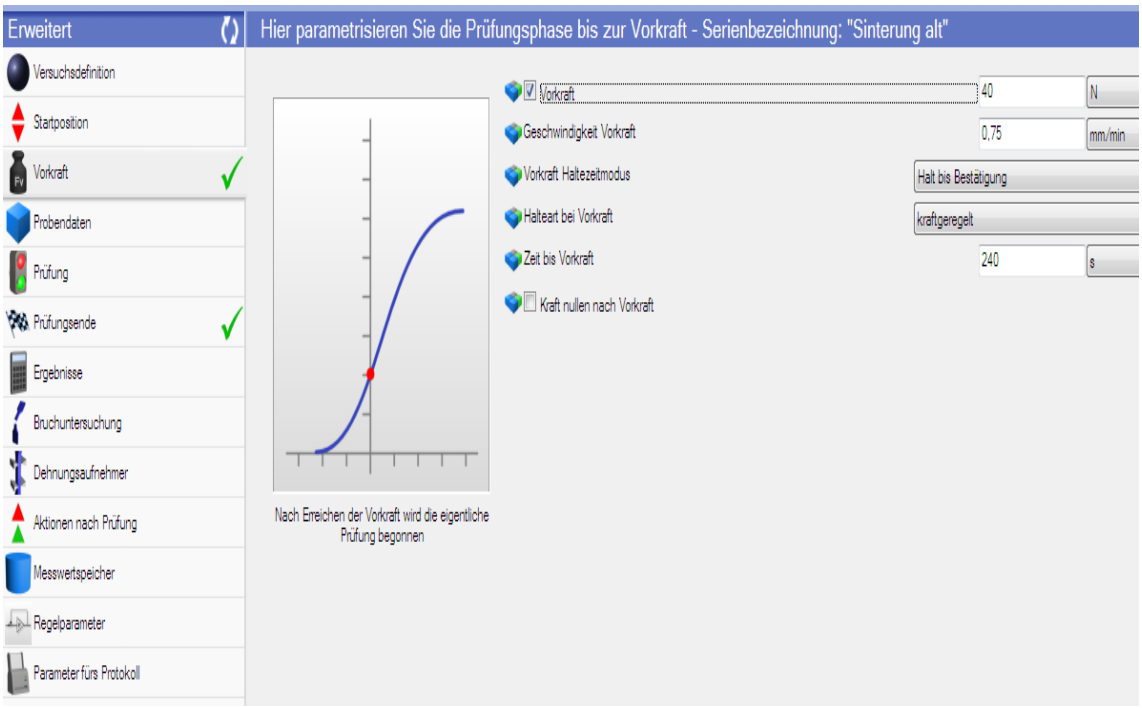

Fig.27: Vrokraft menu

- **Probendaten:** In this section indicate the dimensions of the sample, measuredbefore (initial length and diameter).
-

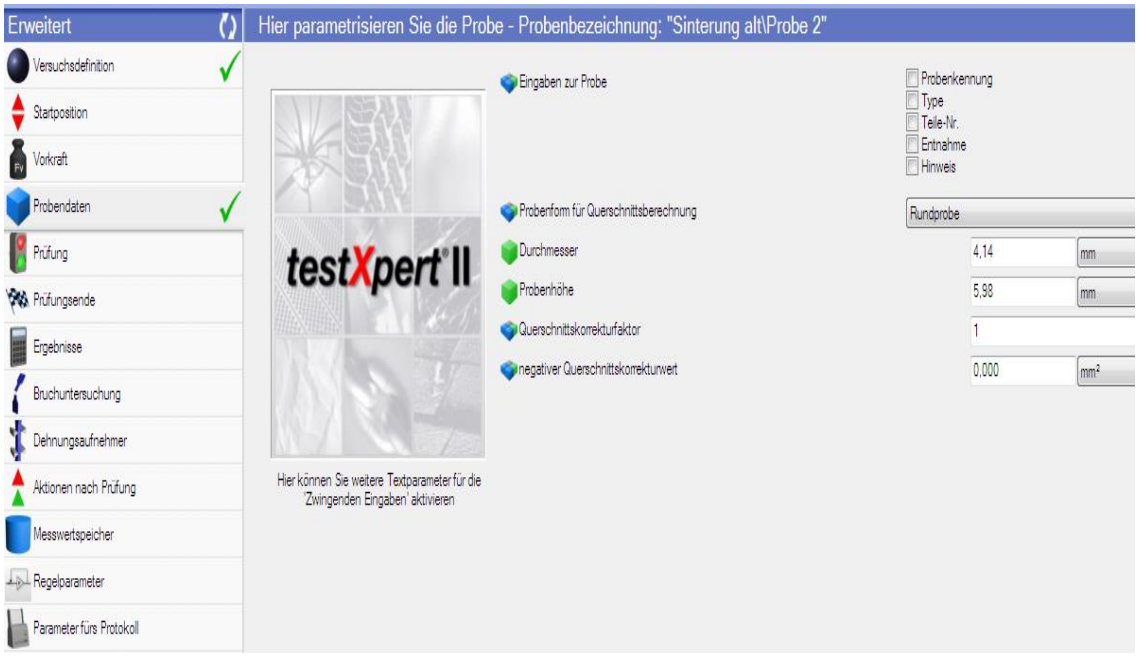

Fig.28: Probendaten menu

- **Prüfung:** Determining the speed of the test. This speed is determined by the product of the initial longitude of the sample and the strain rate of the test.

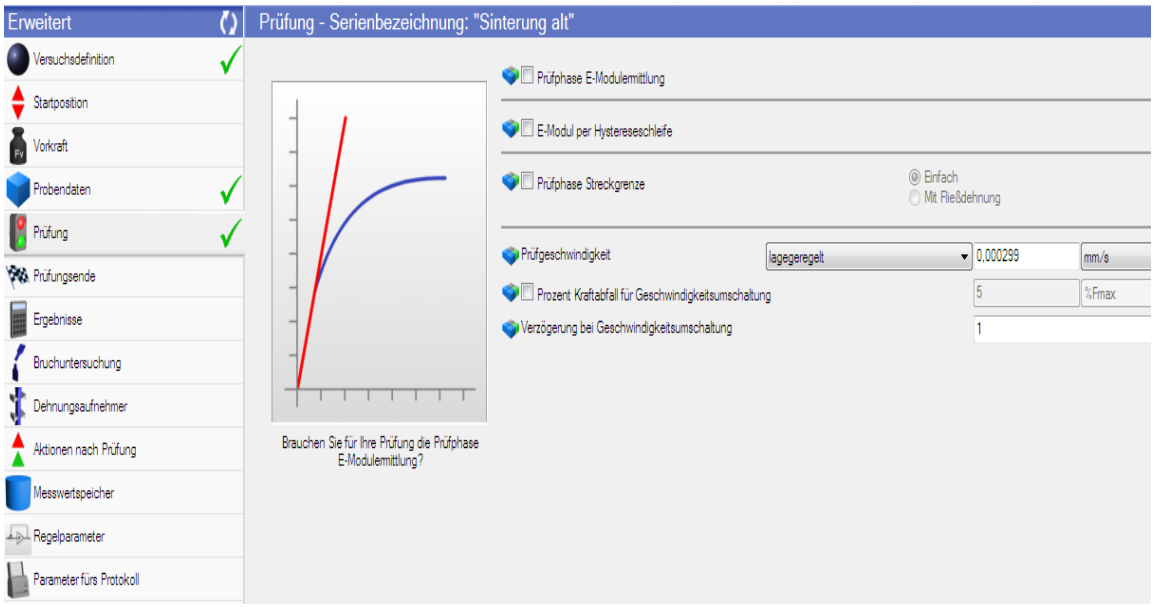

Fig.29: Prüfung menu

- **Prüfungsende:** In this section, the conditions to stop the experiment are given. Whenever one of the three conditions is reached, the experiment is ended. The choice of these conditions is a critical decision, because with a bad choice, it is possible not getting the expected result.

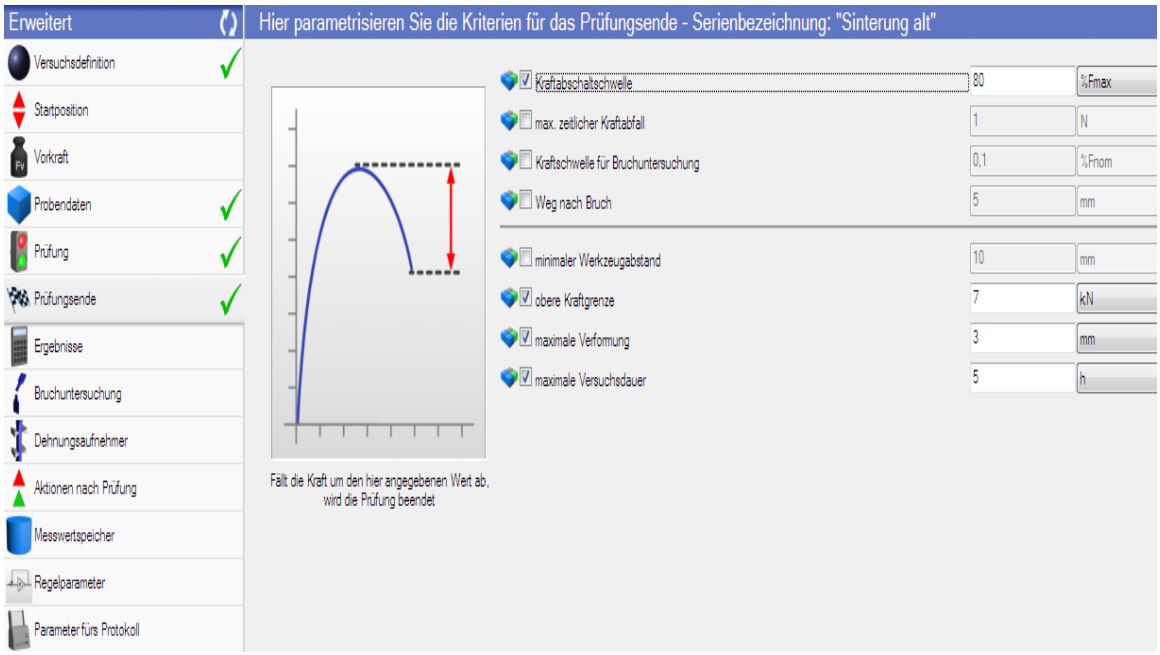

Fig.30: Prüfungende menu

As in testXpert, the end conditions are:

• The time limit of the test, it depends on the speed, type of material and the relative density of the specimen this can vary from four hours to even values close to 20 hours.

• The specimen deformation limit, the maximum length that can be shortened sample. This length ranges from 2.8 to 3 mm.

• The limit force applied on the specimen. The value we choose will come also determined by the type of material, its relative density, even the speed at which we perform the test.

After setting up the test program, the START button located on the top of the screen is pressed. When this button is pressing, the lower punch begins to go up until the force reaches the preload value(40N).

We get a message on the screen when it has reached approximately the preload, asking for continue or cancel the experiment. This is the moment for begin to heat the piece until it reaches the desired temperature for the test.

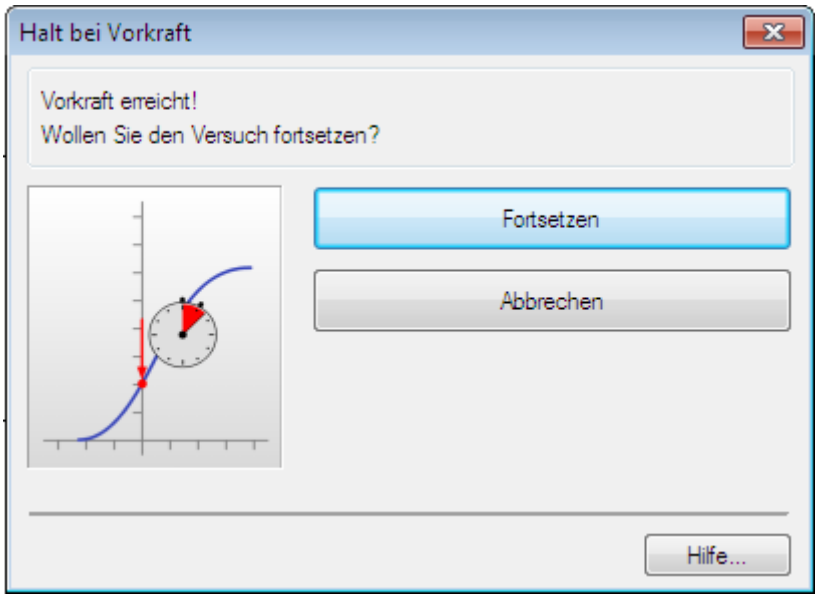

Fig.31: Stop at pre-load

It can be seen that in this case the bottom numbers are not on green background, because now the option to move the lower punch is not enabled.

Once the desired temperature is reached, it is necessary to wait until the temperature is homogeneous and stabilized. Afterwardthe button Fortsetzen can be pressed.

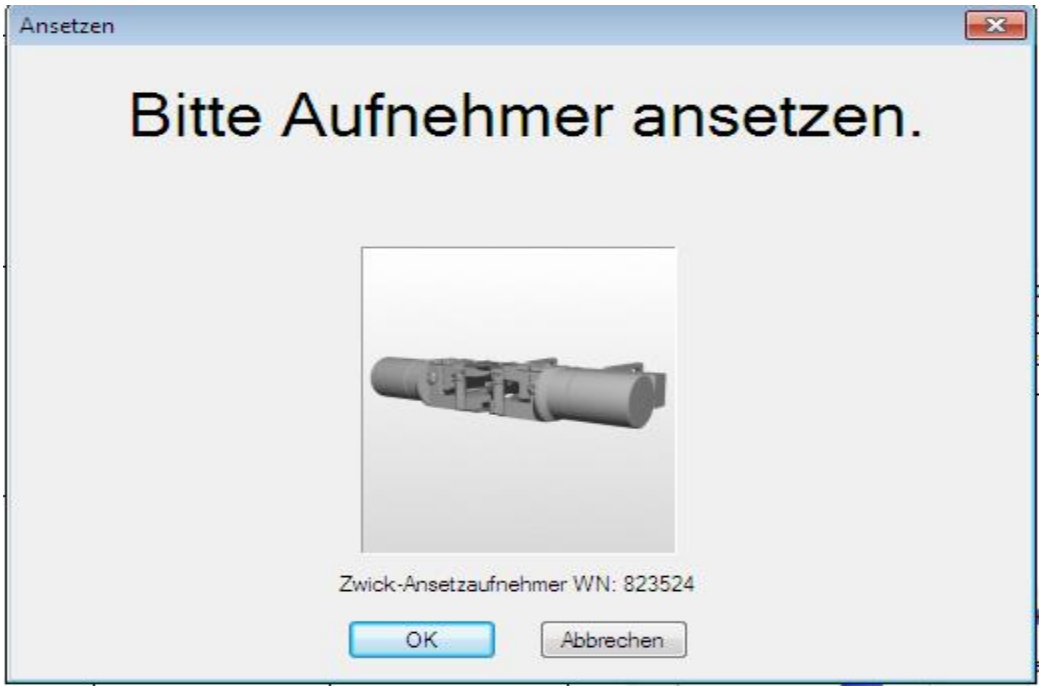

Fig.32: Place the extensometer

This is the message that appears asks for the place of extensometer (MAYTEC PMA-12/V7-1).

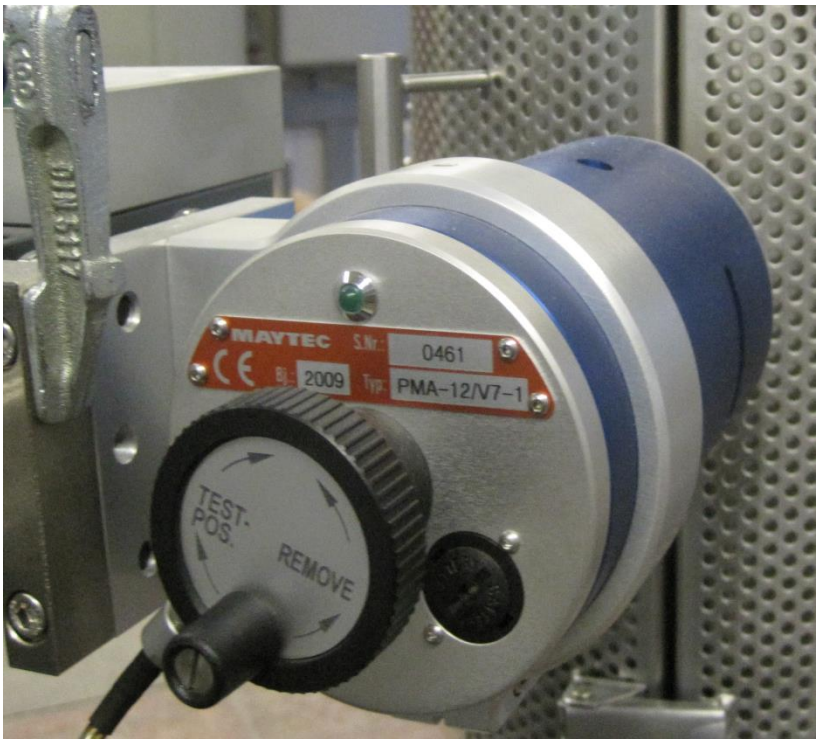

Fig.33: MAYTEC PMA-12/V7-1 turned off

For the extensometer pins come in contact with the walls of the punches, the wheel is rotated until the light turns green located in the extensometer.

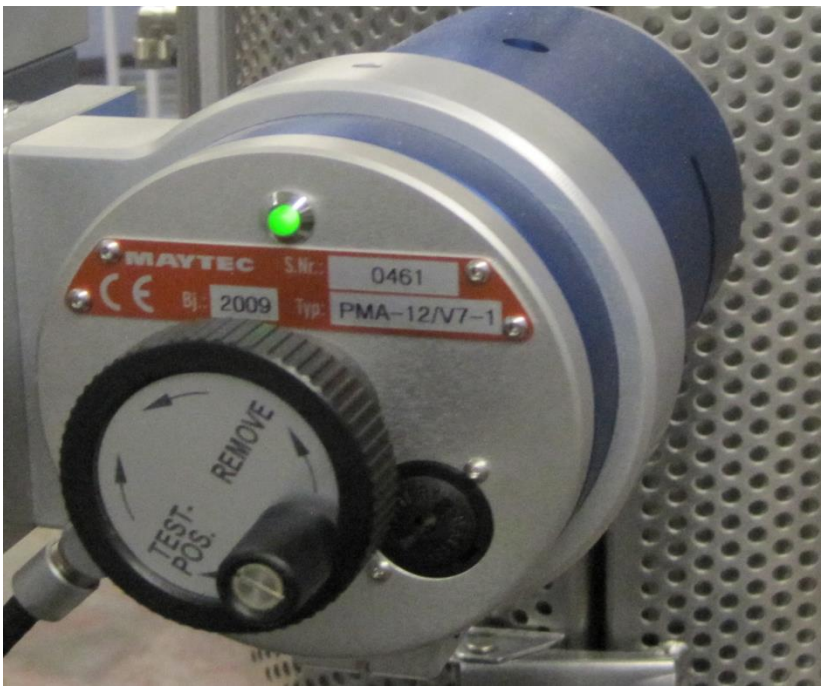

Fig.34: MAYTEC PMA-12/V7-1 turned on

Once the extensometer is well placed, the *OK* button is pressed, and automatically starts the compression of the sample with the defined parameter.

This is the aspect that is displayed while the experiment is underway:

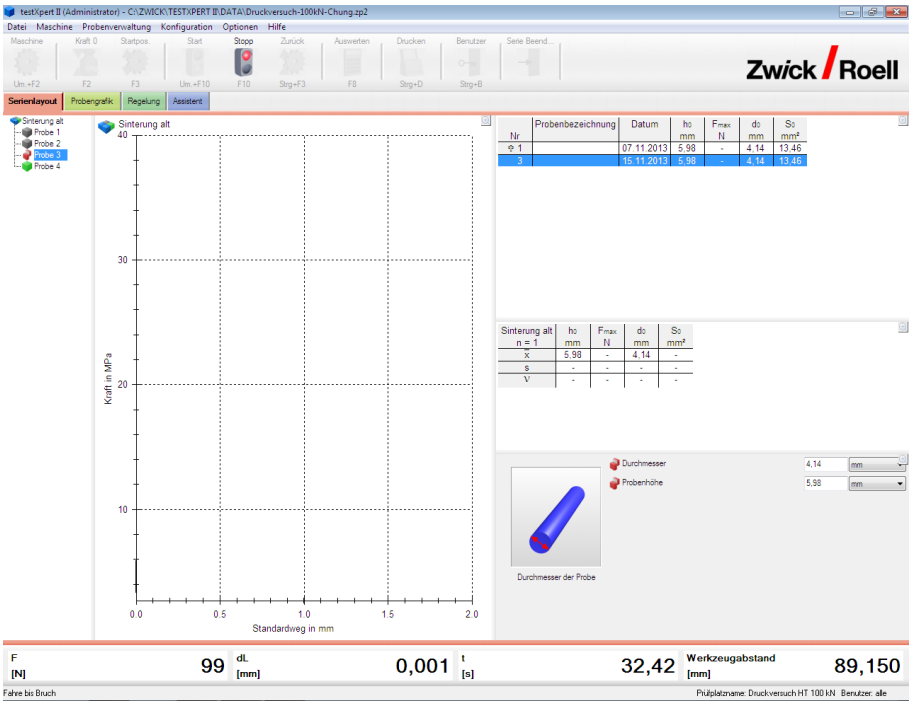

Fig.35: Test running

On this screen are four markers in the lower part of the screen. In order from left to right:

• The force applied on the sample.

• The distance has narrowed the sample.

• The time since compression has begun.

• The distance between the two legs of the extensometer.

Once it reaches one of the three limits defined, the test stops. A message asking to remove the extensometer is appeared.

To remove the pins extensometer, the wheel should be moved in anti-clockwise direction. When it has been retired, the OK button is pressed.

An excel document is automatically generated in place and with the name that defined at the beginning of the experiment. In this excel document there are four columns, from left to right:

• Time, in seconds.

• Applied force in Newtons.

• Shortening measured by the extensometer in millimeters.

• Position of the lower perforated, in millimeters.

5. Data analysis.

5.1. Data collected.

Once the experiments are done, the data are analyzed. This analysis is done on a Microsoft Excel spreadsheet.

In the case of the experiments conducted by Instron / ZWICK 1362, data obtained are directly in Excel format. However, in the case of low temperature experiments, which are conducted in the machine Zwick / Roell Z020 are in Notepad format. With these, we need a transformation to a Microsoft Excel document. In the excel document, there are some difference in the data:

In the case of test data at low temperature, obtained from the machine ZWICK / Roell Z020, we have the following data:

- At the top of the document we have data concerning the experiment, for example, the initial area in contact with the sample, the speed or the starting position of the mobile punch.

In the lower part of the document, there is a table. The respective columns are:

- Test time, measured in seconds.

- Position of the lower end from the machine moving part, the top one. Measured in millimeters from the bottom of the machine.

- Applied force on the sample, measured in Newtons. Recall that when we started testing, we reset it to zero. Later reaches the value of 20 Newtons preload before starting to heat up.

- Difference in length of the sample, measured in millimeters. Positive values are considered for shortening. This is the distance to the initial position.

  Distance between the two pins of the extensometer, measured in millimeters. The extensometer should be regularly calibrated to be sure about the accuracy of the measurement.
- With data from INSTRON/ZWICK 1362, three sheets are generated into the Excel file:

1. Machine data

2. Testing data, such as speed, or the initial area of the contact surface of the sample.

3. The data sheet that interest us to carry out the analysis.

The following columns are in this sheet:

- Test time, measured in seconds.

- Applied force on the sample, measured in Newtons. Recall that when test started, it was reset to zero. Later reaches the value of 40 Newtons preload before starting to heat up.

- Difference in length of the sample, measured in millimeters. Positive values are considered for shortening. This is the distance to the initial position.

- Position of the lower end from the machine moving part, the lower one. Measured in millimeters from the bottom of the machine.

5.2. Data processing

The goal is to analyze the curve of true stress versus true strain. To do this, from the data we have in our Excel documents, the following calculations should be done [20]:

1. Engineer strain = Length variation / Initial length

$$\varepsilon_{eng} = {}^{\Delta l}/_{l_0} \qquad (5.1)$$

2. Engineer stress = Load applied to the sample / Initial Area

$$\sigma_{eng} = {}^{F}/_{A_0} \qquad (5.2)$$

3. True strain = - Ln (1 - Engineer strain)

$$\varepsilon_{true} = -\ln(1 - \varepsilon_{eng}) \qquad (5.3)$$

4. True stress = Engineer stress * (1 - Engineer strain)

$$\sigma_{true} = \sigma_{eng} * (1 - \varepsilon_{eng}) \qquad (5.4)$$

Once the values of true strain and true stress throughout the test are calculated, the graph can be done.

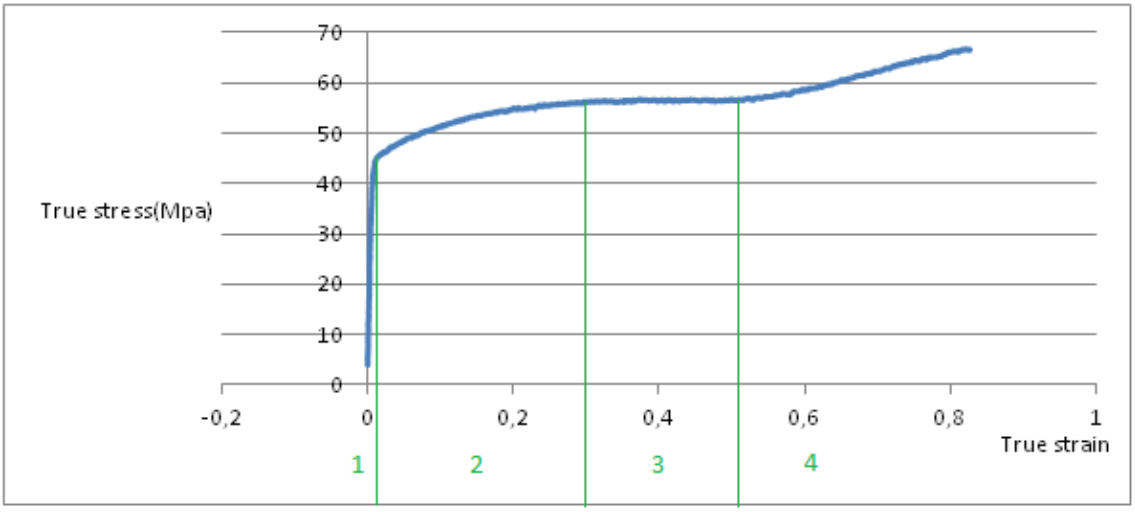

Fig.36: True stress vs. True strain (CN-316L-980°C-RD93-0p0001)

Can be observed four different areas:

1. Linear phase, it corresponds with the elastic region.

2. Decreasing slope until null. It is the primary creep zone.

3. Almost zero slope area. In this phase is almost constant stress producing a strain on the part. It is the secondary creep region.

4. Area with a progressive increase on the slope in which the piece suffers more stress and deforms until it reaches its breaking point. It is the tertiary creep area.

The goal is to find for each test the value of constant stress on the second stage to calculate subsequently creep parameters.

5.3. Secondary creep analysis.

5.3.1. Full dense material.

From the secondary creep analysis, A and n parameters will be determined. A and n for each temperature are identify with axial tests on the completely dense specimen of the material. These tests are carried out in different axial deformation rates in order to identify the constant, maximum axial stress in which the power law is established. In this condition, the axial viscoplastic deformation rate becomes equal to the applied axial deformation rate. Therefore, following equation can be written:

$$\dot{\varepsilon}_{eq} = A\sigma^n \tag{5.5}$$

For obtain stress value needed for previous equation, should only be considered constant stress on secondary creep area:

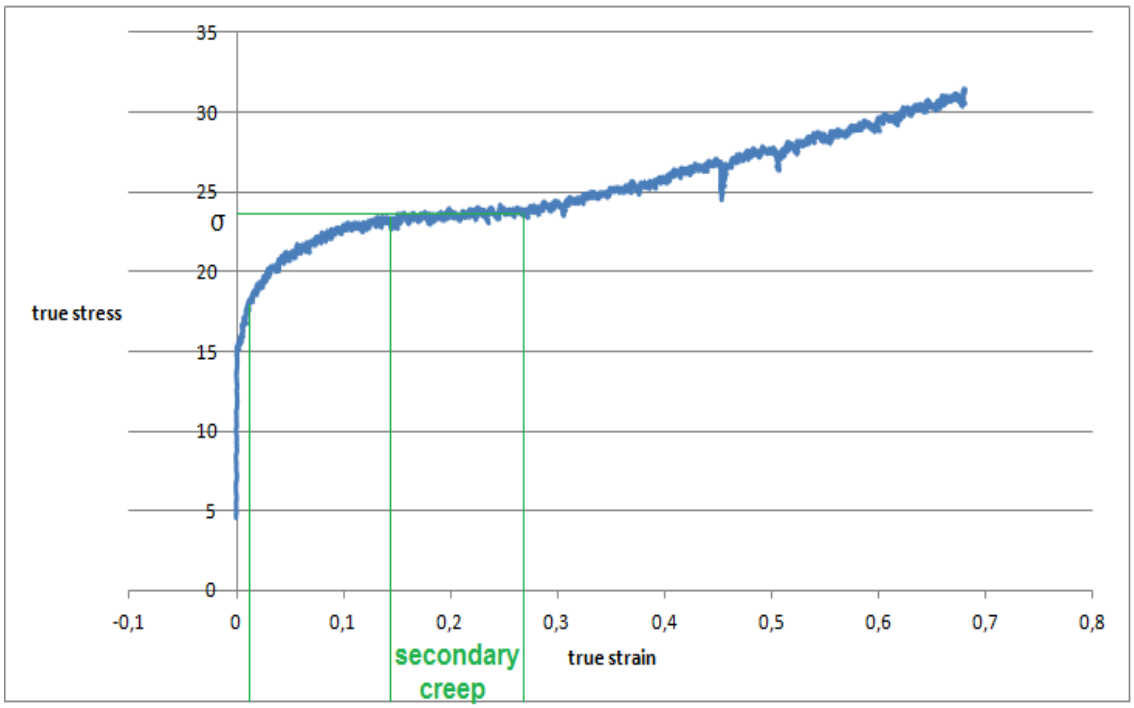

Fig.37: Secondary creep graph (CN-316L-1125°C-0p00005)

For the same material and the same temperature are obtained four couples of related values, due the four different values of strain rates. Charting these four couples of values followings graphs are obtained:

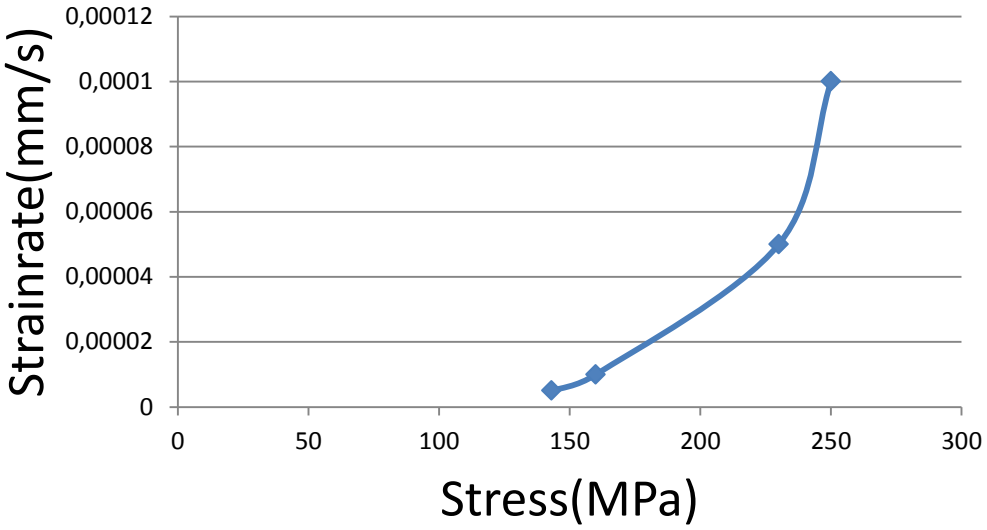

Fig.38: Strain rate vs Stress (CN-316L-800°C)

Therefore, in each temperature, constants A and n are determined from fitting on the experimental curve (strain rate vs stress). Software OriginPro 9 is used to fit the necessary regression to obtain A and n.

To perform a regression with a lower complexity is possible to use a modification of the previous expression:

$$\ln\left(\dot{\varepsilon}_{eq}\right) = \ln(A) + n * \ln(\sigma) \tag{5.6}$$

Using it, the result is reached from a linear regression

5.3.2. Porous material.

Proceeding in the same procedure as done for full dense materials, four couples of values are obtained for each temperature and relative density of 316L material.

As have been introduced in the theoretical basis chapter, the equivalent Misses stress (σ_{eq}) for a porous material can be written as:

$$\boldsymbol{\sigma}_{eq}^{2} = 3cJ_2 + fI_1^2 \quad (5.7)$$

Charting in the same graph the different relative densities of the same material exposed to the same conditions of temperature:

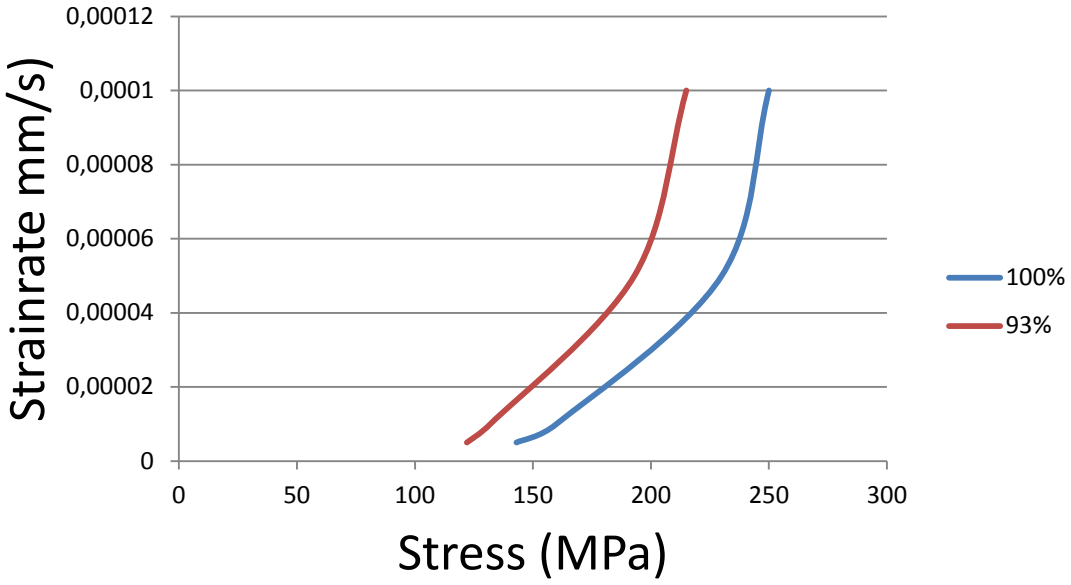

Fig.39: Strain rate vs Stress for different relative densities (CN-316L-800°C)

Measuring the difference between intercepts of three curves is obtained the value of $s(\rho)$, used on (5.8) for obtain the value of $c(\rho)$:

$$c(\rho) = s(\rho)^{-2n/n+1} - f(\rho) \quad (5.8)$$

The value of *n* has been already calculated on the full dense material analysis and the f values have been calculated by HIP tests

5.4. Primary creep analysis.

Plots as following will be the starting point to calculate primary creep parameters:

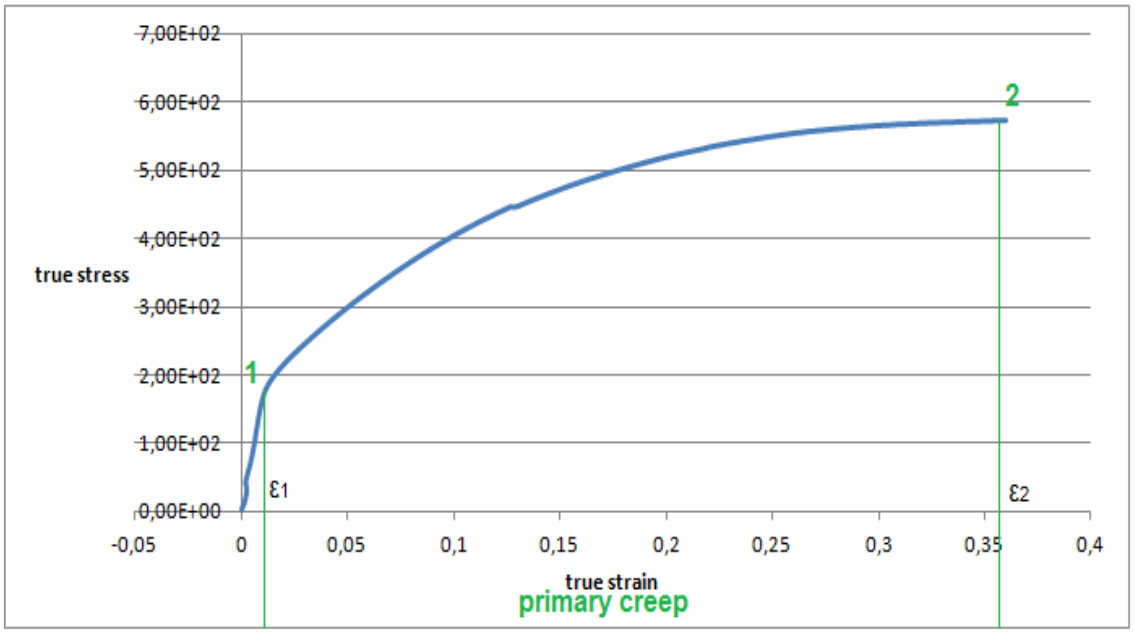

Fig.40: Primary creep graph (CN-316L-600-0p00001)

The point 1 is where primary creep starts. The point 2 is where primary creep ends and starts secondary creep. A collection of data (x, y) is generated for the exponential regression. This collection is made from point 1 to point 2.

The value of creep strain is different from the true strain on the current point to the point 1. For example, on the point 2:

$$\varepsilon_c = \varepsilon_2 - \varepsilon_1 \tag{5.9}$$

Stress value is the current value of true stress on the point. The strain rate is obtained. The strain rate is obtained by dividing the difference of the length of the sample with the previous measurement by the time elapsed between two actions.

Once collected necessary values to carry on the analysis, software OriginPro 9 is used to fit the regression.

6. Results.

In this chapter, results of every experiment are presented. At first secondary creep results are showed and later primary creep results. These results can be observed in groups depending on material type and temperature.

6.1. Secondary creep.

The way chosen in this thesis to show the results of the secondary flow is explained below:

- A graph with experiments results performed at four different strain rates for the same temperature.

- A table summarizing the values with the stress at which secondary creep occurs for each strain rate.

- A graph representing the approaches suggested in this thesis for the values shown above (stress / strain rate). The three approaches on the same graph to give a joint vision and determine which one best fits the data set obtained from the experiments are shown. These approaches are shown in the graph by the following colors:

    - Power creep law is represented in red as shown in (3.3)

    - Unified creep law is represented in blue. as shown in (3.4)

    - Exponential creep law is represented in green. as shown in (3.5)

- A table summarizing the different parameters values of every approach.

6.1.1. 304 stainless steel

- **600ºC**

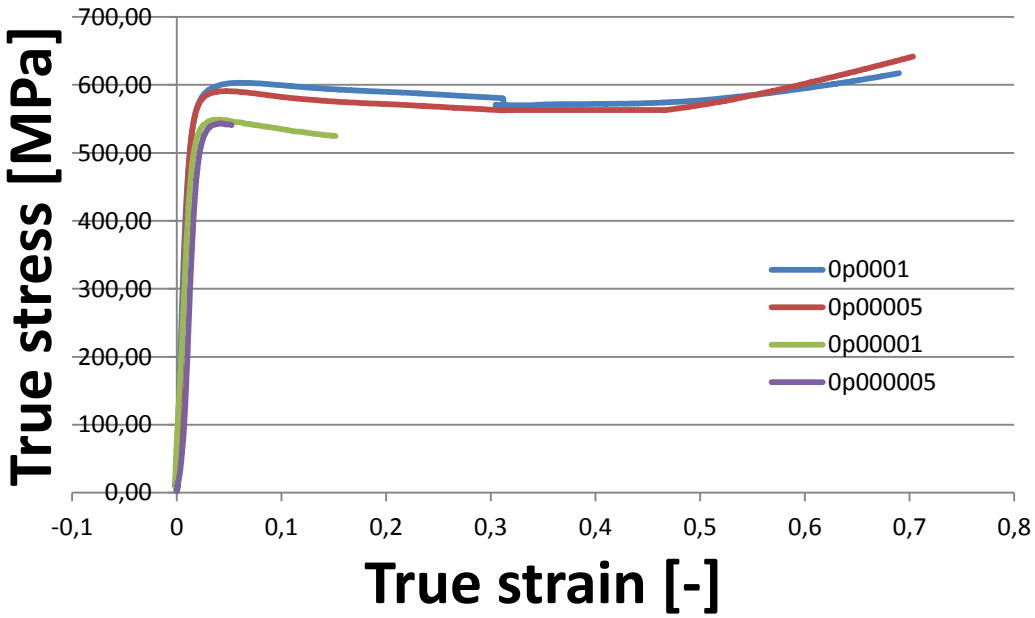

Fig.41: CN-304-600ºC

strain rate	0,0001	0,00005	0,00001	0,000005
stress	603	588	548	542

Fig. 42: 304-600ªC-results

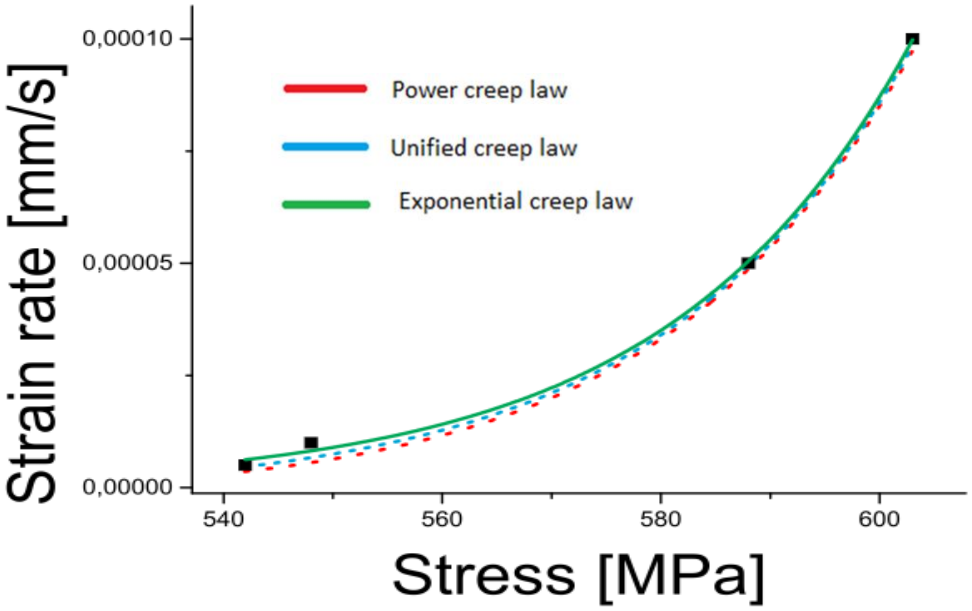

.

Fig.43: CN-304-600ºC Fitting

Some authors prefer the fit from the ln (strain rate) vs ln (stress) graph (eq. 5.6). The reason is because the result plot is linear.

$$\ln\left(\dot{\varepsilon}_{eq}\right) = \ln(A) + n * \ln(\sigma) \qquad (5.6)$$

This formula can be compared with the common linear equation: y = a1 + a2*x. Where exit two variables (y, x) and two parameters (a1, a2). The relation between eq. 5.6 and the common linear equation is as follows:

$\ln\left(\dot{\varepsilon}_{eq}\right)$ = y

$\ln(A)$ = a1

n = a2

$\ln(\sigma)$ = x

So, having couples of variables data ($\ln\left(\dot{\varepsilon}_{eq}\right)$, $\ln(\sigma)$), is possible to make a linear regression to fit the two parameters ($\ln(A)$, n) . An example from this kind of fitting is presented for this case where is possible to check the same success on the fit.

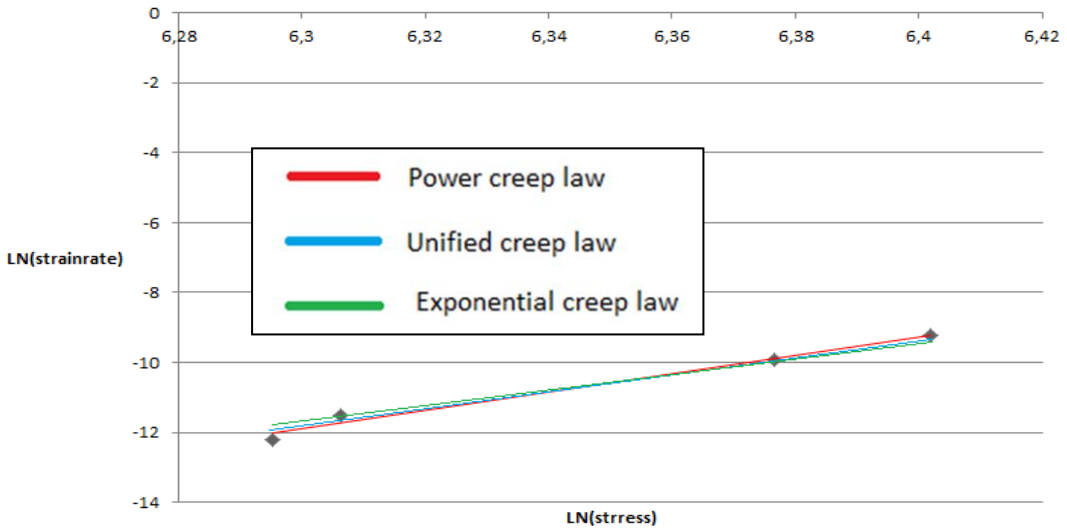

Fig.44: CN-304-600ºC Logarithm Fitting

	Power law		Unified law		Exponenital law	
	Value	error	Value	error	Value	error
A	7,02E-79	5,54E-78	2,45E-16	1,59E-12	1,22E-16	1,33E-16
n	26,6705	1,23442	0,21352	9377,9929	0,04548	0,00182
k			0,20874	9161,1276		

Fig.45: CN-304-600ºC Parameters

In the case of this thesis is not necessary due Origin Pro 9 software is used, and this software has the capacity to fit with a very high exactitude the curves analyzed in this section.

- **700ºC**

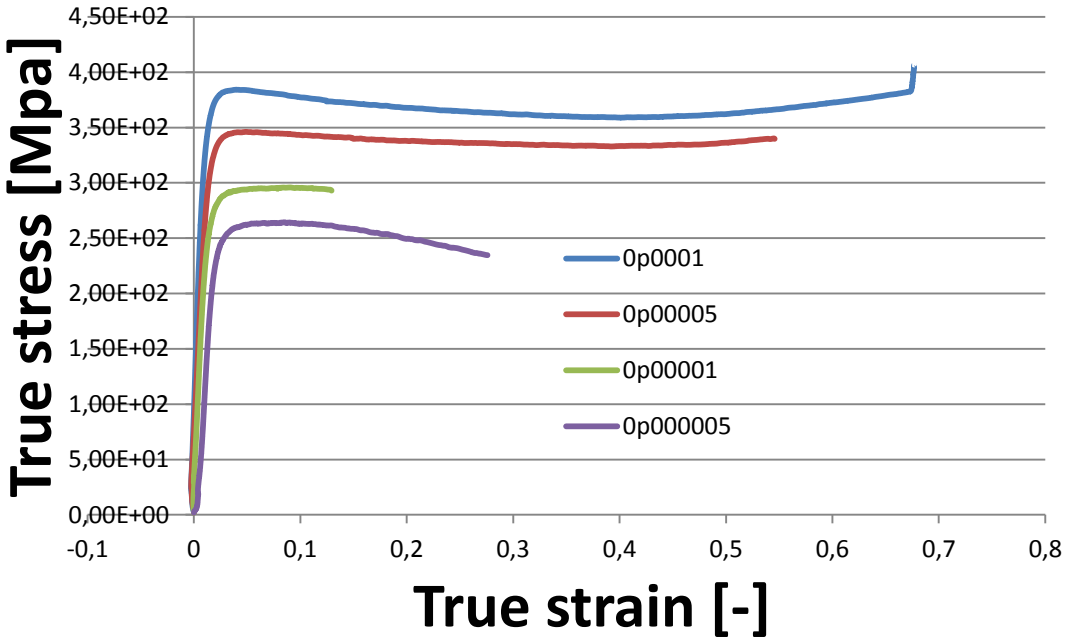

Fig.46: CN-304-700ºC

strain rate	0,0001	0,00005	0,00001	0,000005
stress	383	345	295	263

Fig. 47: 304-700ªC-results

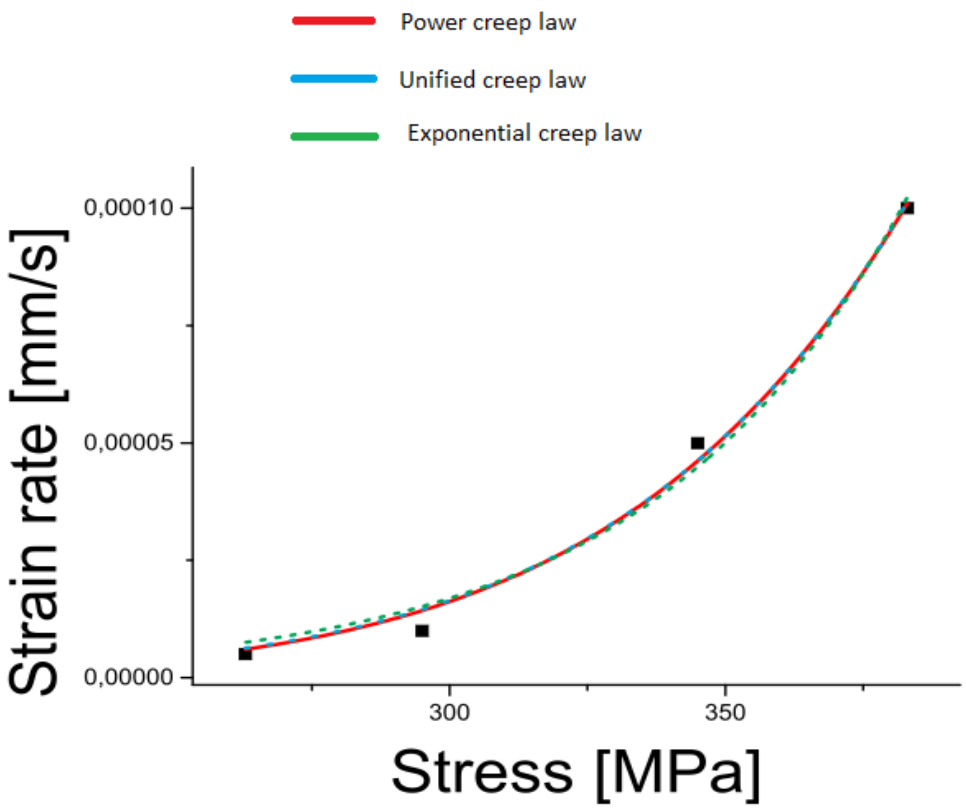

Fig.48: CN-304-700ºC Fitting

	Power law		Unified law		Exponenital law	
	Value	error	Value	error	Value	error
A	3,59E-26	5,54E-78	3,53E-15	1,068E-11	1,22E-16	1,33E-16
n	8,30869	1,23442	4,61847	4388,8295	0,04548	0,00182
k			0,00979	9,15802		

Fig.49: CN-304-700ºC Parameters

- **800ºC**

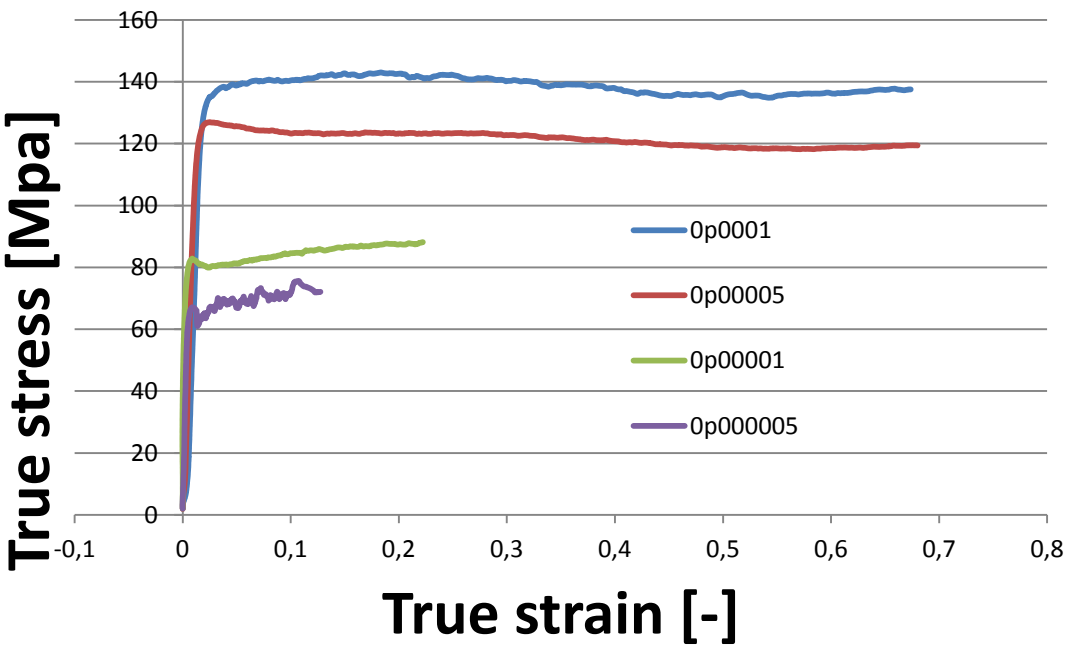

Fig.50: CN-304-800ºC

strain rate	0,0001	0,00005	0,00001	0,000005
stress	142	126	82	67

Fig. 51: 304-800ªC-results

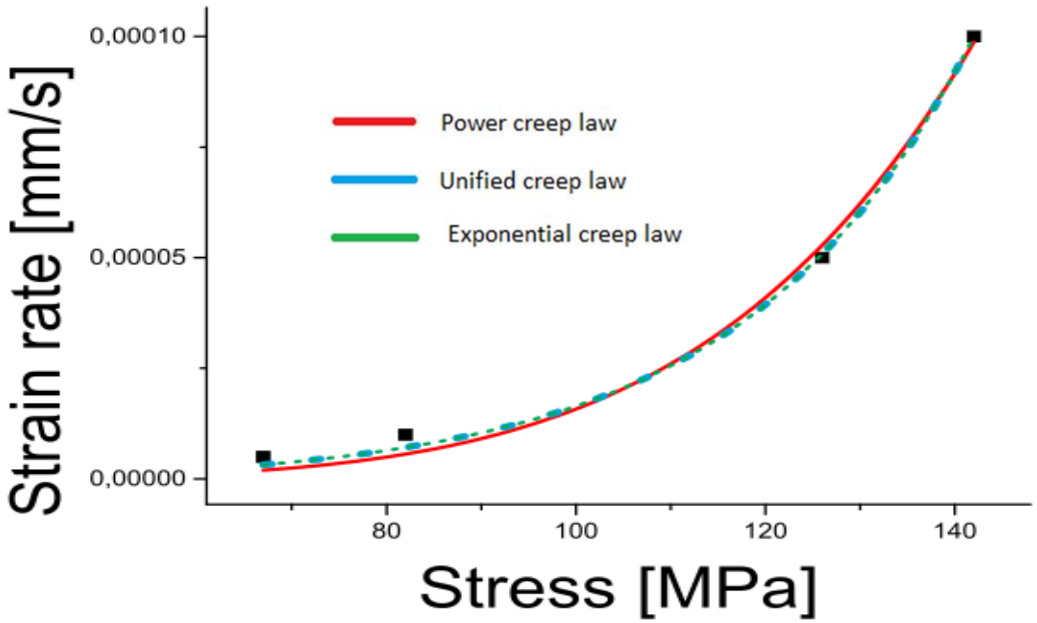

Fig.52: CN-304-800ºC Fitting

Power law	Unified law	Exponenital law

	Value	error	Value	error	Value	error
A	5,41E-16	1,81E-15	3,22E-07	0,01173	2,76E-07	6,65E-08
n	5,23242	0,68081	0,22005	52624,44	0,04145	0,00174
k			0,18839	45018,519		

Fig.53: CN-304-800ºC Parameters

➢ **980ºC**

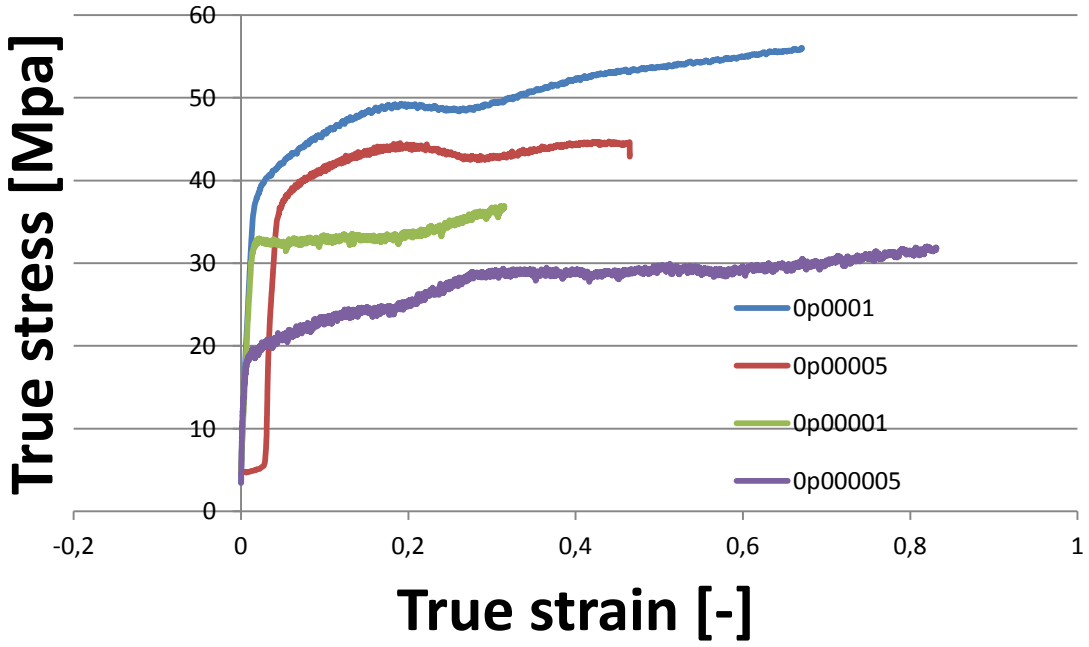

Fig.54: CN-304-980ºC

strain rate	0,0001	0,00005	0,00001	0,000005
stress	49	44	32	24

Fig. 55: 304-980ªC-results

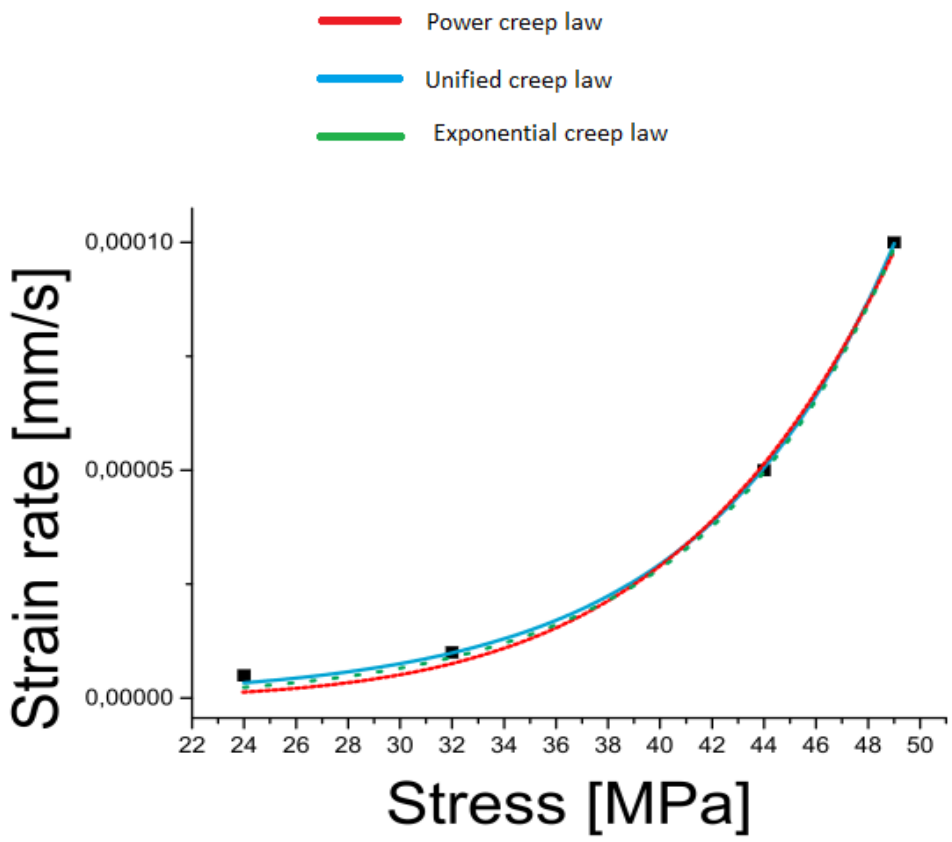

Fig.56: CN-304-980ºC Fitting

	Power law		Unified law		Exponenital law	
	Value	error	Value	error	Value	error
A	7,11E-15	1,58E-14	1,61E-07	0,09154	1,29E-07	2,70E-08
n	6,00213	0,57515	0,32611	36180,983	0,13577	0,00438
k			0,41636	32456,563		

Fig.57: CN-304-980ºC Parameters

- **1125ºC**

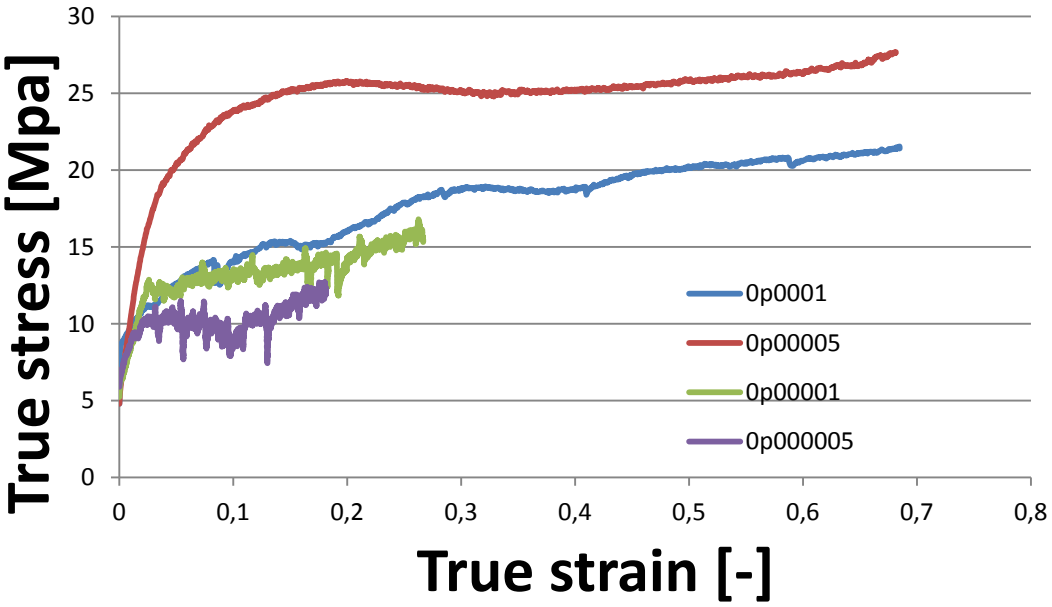

Fig.58: CN-304-1125ºC

strain rate	0,0001	0,00005	0,00001	0,000005
stress		25,7	12,7	9,3

Fig. 59: 304-1125ªC-results

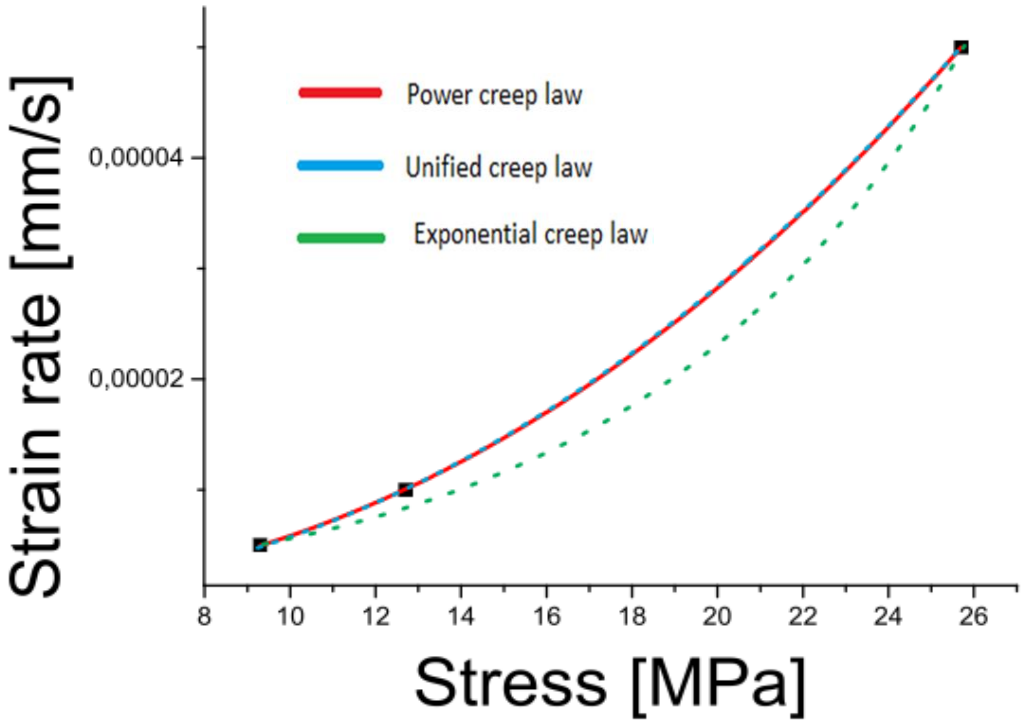

Fig.60: CN-304-1125ºC Fitting

	Power law		Unified law		Exponenital law	
	Value	error	Value	error	Value	error
A	3,08E-08	8,63E-10	2,20E-03	2,00729	1,77E-06	3,58E-07
n	2,27713	0,00872	2,22	1,67256	0,12994	0,00801
k			0,00704	0,30596		

Fig.61: CN-304-1125ºC Parameters

6.1.2. 316L stainless steel

- **600ºC**

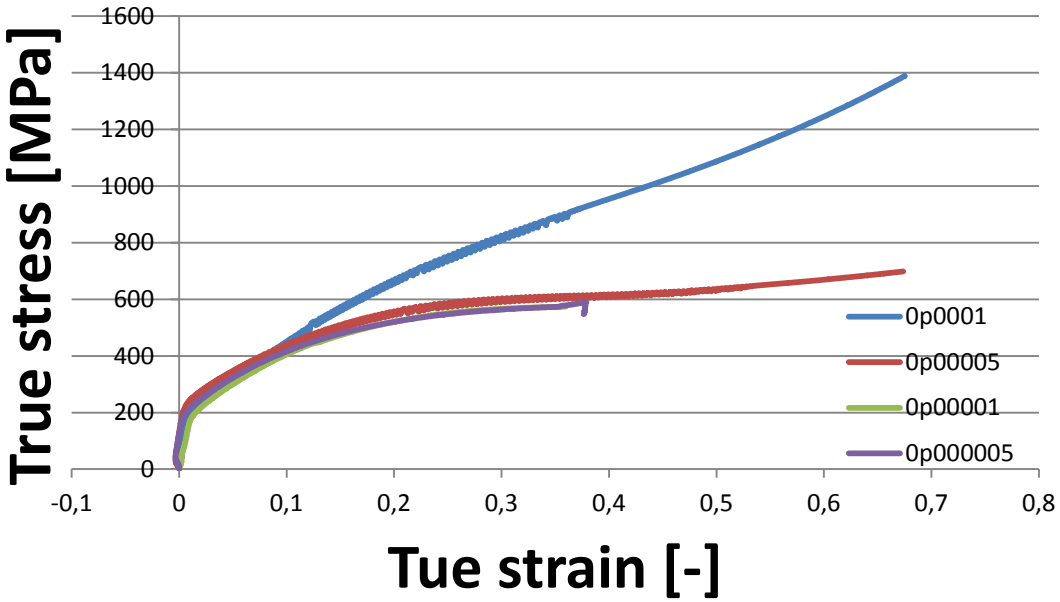

Fig.62: CN-316L-600ºC

For CN-316L-600-0p0001 experiment there is not a clear phase with constant stress. These types of graphs appear at the lower temperature, (as in this case for 316L material at 600ºC). When it happens is possible to say that secondary creep does not occur, and only primary creep happens.

strain rate	0,0001	0,00005	0,00001	0,000005
stress	655	615	580	560

Fig. 63: 316L-600ªC-results

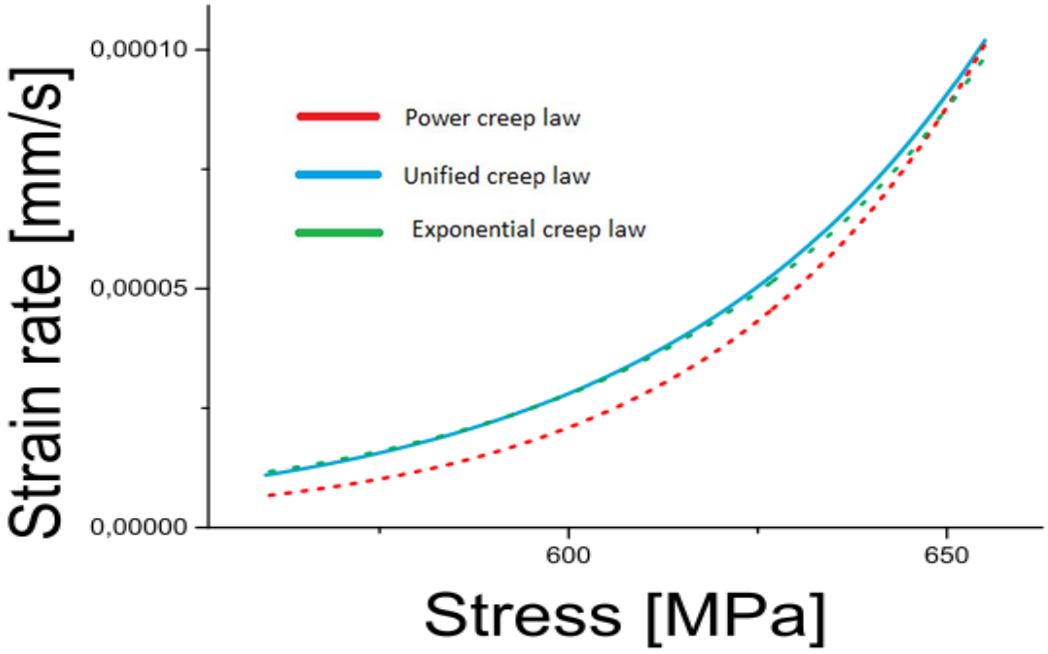

Fig.64: CN-316L-600ºC Fitting

	Power law		Unified law		Exponenital law	
	Value	error	Value	error	Value	error
A	1,24E-56	4,04E-55	2,39E-11	1,77E-06	2,14E-11	6,45E-11
n	18,43904	5,03162	0,15428	106661,33	0,02348	0,00465
k			0,15211	105102,92		

Fig.65: CN-316L-600ºC Parameters

- **700ºC**

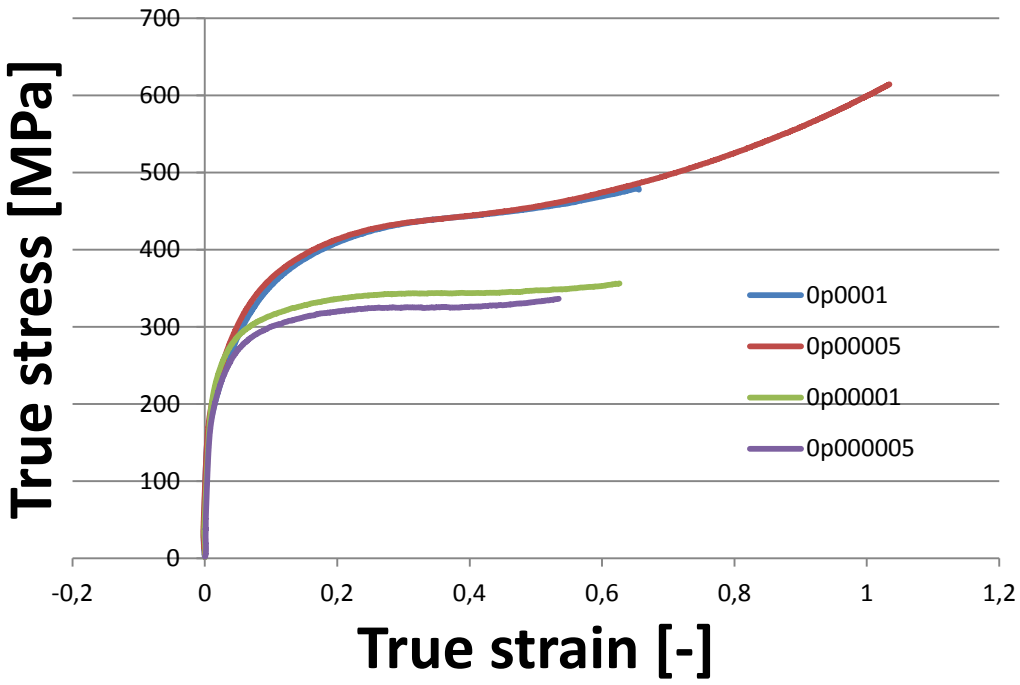

Fig.66: CN-316L-700ºC

strain rate	0,0001	0,00005	0,00001	0,000005
stress	383	345	295	263

Fig. 67: 316L-700ªC-results

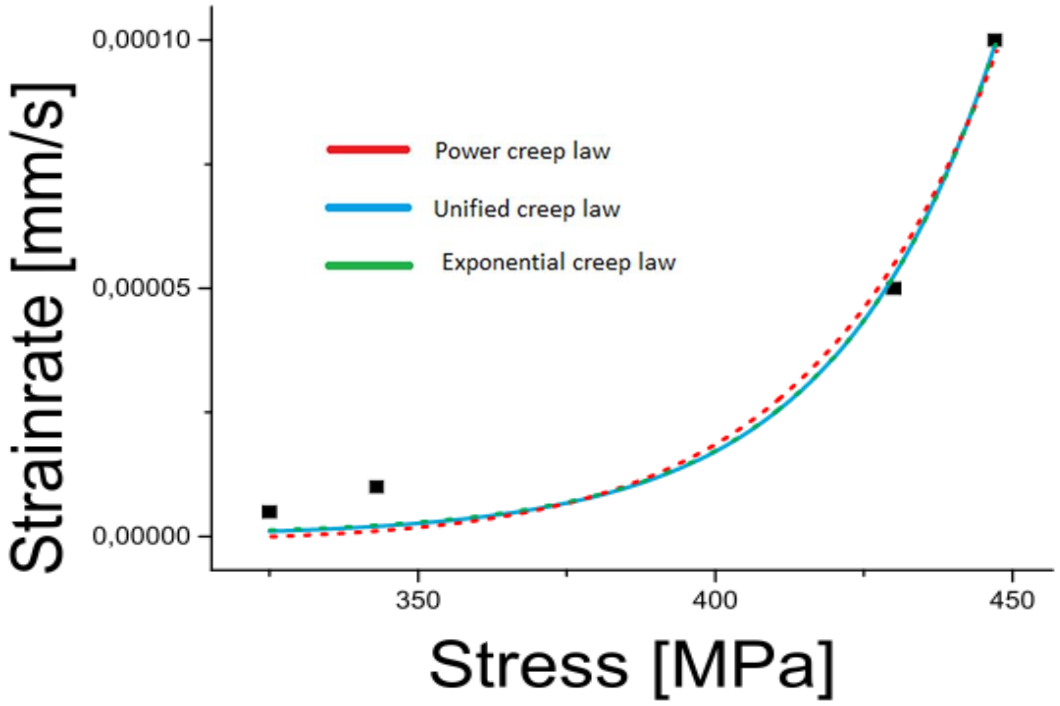

Fig.68: CN-316L-700ºC Fitting

	Power law		Unified law		Exponenital law	
	Value	error	Value	error	Value	error
A	4,40E-43	1,04E-41	6,50E-12	1,068E-11	5,69E-12	2,01E-11
n	14,46769	3,88383	0,19533	4388,8295	0,03729	0,00797
k			0,19095	9,15802		

Fig.69: CN-316L-700ºC Parameters

- **800ºC**

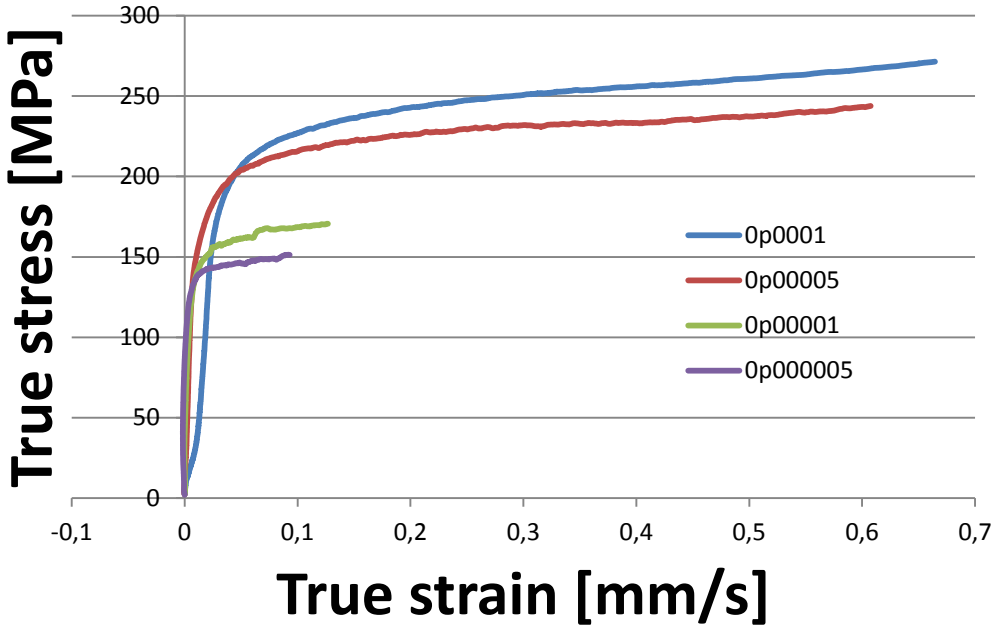

Fig.70: CN-316L-800ºC

strain rate	0,0001	0,00005	0,00001	0,000005
stress	250	230	160	143

Fig. 71: 316L-800ªC-results

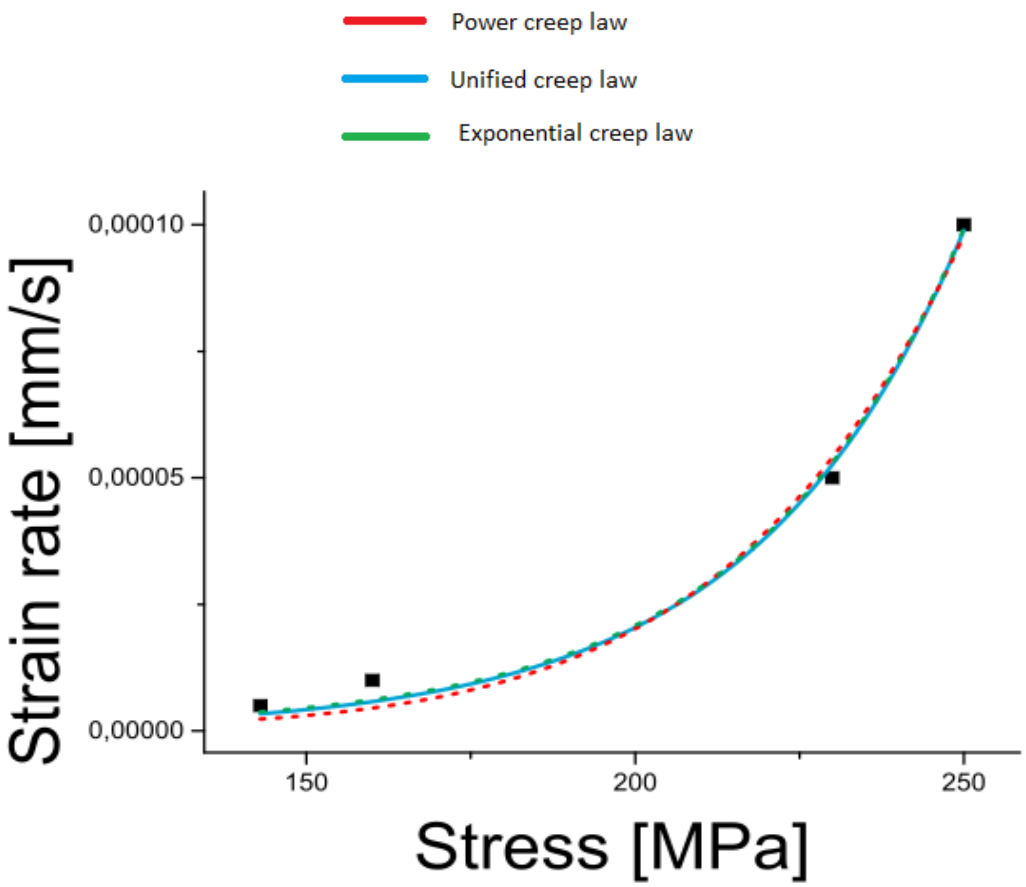

Fig.72: CN-316L-800ºC Fitting

	Power law		Unified law		Exponenital law	
	Value	error	Value	error	Value	error
A	5,81E-22	4,16E-21	4,22E-08	0,01173	4,22E-08	6,65E-08
n	7,18427	1,30219	0,18243	52624,44	0,18243	0,00174
k			0,17292	45018,519		

Fig.73: CN-316L-800ºC Parameters

- **980ºC**

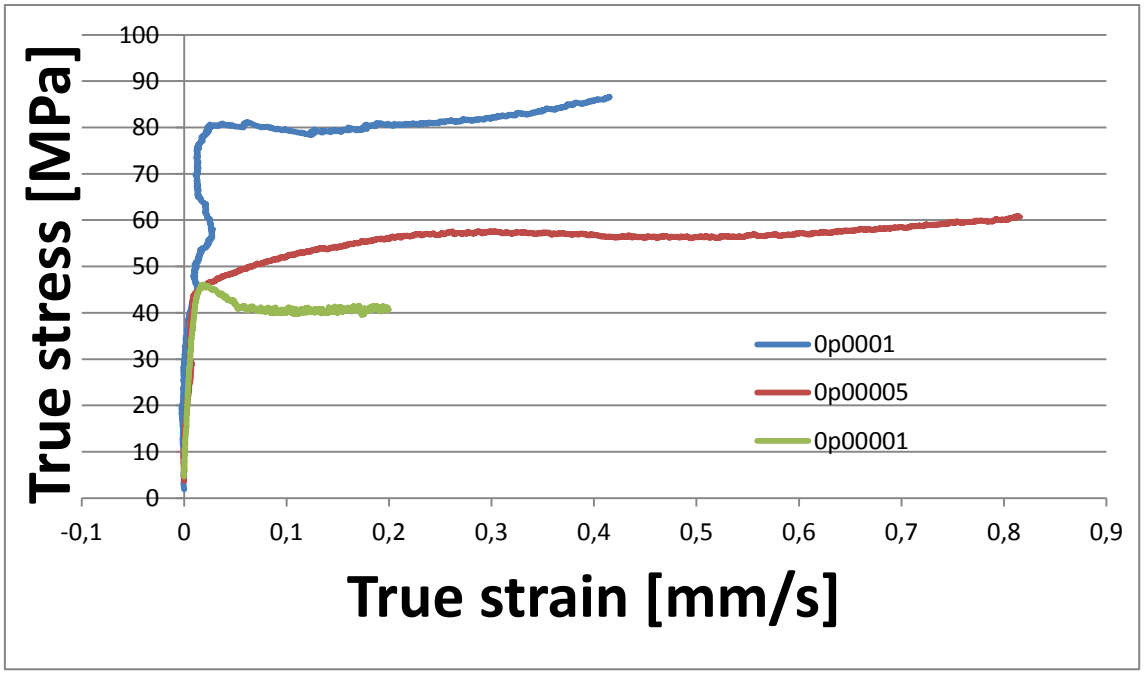

Fig.74: CN-316L-980ºC

strain rate	0,0001	0,00005	0,00001	0,000005
stress	80,2	57,2	40,8	32

Fig. 75: 316L-980ªC-results

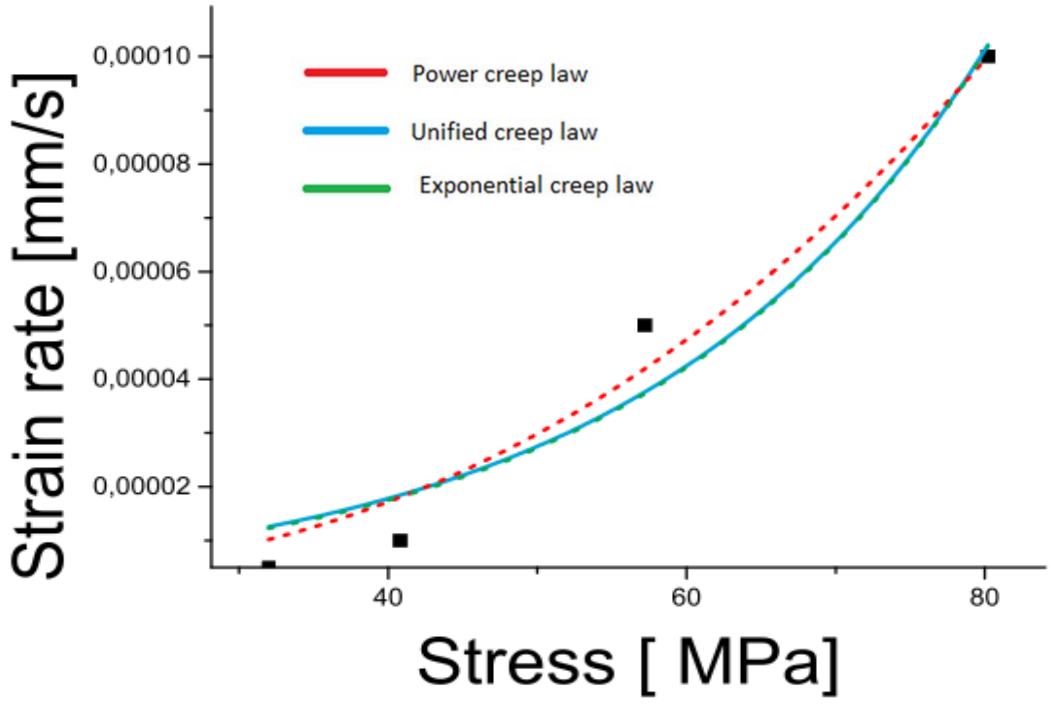

Fig.76: CN-316L-980ºC Fitting

Power law	Unified law	Exponenital law

	Value	error	Value	error	Value	error
A	9,72E-10	1,89E-09	3,65E-06	0,09154	3,13E-06	2,42E-06
n	2,63634	0,44919	0,21996	36180,983	0,04344	0,01009
k			0,19747	32456,563		

Fig.77: CN-316L-980ºC Parameters

- **1125ºC**

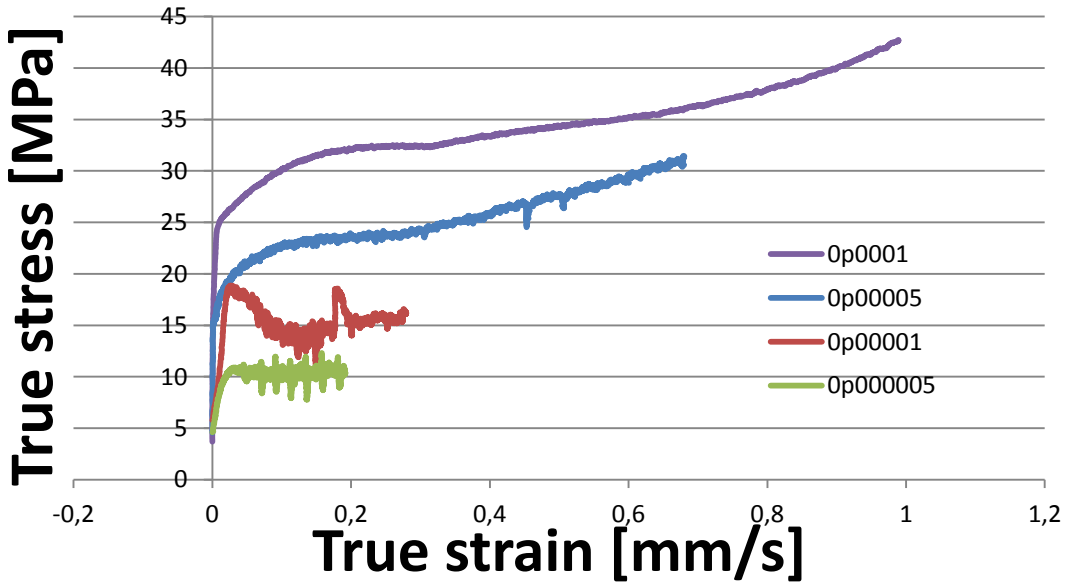

Fig.78: CN-316L-1125ºC

strain rate	0,0001	0,00005	0,00001	0,000005
stress	32	23,5	15	10,9

Fig. 79: 316L-1125ªC-results

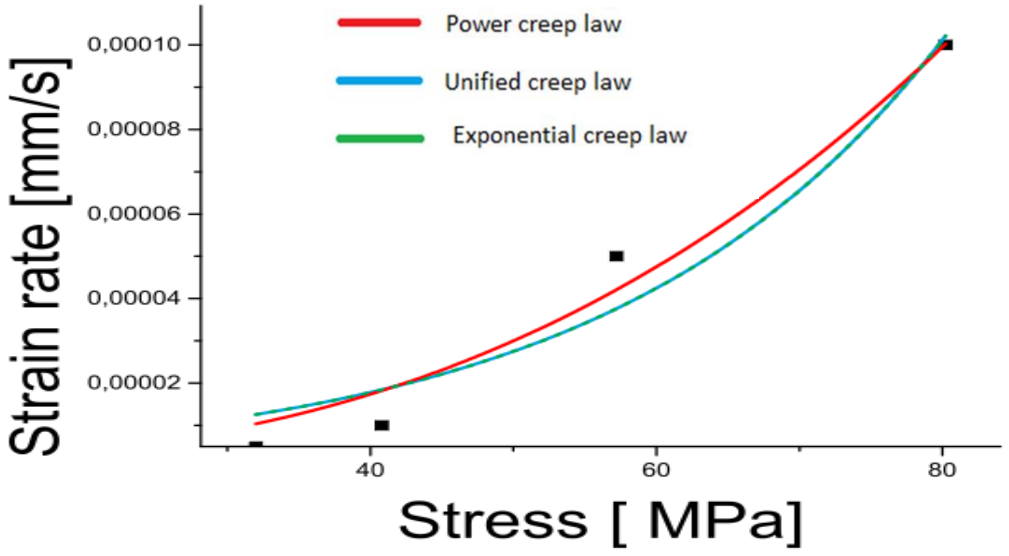

Fig.80: CN-316L-1125ºC Fitting

	Power law		Unified law		Exponenital law	
	Value	error	Value	error	Value	error
A	1,40E-08	1,22E-08	1,20E-02	2,00729	3,33E-06	1,95E-06
n	2,56416	0,25642	2,55073	1,67256	0,10696	0,0192
k			0,00479	0,30596		

Fig.81: CN-316L-1125ºC Parameters

An overview of all the experiments is shown below:

-304

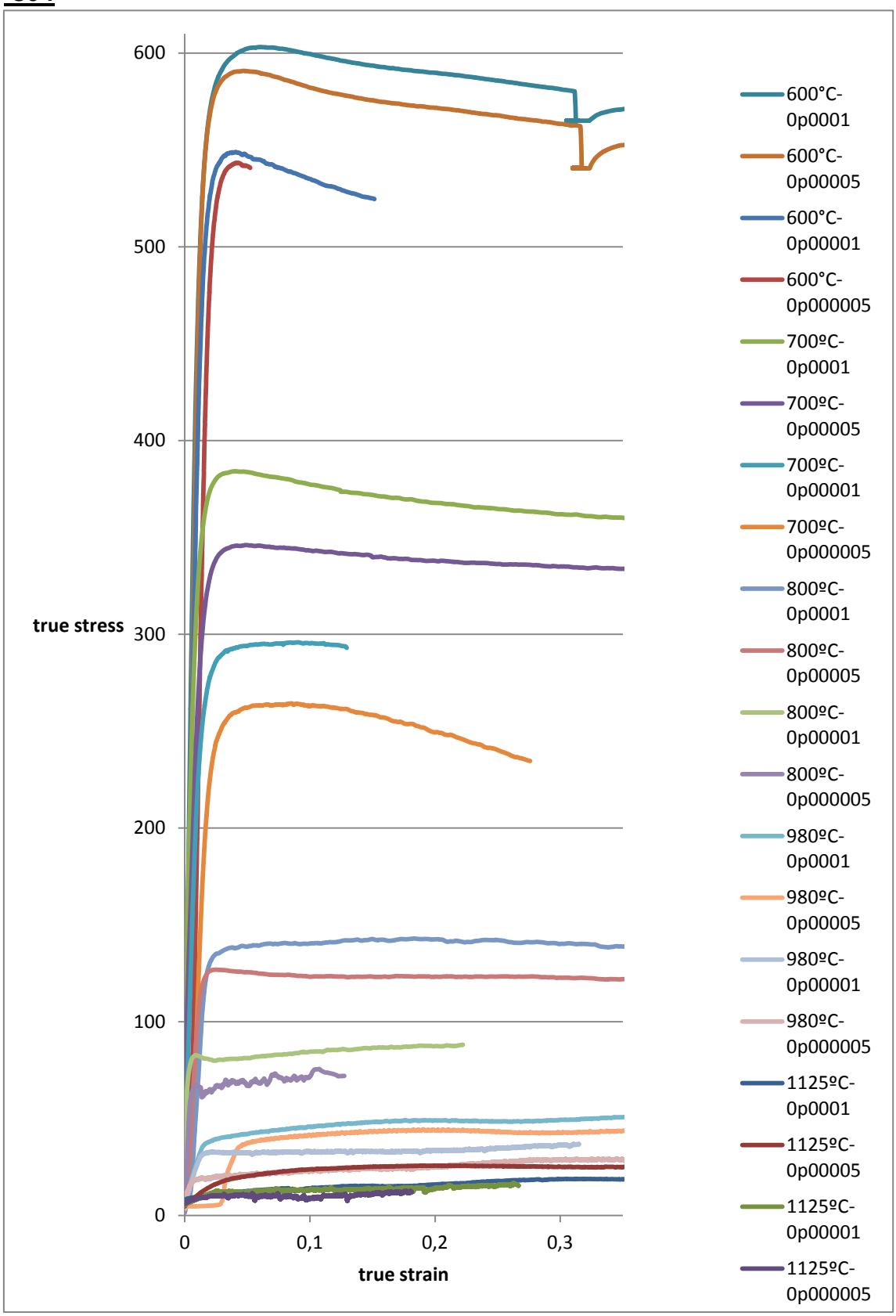
600
500
400
300
200
100
0
true stress
0
0,1
0,2
0,3
true strain
600°C-0p0001
600°C-0p00005
600°C-0p00001
600°C-0p000005
700ºC-0p0001
700ºC-0p00005
700ºC-0p00001
700ºC-0p000005
800ºC-0p0001
800ºC-0p00005
800ºC-0p00001
800ºC-0p000005
980ºC-0p0001
980ºC-0p00005
980ºC-0p00001
980ºC-0p000005
1125ºC-0p0001
1125ºC-0p00005
1125ºC-0p00001
1125ºC-0p000005

Fig.82: 304 Overview.

-316L

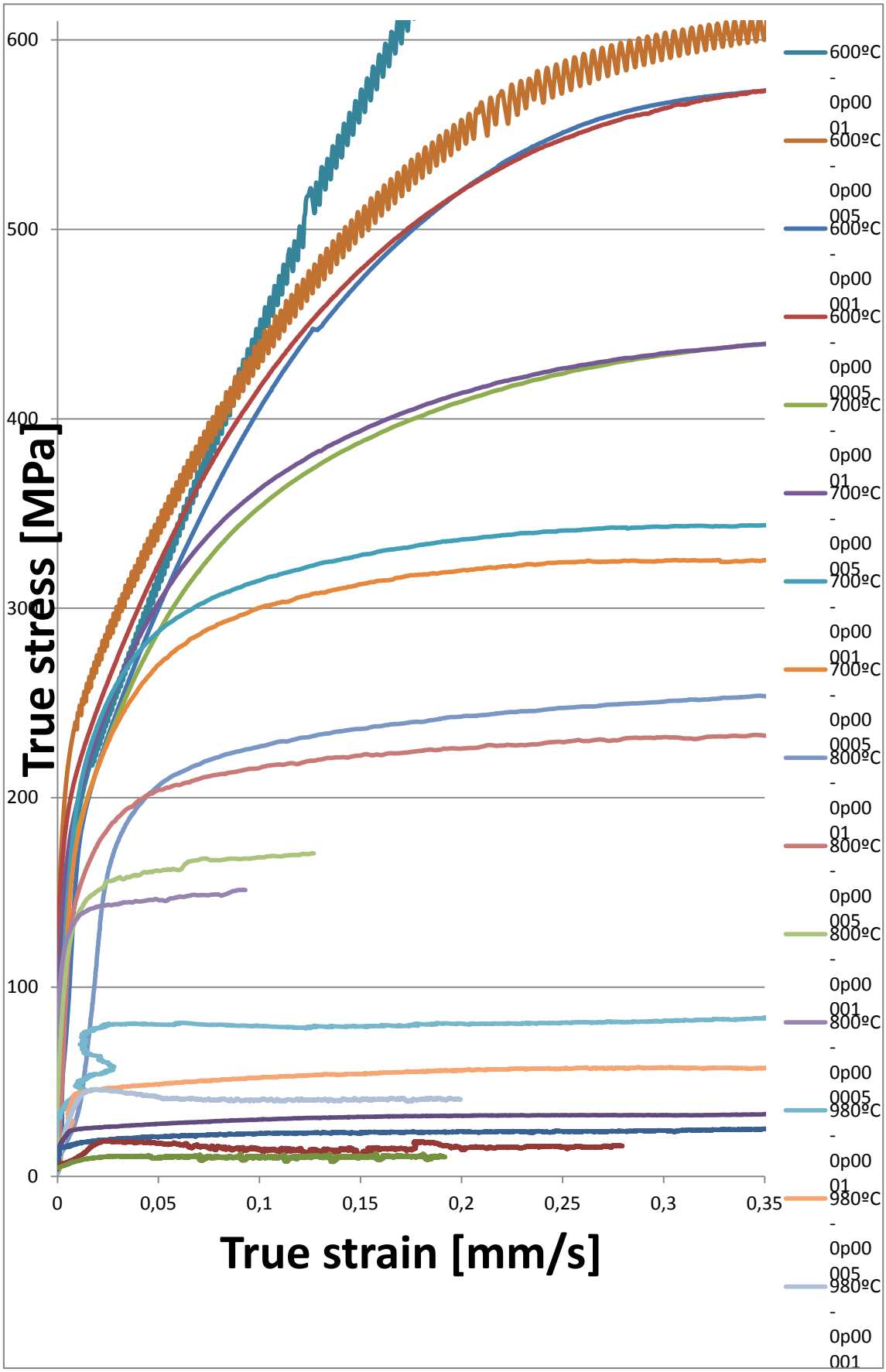

Fig.83: 316L Overview

From previous diagrams some considerations can be observed

- At lower temperatures (600ºC - 700ºC), primary creep is the dominant mechanism, where there is a high stress increment for a low strain, and the constant stress area is too small or it does not exists.
- At medium temperature (800ºC), there is an equilibrium between primary and secondary creep.
- At higher temperatures (980ºC – 1125ºC), the primary creep process is to short, and the dominant mechanism is secondary creep, with a long constant stress area in the graph.

A resume of the calculated parameters are presented:

- 304
    - Power law creeep

Temperature [°C]	A	n
600	7,02E-79	26,6705
700	3,59E-26	8,30869
800	5,41E-16	5,23242
980	7,11E-15	6,00213
1125	3,08E-08	2,27713

Fig.84: 304 Power law creep parameters

    - Unified creeep law

Temperature [°C]	A	n	k
600	2,45E-16	0,21352	0,20874
700	3,53E-15	4,61847	0,00979
800	3,22E-07	0,22005	0,18839
980	1,61E-07	0,32611	0,41636
1125	2,20E-03	2,22	0,00704

Fig.85: 304 Unified creep law parameters

    - Exponential creep law

Temperature [°C]	A	n
600	1,22E-16	0,04548
700	1,22E-16	0,04548
800	2,76E-07	0,04145
980	1,29E-07	0,13577
1125	1,77E-06	0,12994

Fig.86: 304 Exponential creep law parameters

- 316L
    - Power law creeep

Temperature [°C]	A	n
600	1,24E-56	18,43904
700	4,40E-43	14,46769
800	5,81E-22	7,18427
980	9,72E-10	2,63634
1125	1,40E-08	2,56416

Fig.87: 316L Power law creep parameters

- Unified creeep law

Temperature [°C]	A	n	k
600	2,39E-11	0,15428	0,15211
700	6,50E-12	0,19533	0,19095
800	4,22E-08	0,18243	0,17292
980	3,65E-06	0,21996	0,19747
1125	1,20E-02	2,55073	0,00479

Fig.88: 316L Unified creep law parameters

- Exponential creep law

Temperature [°C]	A	n
600	2,14E-11	0,02348
700	5,69E-12	0,03729
800	4,22E-08	0,18243
980	3,13E-06	0,04344
1125	3,33E-06	0,10696

Fig.89: Exponential creep law parameters

Given the graphical approach and the relationship between the values and their errors is considered that, for most cases, the model that best adjusts the behavior of secondary creep to such materials is the **Power creep law.**

Theoretical results, for some temperatures for 316L stainless steel, collecting from some authors [21] [22] [23] are compared with the obtained in this thesis for power creep law analysis:

T(ºC)	A		
	Paper [21]	Paper [23]	Thesis
600	8,13E-21	5E-21	1,24E-56
700	8,22E-14	3,87E-18	4,40E-43
800		7,47E-18	5,81E-22
980		1,87E-17	9,72E-10

1125	4,98E10-7	5E-7	1,40E-08

Fig.90: Parameters comparison.

T(ºC)	n			
	Paper [21]	Paper [22]	Paper [23]	Thesis
600	8,20		8	18,43904
700	5,30		2,7	14,46769
800		5	2,18	7,18427
980			1,53	2,63634
1125	2,02	2	2	2,56416

In the case of A value the differences in the values correspond to, as explained the chapter 3.1 of this thesis, theoretical value correspond to A*, and in case of thesis values correspond to A. Relation is showed in equation 3.6. The calculated of A* values is planned for further works.

Values corresponding to n variable, can be seen that for low temperatures theoretical and values calculated in the thesis have a bigger difference for lower temperatures than for higher. This is because the linear stress region is more clear for higher temperature, and the chosen values for make regressions are more reliable.

Taking account all these considerations can be considered that the experiments carried out in this thesis have a good resolution.

6.1.3. Porous material.

In this chapter two different relative densities for stainless steel 316L have been analyzed. These relative densities are 93% and 67%. Results are presented ordered by its temperature and comparing different materials at same temperature.

- **600ºC**
  - **93%**

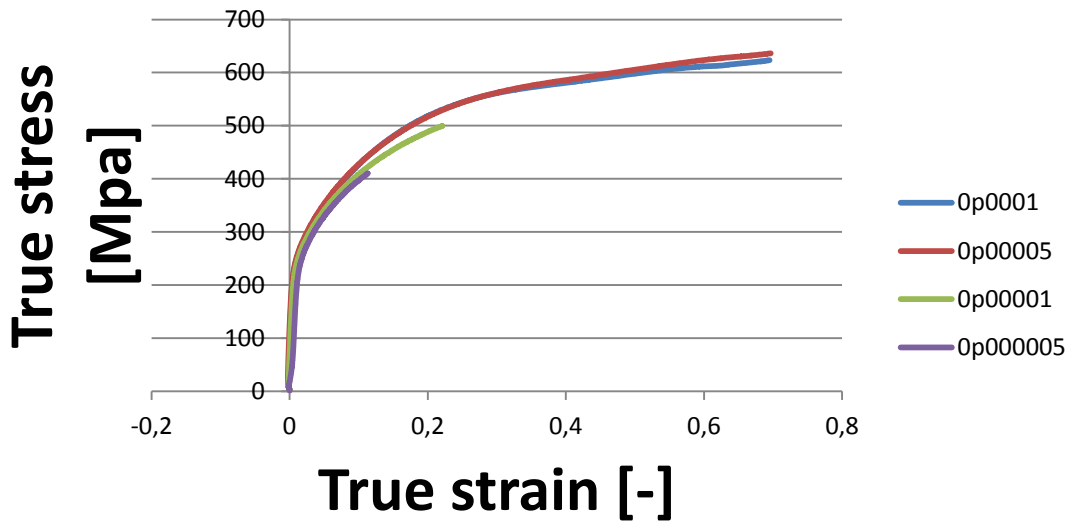

Fig.89: CN-316L-RD93-600ºC

These experiments could not reach the constant stress, so a fitting approximation was made for take this constant stress value.

strain rate	0,0001	0,00005	0,00001	0,000005
stress	685	650	550	485

Fig. 90: 316L-RD93-600ªC-results

❖ **67%**

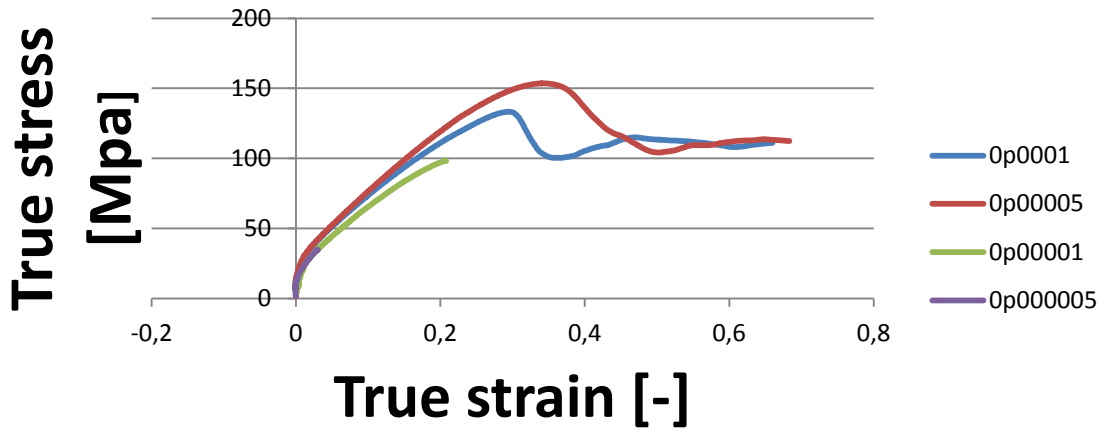

Fig.91: CN-316L-RD67-600ºC

For lower speeds the constant stress values were not reached, so a fitting approximation was made to obtain these stress values. In case of higher speeds there is an irregularity state before the secondary stage. For calculations the constant stress values was taken into account.

strain rate	0,0001	0,00005	0,00001	0,000005
stress	115	109	98	88

Fig. 92: 304-RD67-600ªC-results

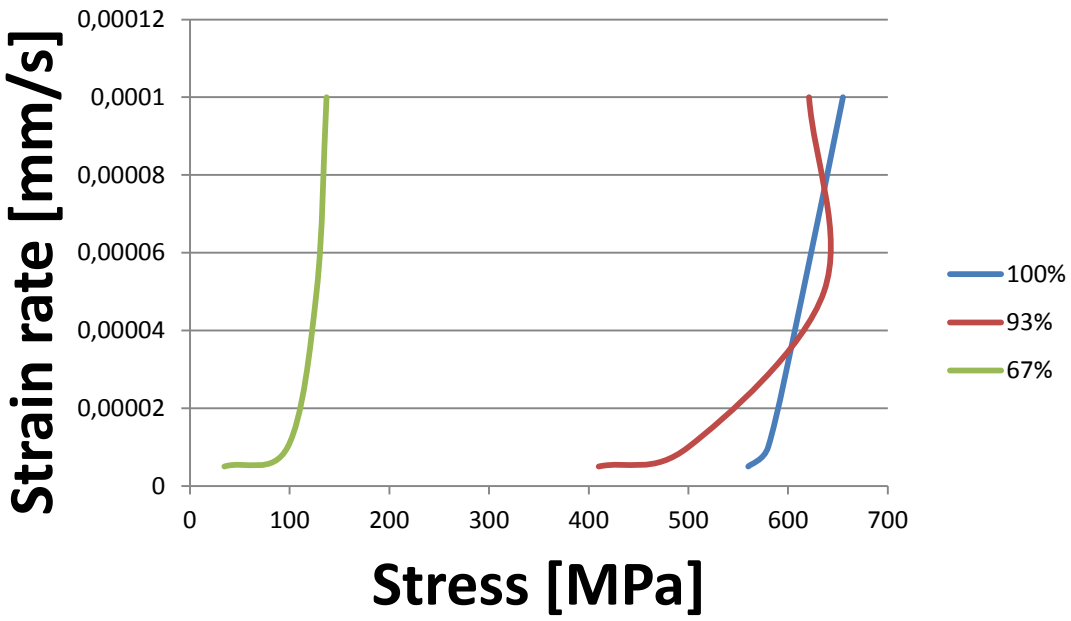

In this case a strange value was obtained for 93% relative density and 0,00005 mm/s strain rate. This value was no taken into account. Ignoring this value, the curves relation is enough good to analyze the desired parameters.

Fig. 93: 316L-600ªC-relative densities

As has been explained in chapter 5.3, messuring the difference between intercepts of three curves ($s(\rho)$) and using eq 5.8, the c and f parameters can be calculated. Having the HIP results, where f values are obtained, c values can be calculated from the followings relations.

$$c(\rho) = s(\rho)^{-2n/n+1} - f(\rho) \quad (5.8)$$

c + f (93%, 600ºC)= 2,71E+52

c + f (67%, 600ºC)= 2,26E+83

- **800ºC**
  - **93%**

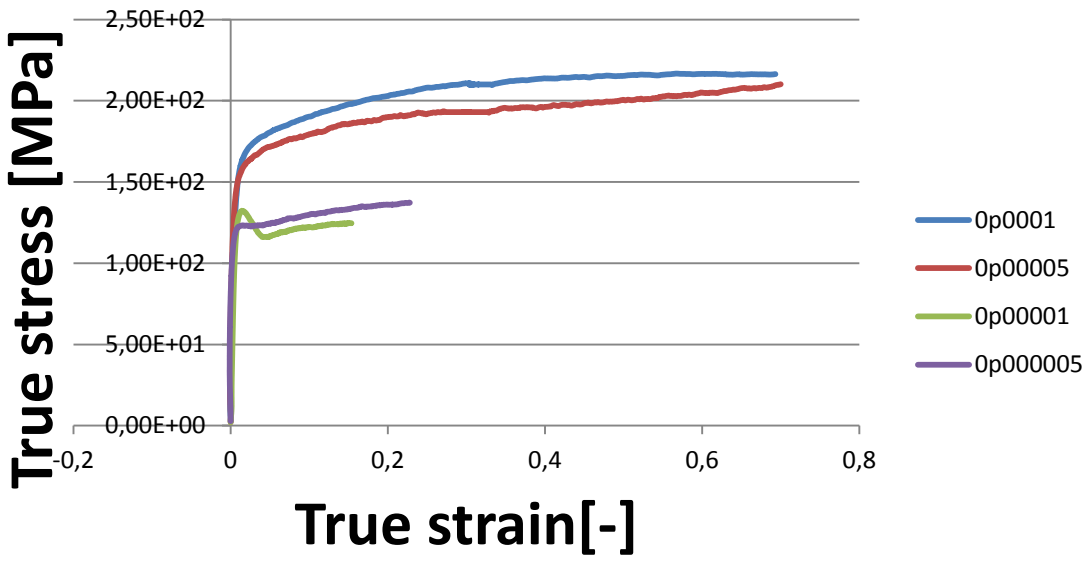

Fig.94: CN-316L-RD93-800ºC

strain rate	0,0001	0,00005	0,00001	0,000005
stress	210	193	132	123

Fig. 95: 304-RD93-800ªC-results

❖ **67%**

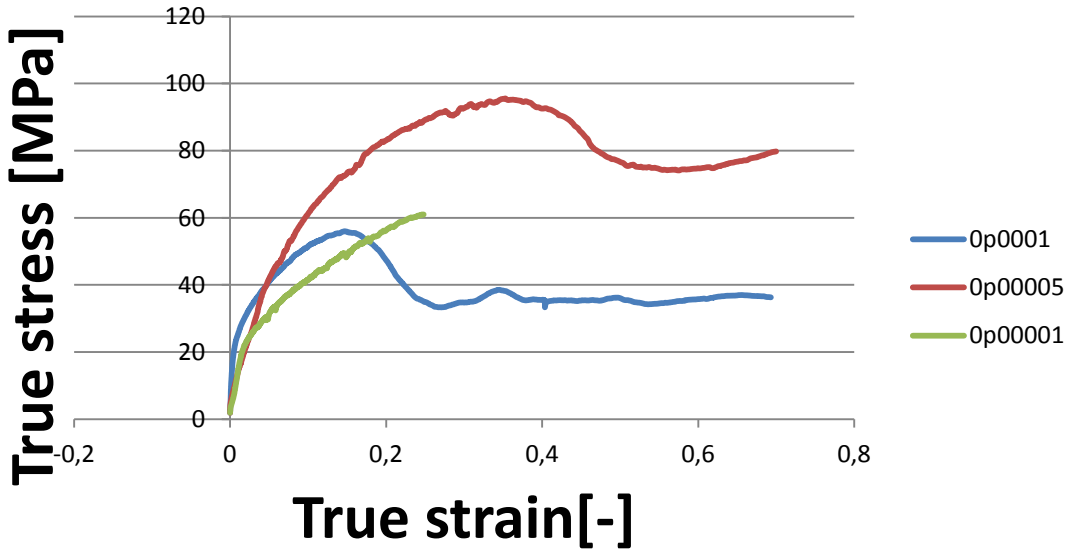

Fig.96: CN-316L-RD67-800ºC

For lower speed the constant stress value was not reached, so a fitting approximation was made to obtain these stress values. In case of higher speeds there is an irregularity state before the secondary stage. For calculations the constant stress values was taken into account.

strain rate	0,0001	0,00005	0,00001	0,000005

stress	43,3	84,4	60,9	

Fig. 97: 316L-RD67-800ªC-results

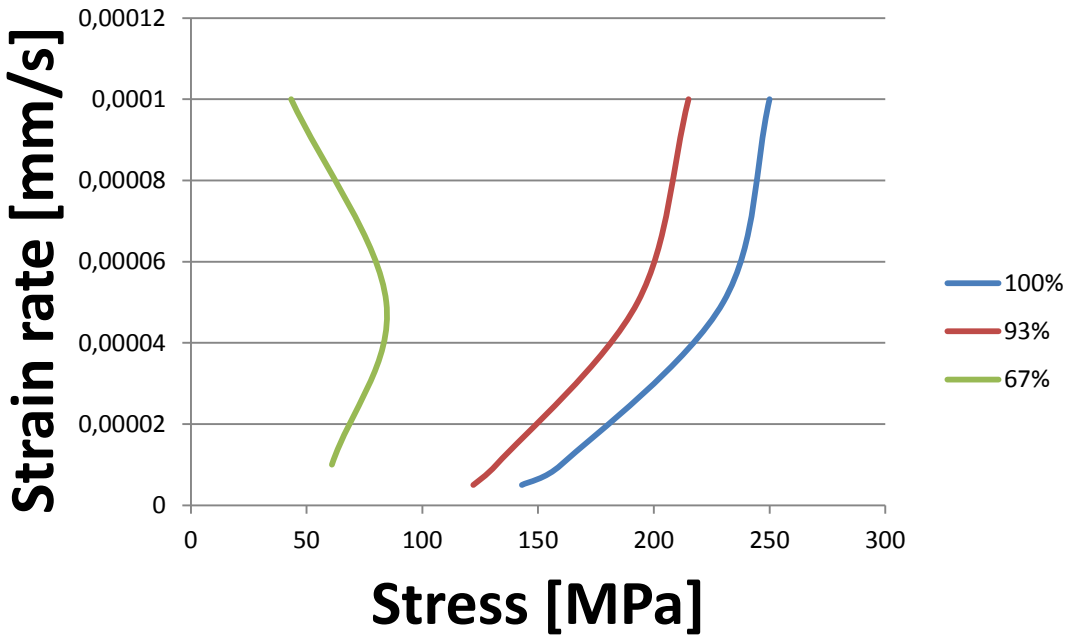

Fig. 98: 316L-800ªC-relative densities

In this case a strange value was obtained for 67% relative density and 0,0001 mm/s strain rate. This value was no taken into account. Ignoring this value, the curves relation is enough good to analyze the desired parameters.

c + f (93%, 800ºC)= 1,677051859

c + f (67%, 800ºC)= 7,214846399

- **980ºC**
  - **93%**

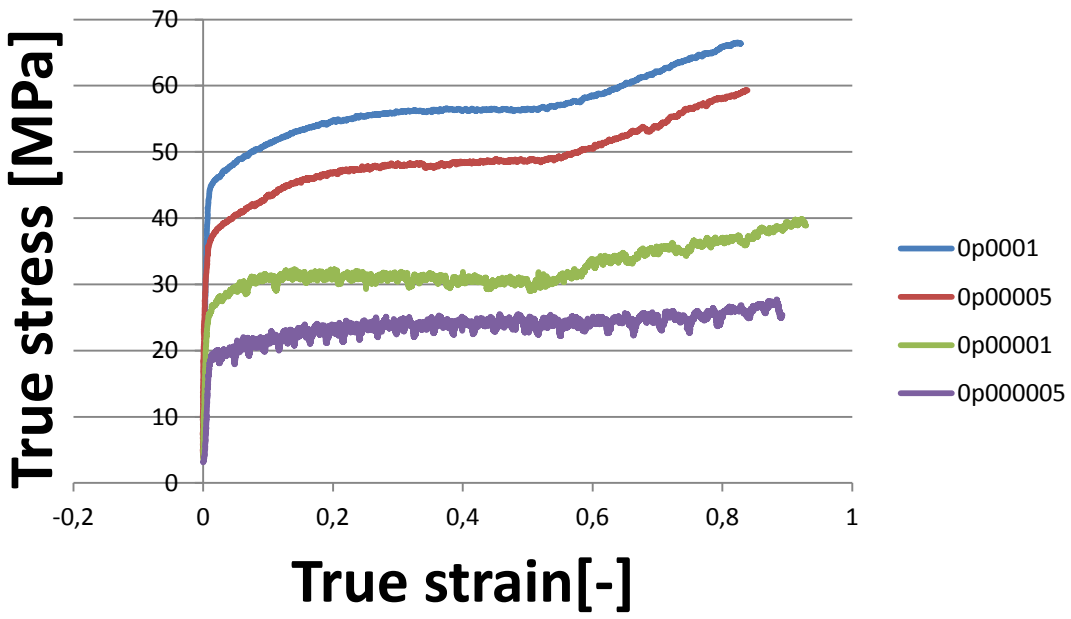

Fig.99: CN-316L-RD93-980ºC

strain rate	0,0001	0,00005	0,00001	0,000005
stress	56,46	48,5	31,8	25

Fig. 100: 316L-RD93-980ªC-results

❖ **67%**

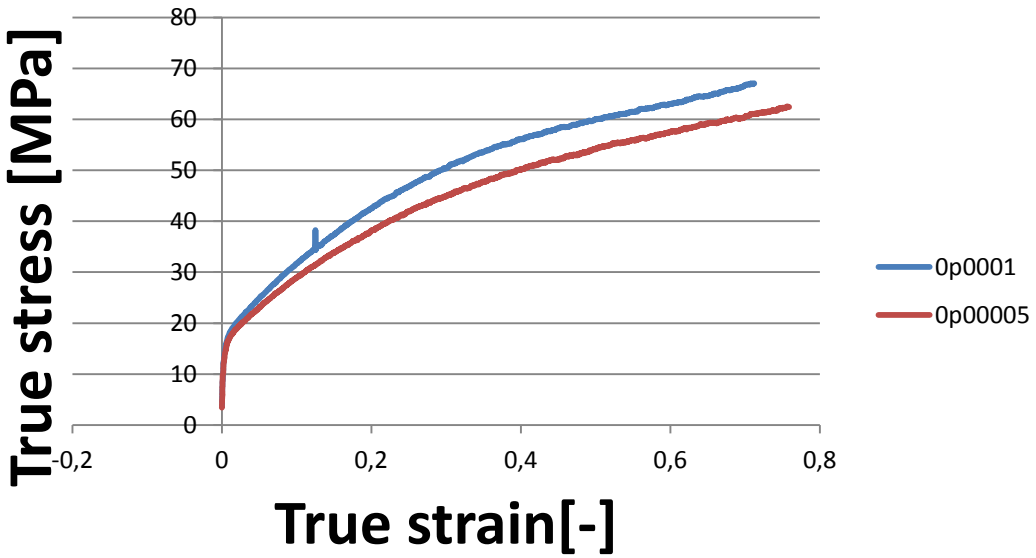

Fig. 101: 316L-RD93-980ªC-results

For these experiments the constant stress value was not reached, so a fitting approximation was made to obtain these stress values. As no satisfactory

results of these experiments were obtained, it was decided to perform the analysis without taking into account this relative density.

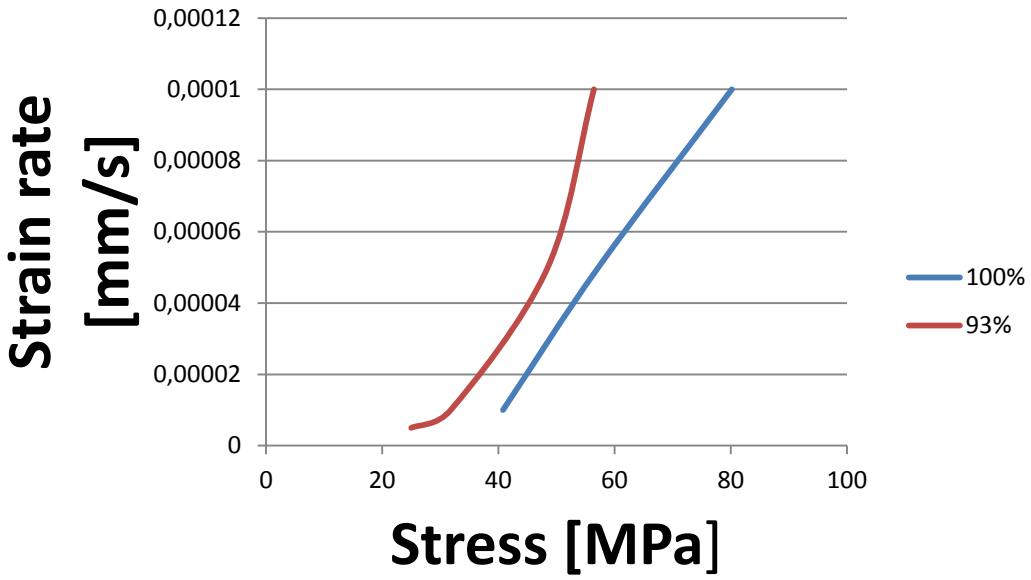

Fig. 102: 316L-980ªC-relative densities

- **1125ºC**
  - **93%**

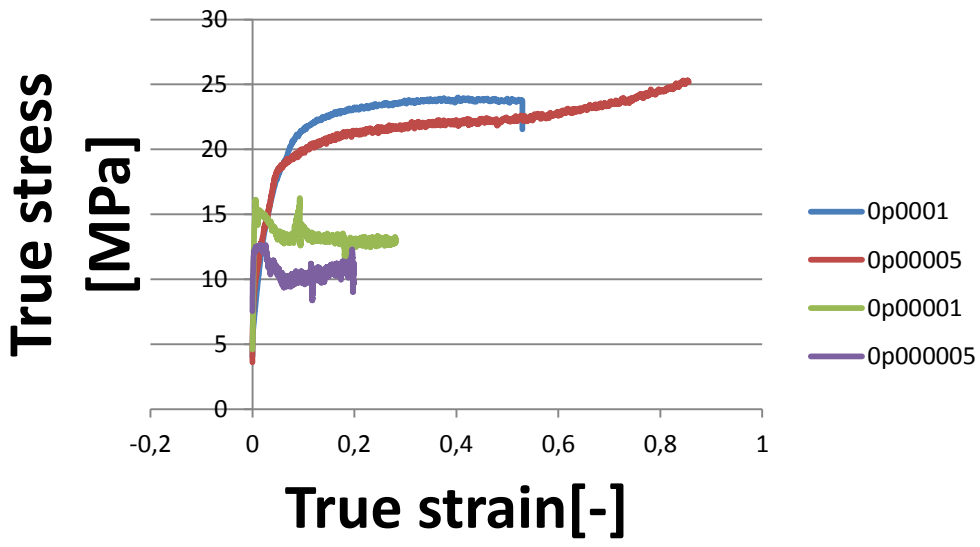

Fig.103: CN-316L-RD93-1125ºC

strain rate	0,0001	0,00005	0,00001	0,000005
stress	23	21	13	9

Fig. 104: 316L-RD93-1125ªC-results

- **67%**

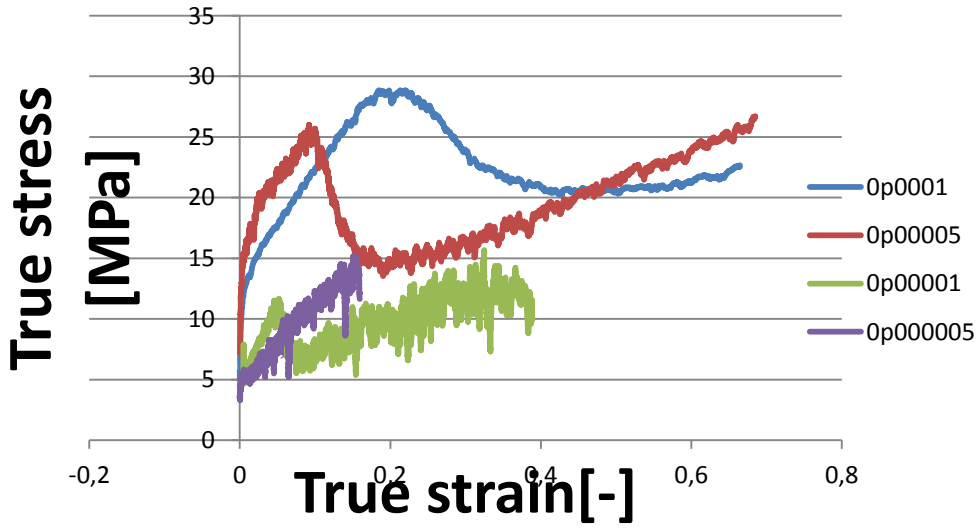

Fig. 105: 316L-RD67-1125ªC

For higher speeds there is an irregularity state before the secondary stage. For calculations the constant stress values was taken into account. In case of lower speeds the constant stress region stage is to short.

strain rate	0,0001	0,00005	0,00001	0,000005
stress	24,3	19,9	8,3	5,1

Fig. 106: 316L-RD67-1125ªC-results

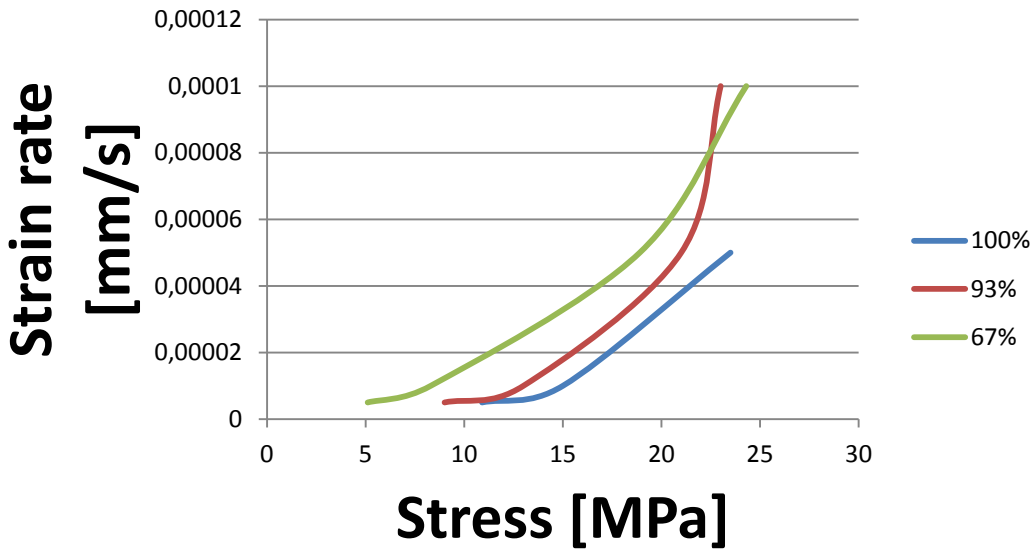

Fig. 107: 316L-1125ªC-relative densities

c + f (93%, 1125ºC) = 1,198492

c + f (67%, 1125ºC) = 9,181706

An overview of all experiments for porous materials is presented:

-93%

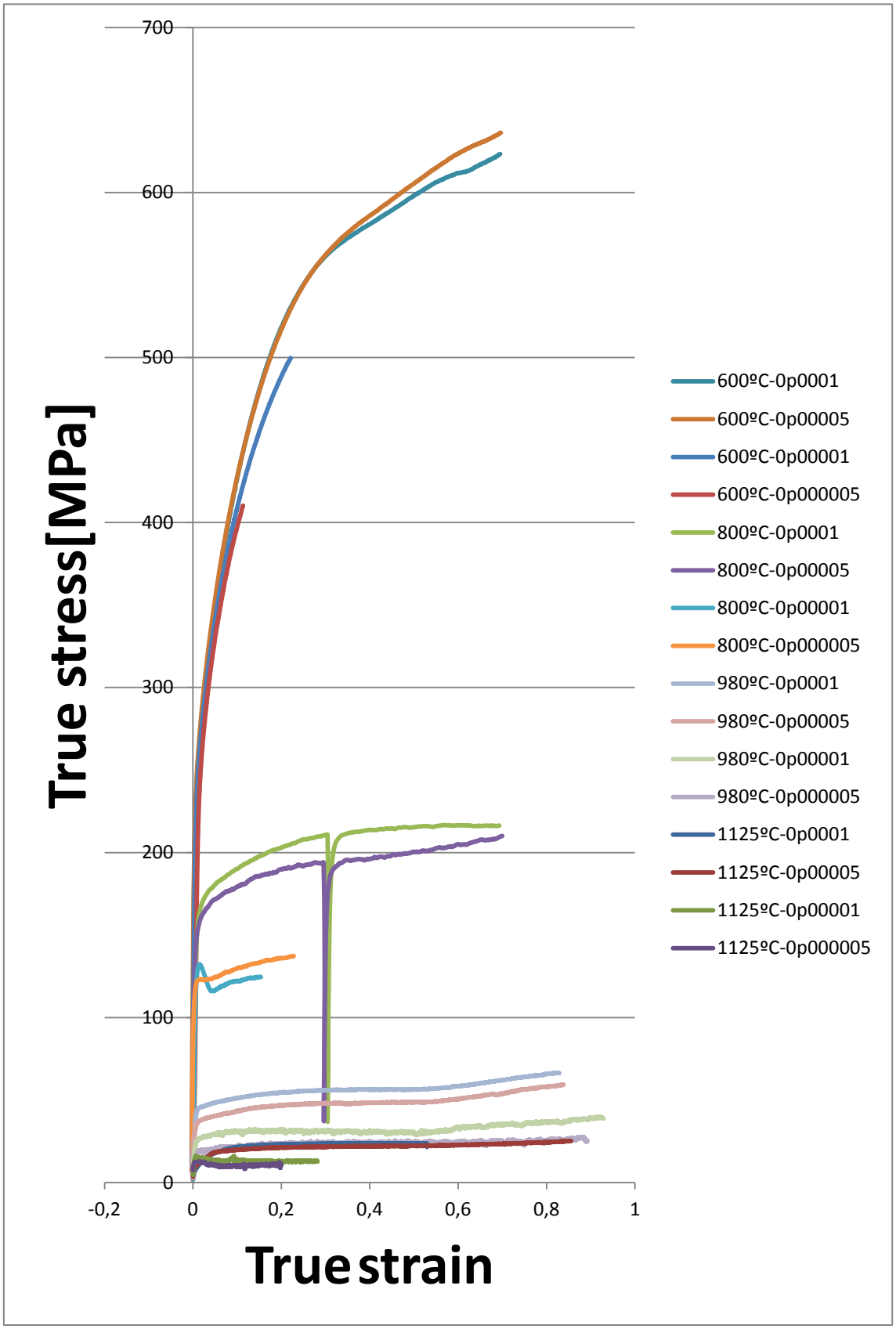

Fig. 108: 316L-93% relative density

-67%

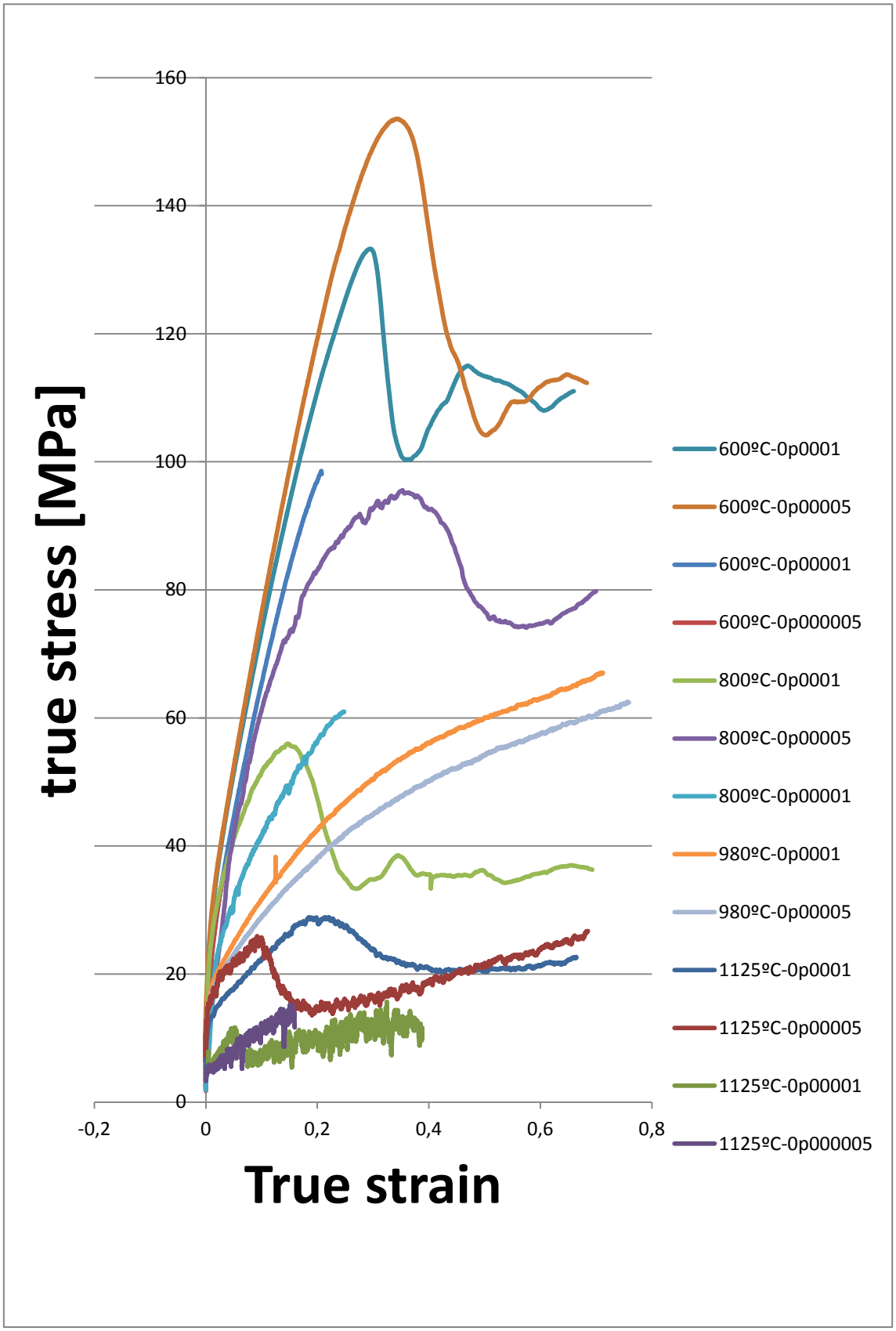

Fig. 109: 316L-67% relative density

6.2. Primary creep.

For the primary creep analysis, in each experiment, (constant temperature and deformation speed) different parameters values are calculated. Besides the parameters calculated in the secondary creep, which are necessary for primary creep analysis.

In each experiment, from data obtained in the tests, there is a collection of values for variables stress, time, strain rate and deformation. There will be two models (Strain hardening and Modified strain hardening approaches) that use the variables stress, strain rate and strain. And the other model (Time hardening) will use the variable time, stress and strain rate.

The way to present the results of the primary creep in this thesis is as follows:

- A graph of stress vs. strain rate at which the three approaches will be represented.

- Another graph of strain vs. strain rate, which is represented only equations with depends of the deformation variable.

- Finally a table of parameter values on the three approaches is presented.

The same as in secondary creep analysis, in this section each approach is represented by one color:

- Time hardening law as shown in equation (3.7), chapter 3.1 is represented in red

- Strain hardening law as shown in equation (3.8), chapter 3.1 is represented in blue.

- Modified strain hardening law as shown in equation (3.9), chapter 3.1 is represented in green.

5.2.1. 304 stainless steel

- **600ºC**
  - **0p0001**

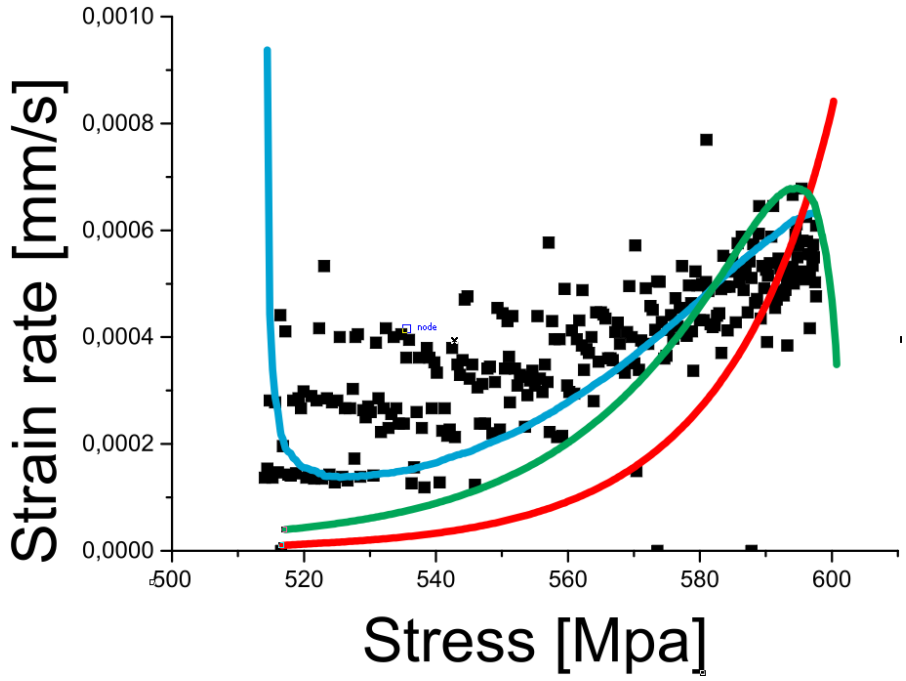

Fig. 108: 304-600º-0p0001-Fitting I

In experiments are collected instantaneous data on stress and strain rate and, using software OringinPro 9 adjustment is performed based on the characteristics of the equations discussed above. Stress is measured by the machine, and the strain rate is calculated dividing the difference in length of the sample between the elapsed time since the last couple of measures.

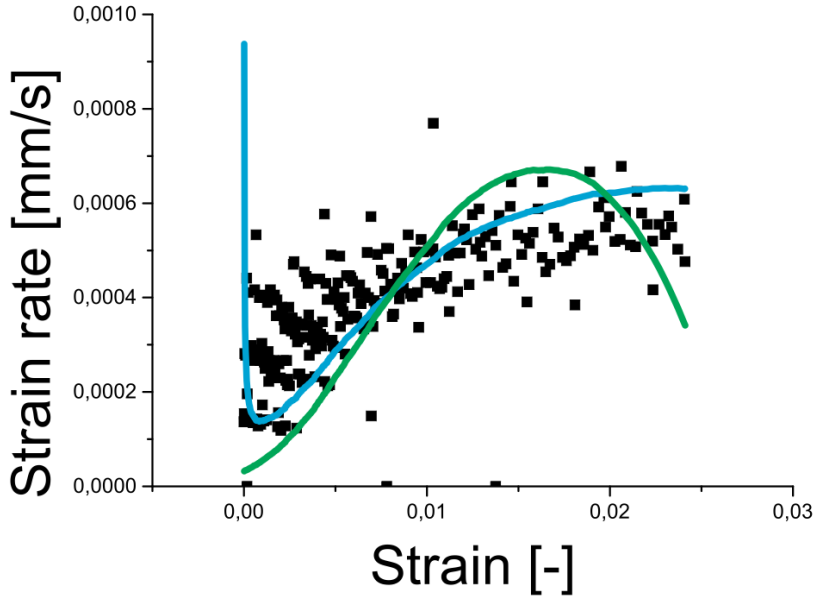

Fig. 109: 304-600º-0p0001-Fitting II

In this case have been collected strain and strain rate values. Strain is calculated as the difference in length of the sample, and in case of strain rate as difference in length of the sample.

	Time hardening		Strain hardening		Modified strain h.	
	Value	error	Value	error	Value	error
m	1,35363	0,01081	-0,55696	0,01023	15,63648	1,03658
k					-104,635	7,01038

Fig. 110: 304-600º-0p0001-parameters

❖ **0p00005**

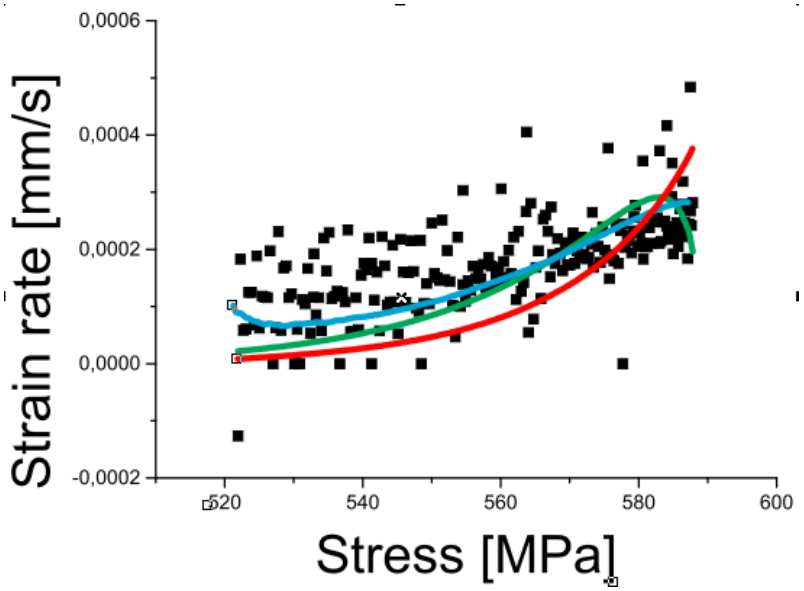

Fig. 111: 304-600º-0p00005-Fitting I

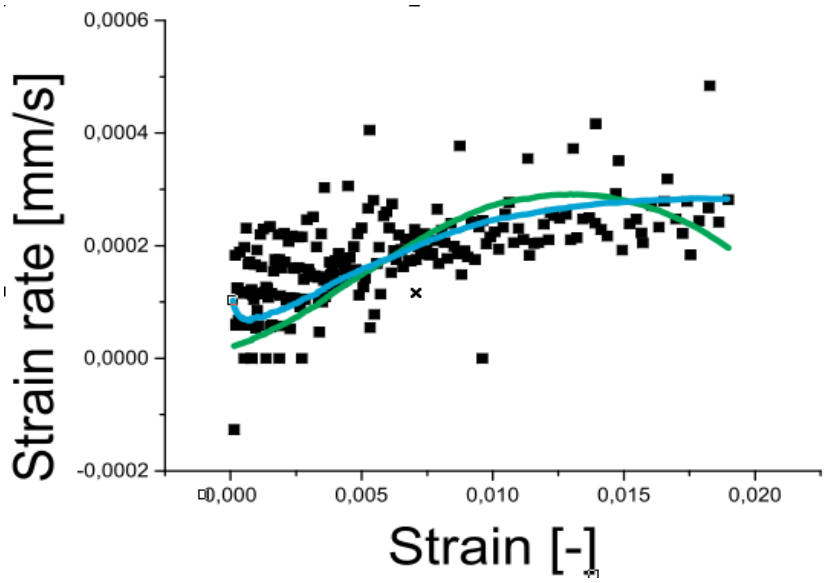

Fig. 112: 304-600º-0p00005-Fitting II

	Time hardening		Strain hardening		Modified strain h.	
	Value	error	Value	error	Value	error
m	1,27423	0,00631	-0,43833	0,00526	9,85843	0,41951
k					-102,784	6,45308

Fig. 113: 304-600º-0p00005-parameters

❖ **0p00001**

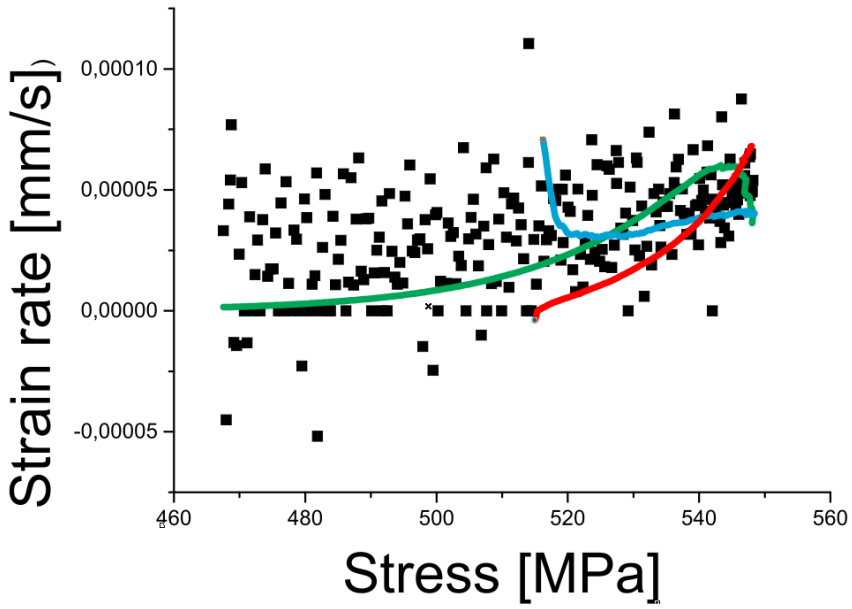

Fig. 114: 304-600º-0p00001-Fitting I

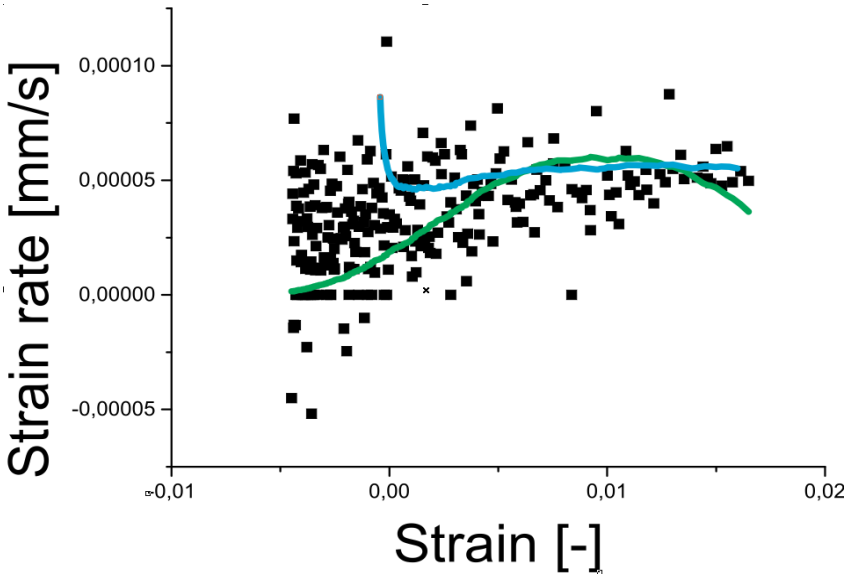

Fig. 115: 304-600º-0p00001-Fitting II

	Time hardening		Strain hardening		Modified strain h.	
	Value	error	Value	error	Value	error
m	1,25457	0,00824	-0,41132	0,01034	11,56117	0,66914
k					-126,8	11,67828

Fig. 116: 304-600º-0p00001-parameters

❖ **0p000005**

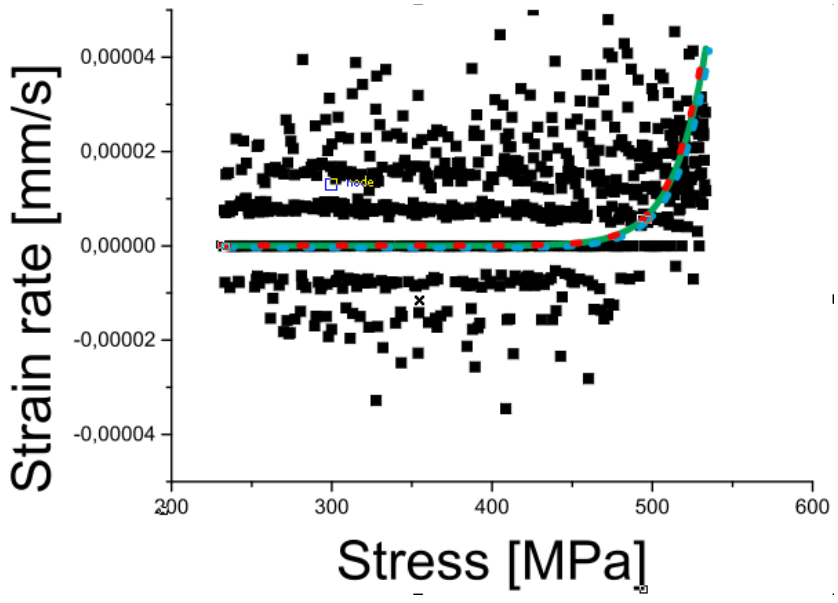

Fig. 117: 304-600º-0p000005-Fitting I

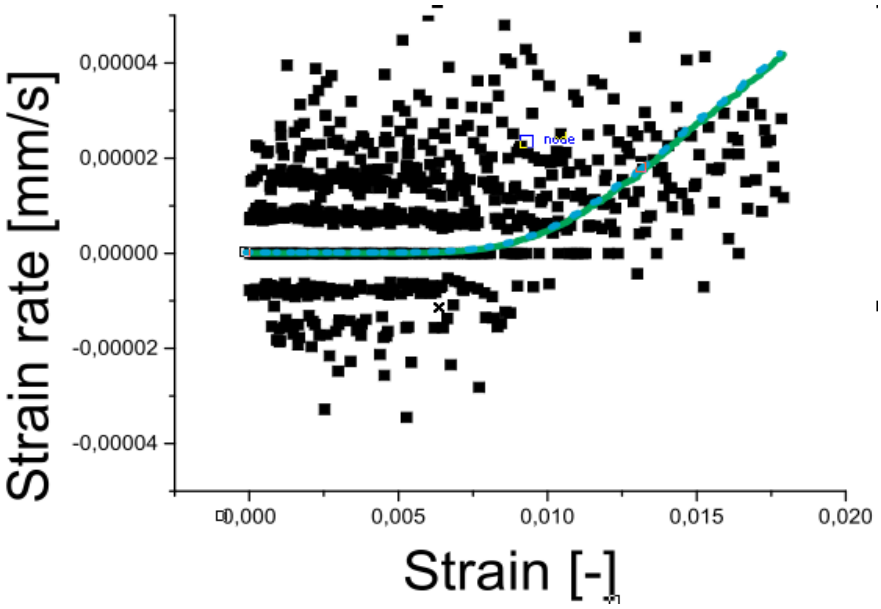

Fig. 118: 304-600º-0p000005-Fitting II

	Time hardening		Strain hardening		Modified strain h.	
	Value	error	Value	error	Value	error
m	1,23207	0,00886	-0,01386	0,0005329	9,80126	0,99215
k					2,1E+14	0,46929

Fig. 119: 304-600º-0p00005-parameters

- **700ºC**
  - **0p0001**

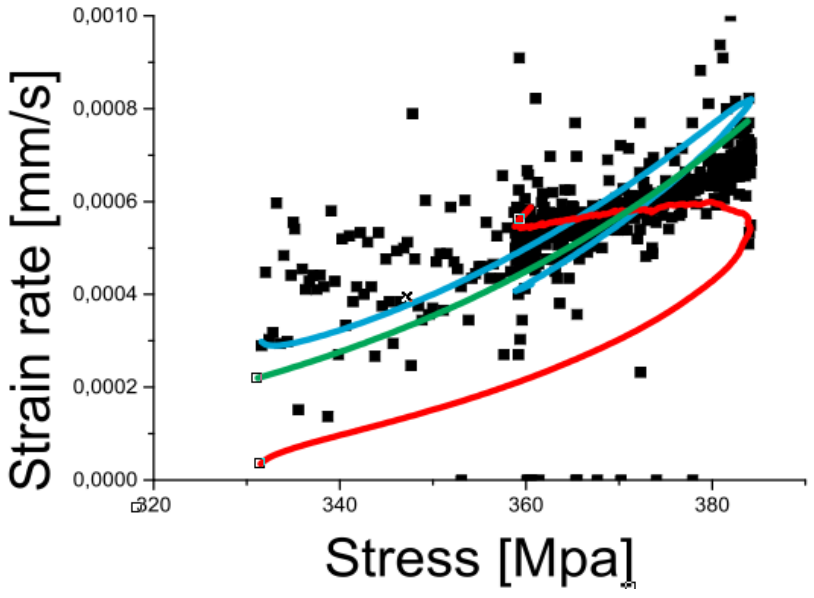

Fig. 120: 304-700º-0p0001-Fitting I

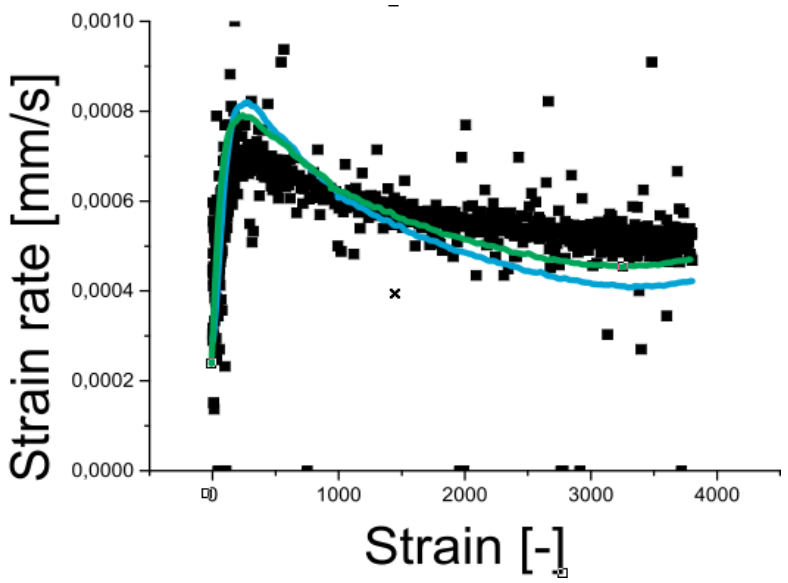

Fig. 121: 304-700º-0p0001-Fitting II

	Time hardening		Strain hardening		Modified strain h.	
	Value	error	Value	error	Value	error
m	1,23278	0,00442	-0,04209	0,0007584	6559,341	227,62839
k					61868100	0,38312

Fig. 122: 304-700º-0p0001-parameters

❖ **0p00005**

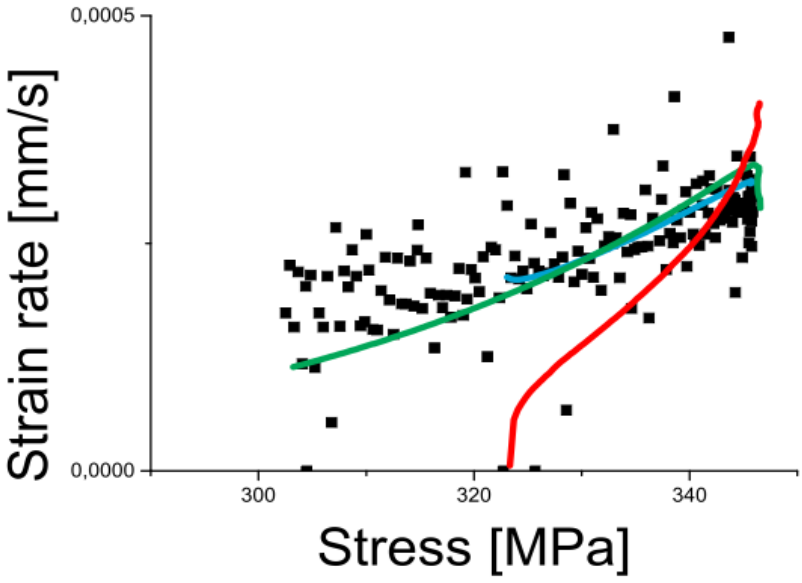

Fig. 123: 304-700º-0p00005-Fitting I

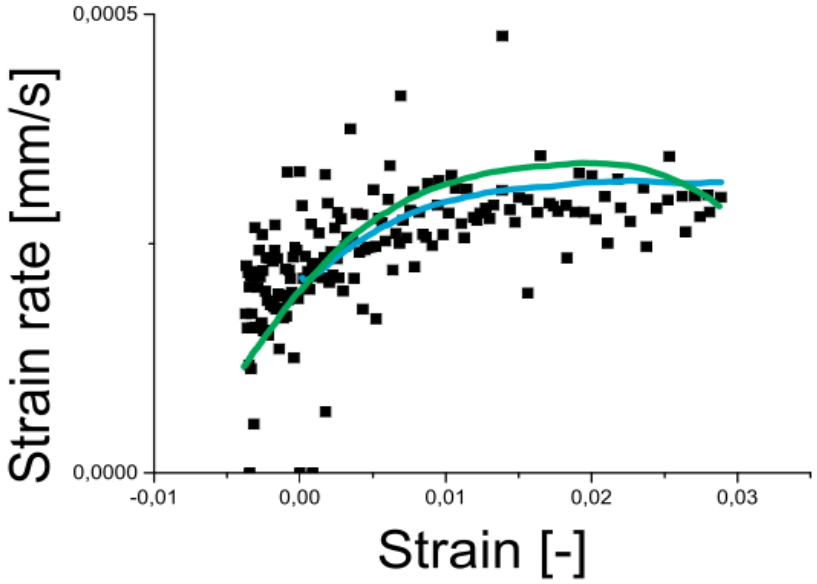

Fig. 124: 304-700º-0p00005-Fitting II

	Time hardening		Strain hardening		Modified strain h.	
	Value	error	Value	error	Value	error
m	1,28588	0,00812	-0,03423	0,000824	-244,694	28,47661
k					6887,437	383,39788

Fig. 125: 304-700º-0p00005-parameters

- **0p00001**

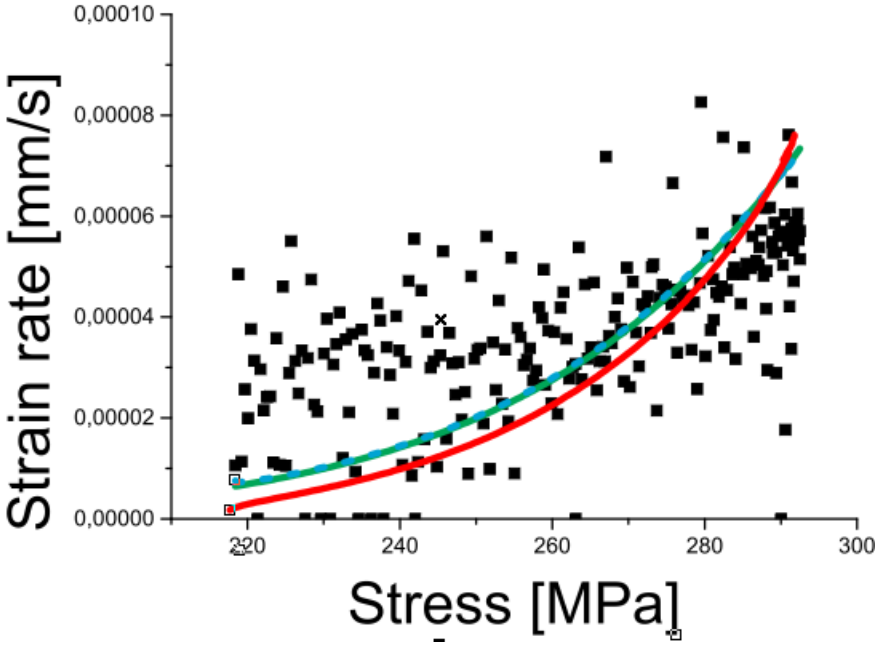

Fig. 126: 304-700º-0p00001-Fitting I

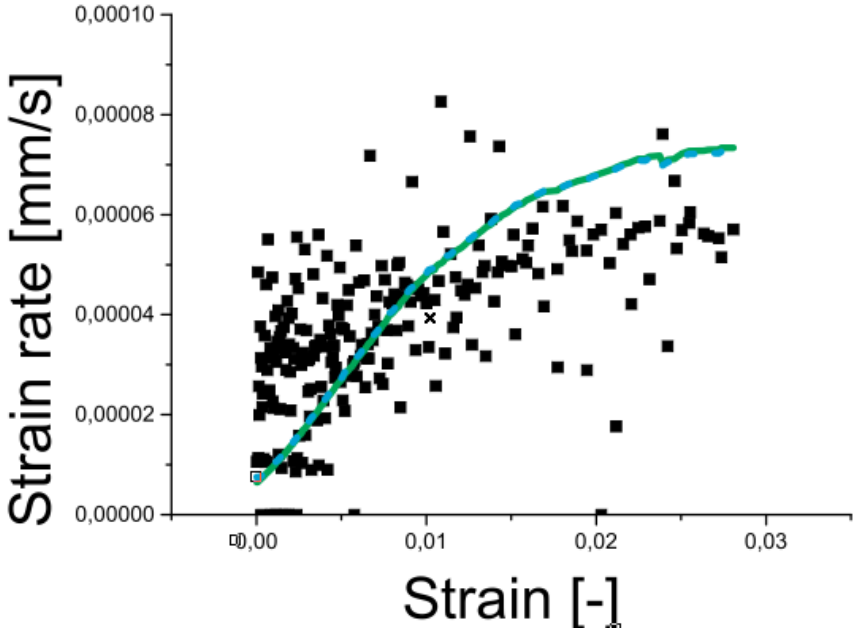

Fig. 127: 304-700º-0p00001-Fitting II

	Time hardening		Strain hardening		Modified strain h.	
	Value	error	Value	error	Value	error
m	1,19843	0,00987	-0,03365	0,00146	5920,356	476,04769
k					1,02E+09	2034,0743

Fig. 128: 304-700º-0p00001-parameters

❖ **0p000005**

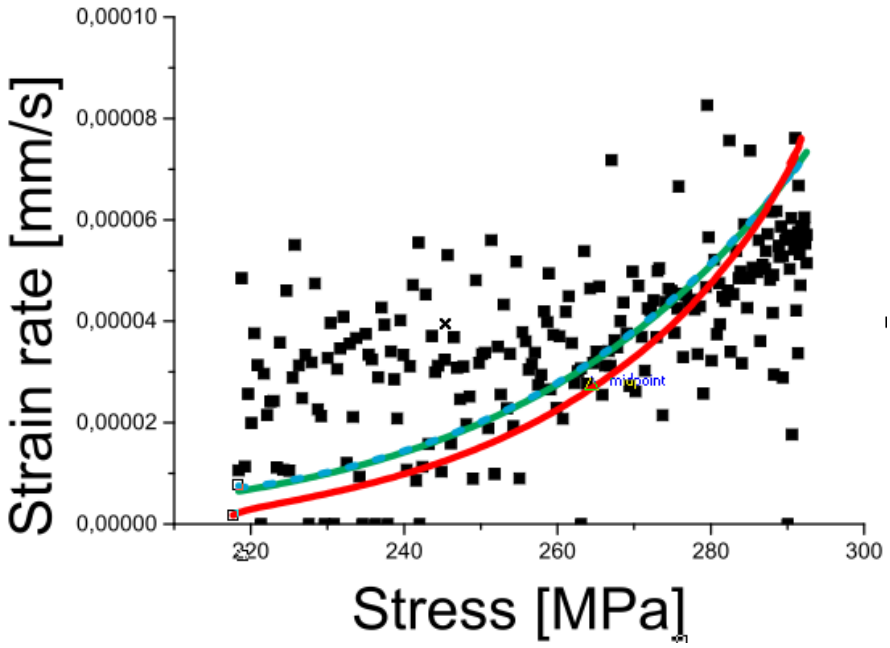

Fig. 129: 304-700º-0p000005-Fitting I

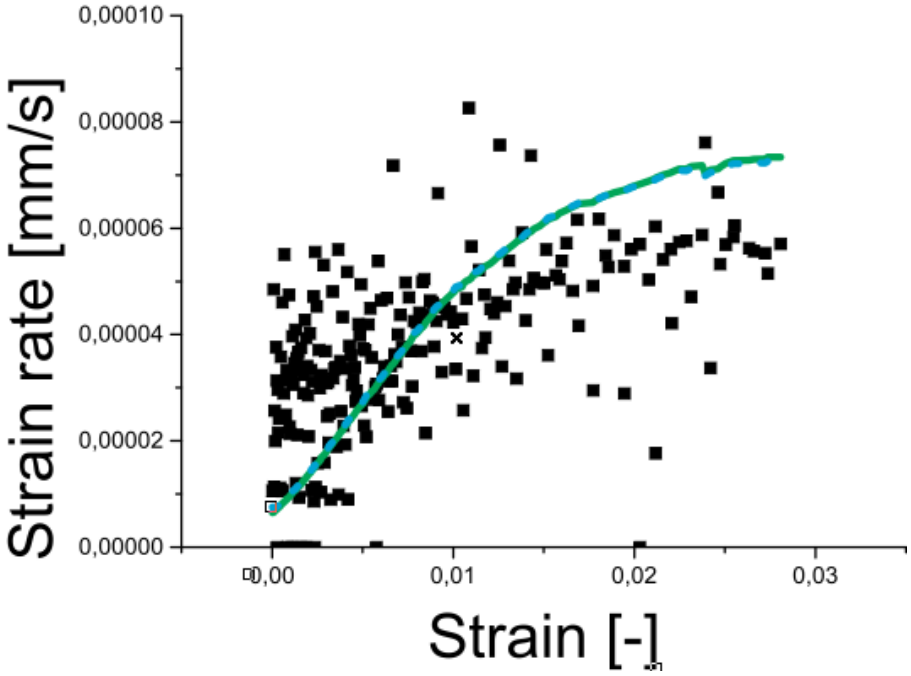

Fig. 130: 304-700º-0p000005-Fitting II

	Time hardening		Strain hardening		Modified strain h.	
	Value	error	Value	error	Value	error
m	1,20055	0,00654	-0,03708	0,00101	6887,437	383,39788
k					1,62E+11	267,90085

Fig. 131: 304-700º-0p000005-parameters

- **800ºC**
  - **0p0001**

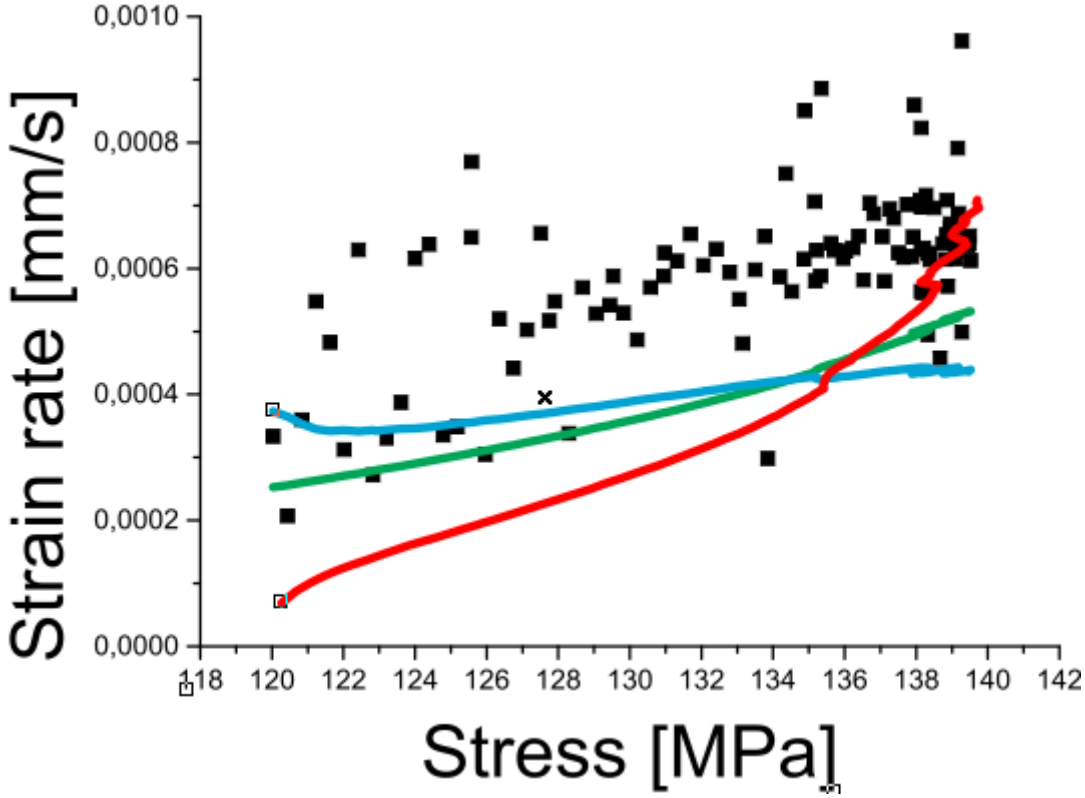

Fig. 132: 304-800º-0p0001-Fitting I

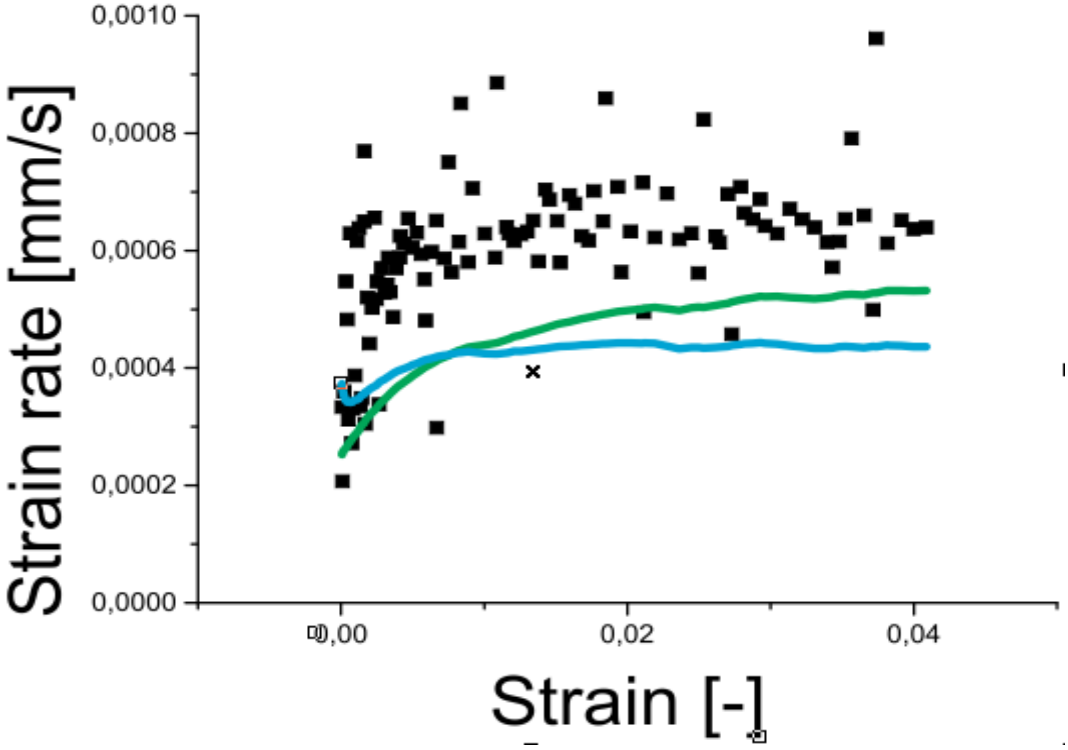

Fig. 133: 304-800º-0p0001-Fitting II

	Time hardening		Strain hardening		Modified strain h.	
	Value	error	Value	error	Value	error
m	1,313	0,06581	-0,06912	0,01626	5,46649	7,888
k					70,59815	2034,0743

Fig. 134: 304-800º-0p0001-parameters

❖ **0p00005**

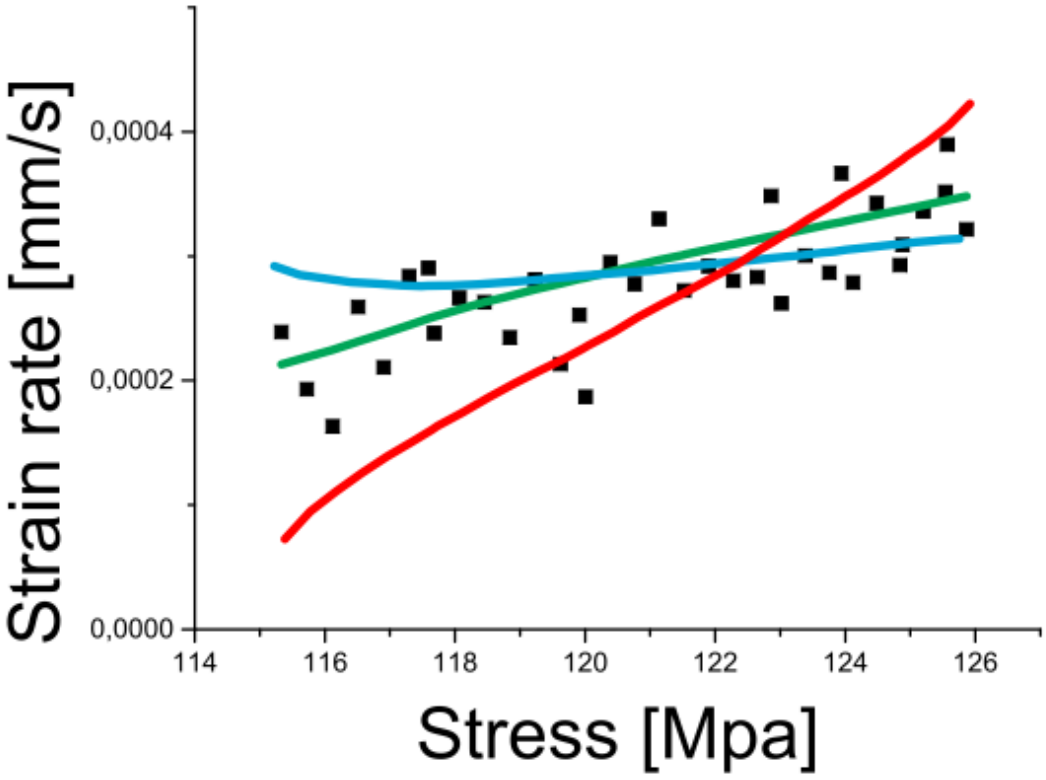

Fig. 135: 304-800º-0p00005-Fitting I

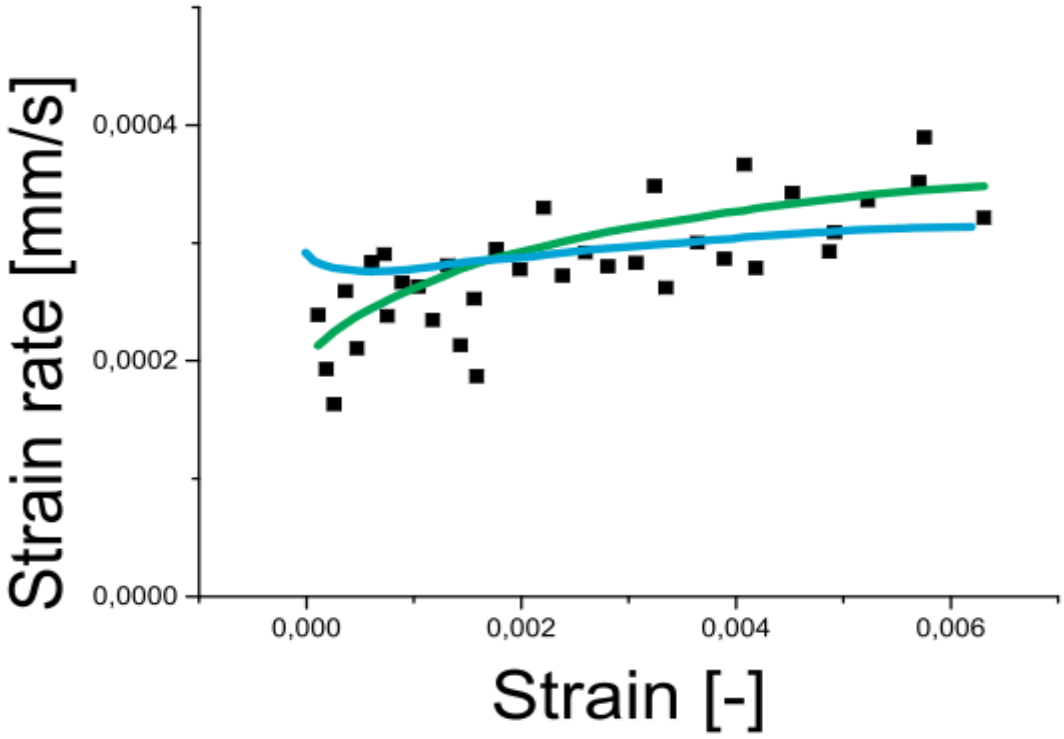

Fig. 136: 304-800º-0p00005-Fitting II

	Time hardening		Strain hardening		Modified strain h.	
	Value	error	Value	error	Value	error
m	1,35522	0,01199	-0,06715	0,00168	5,26733	0,41424
k					1266,411	2721,1355

Fig. 137: 304-800º-0p00005-parameters

- **0p00001**

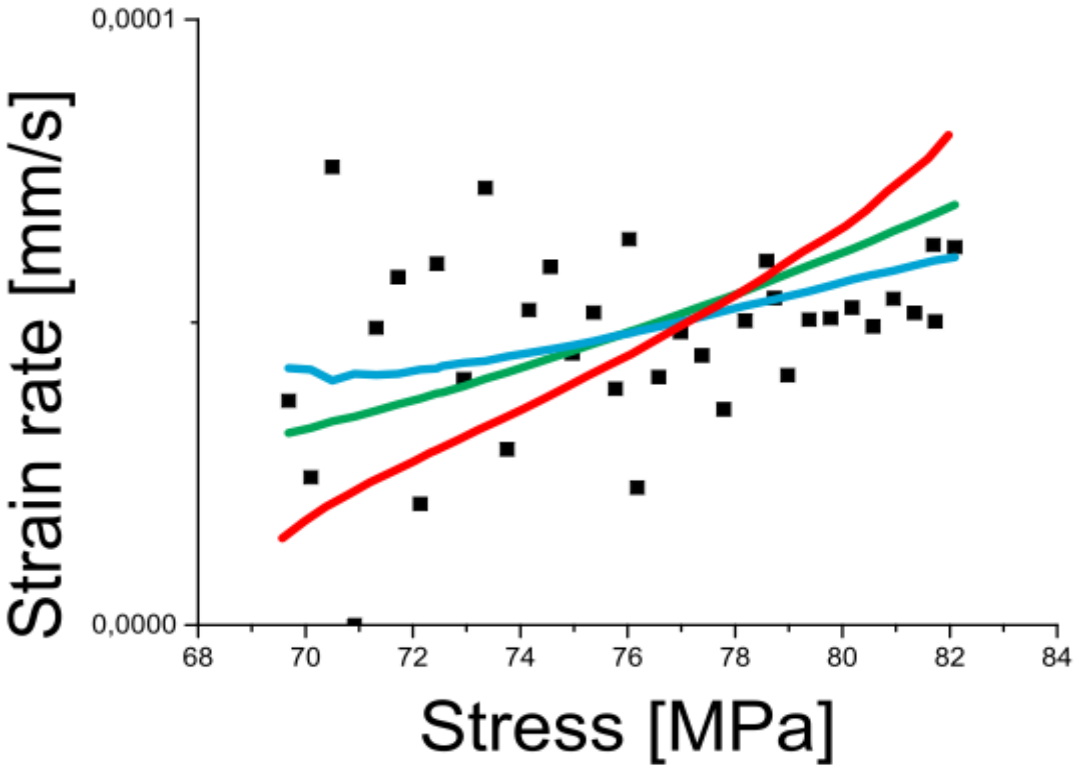

Fig. 138: 304-800º-0p00001-Fitting I

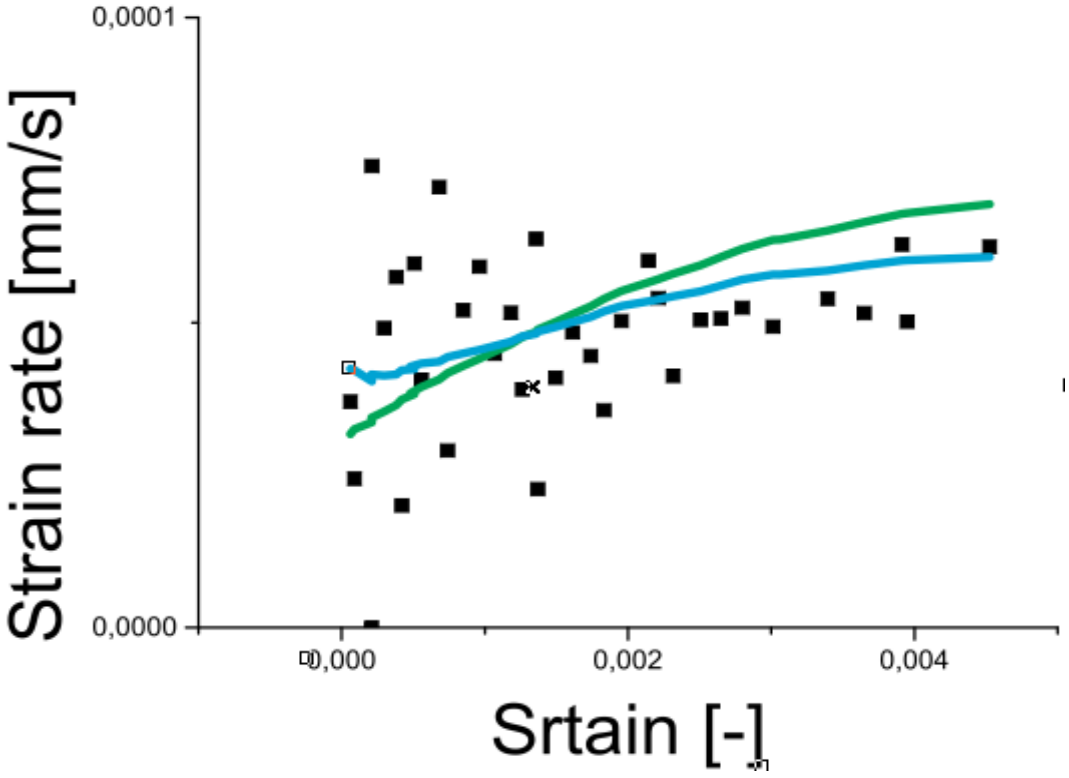

Fig. 139: 304-800º-0p00001-Fitting II

	Time hardening		Strain hardening		Modified strain h.	
	Value	error	Value	error	Value	error
m	1,28543	0,01722	-0,07235	0,00403	5,72362	2,64122

k					566,9838	5011,8897

Fig. 140: 304-800º-0p00001-parameters

- **0p000005**

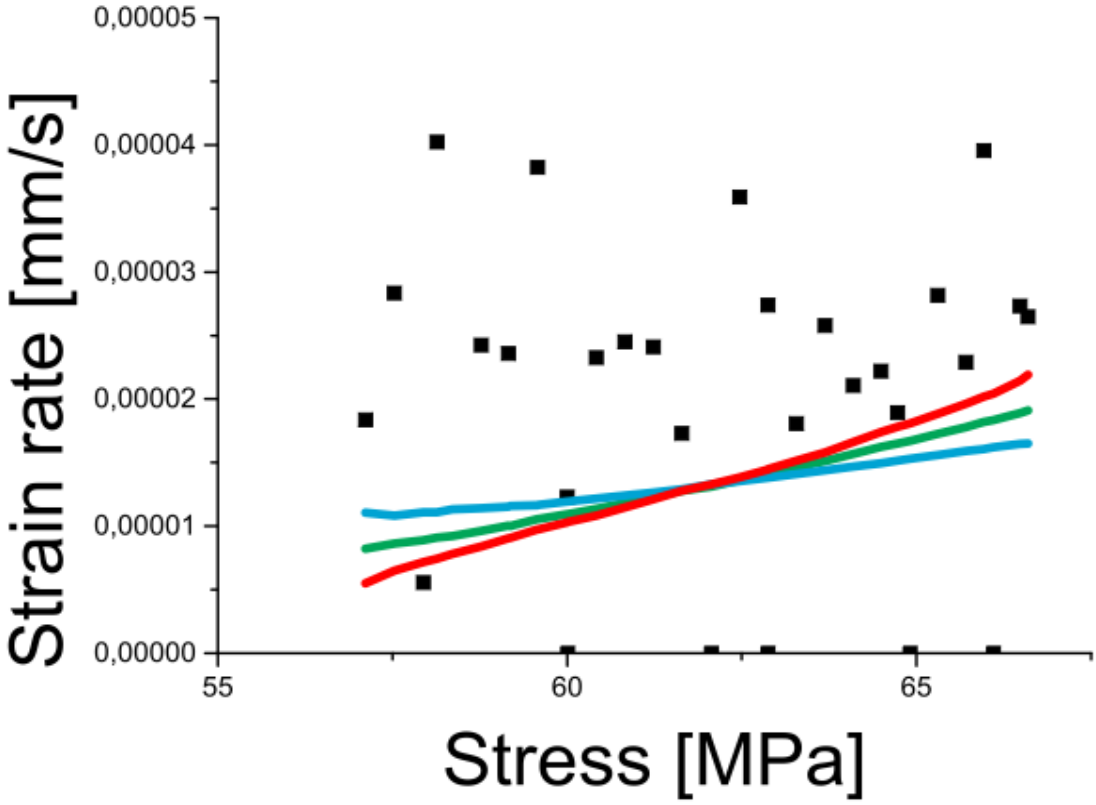

Fig. 141: 304-800º-0p00005-Fitting I

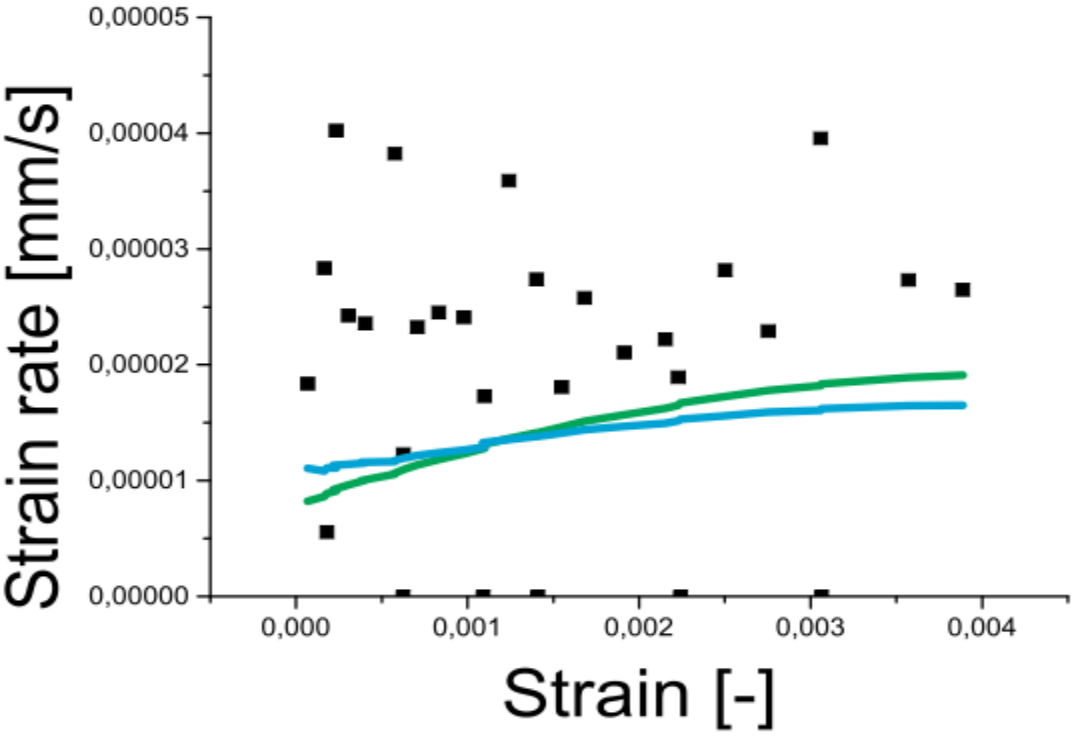

Fig. 142: 304-800º-0p00005-Fitting II

	Time hardening		Strain hardening		Modified strain h.	
	Value	error	Value	error	Value	error
m	1,19957	0,05311	-0,0545	0,01598	37	5,66392
k					35	13931,91

Fig. 143: 304-800º-0p000005-parameters

- **980ºC**
  - **0p0001**

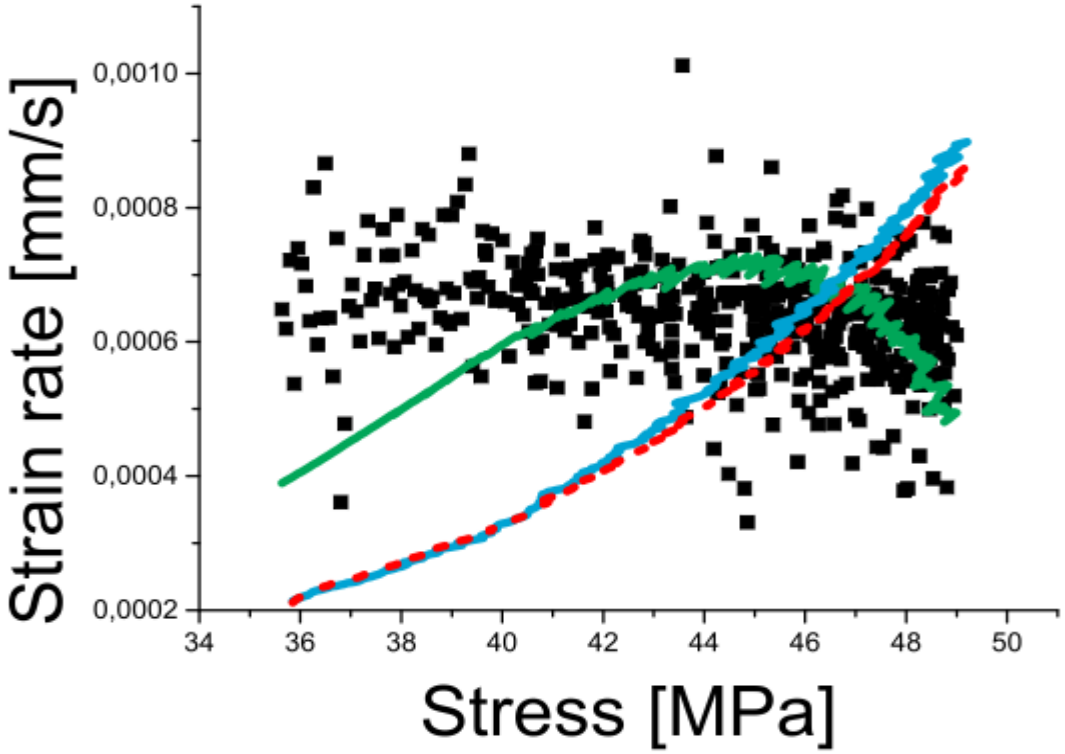

Fig. 144: 304-980º-0p0001-Fitting I

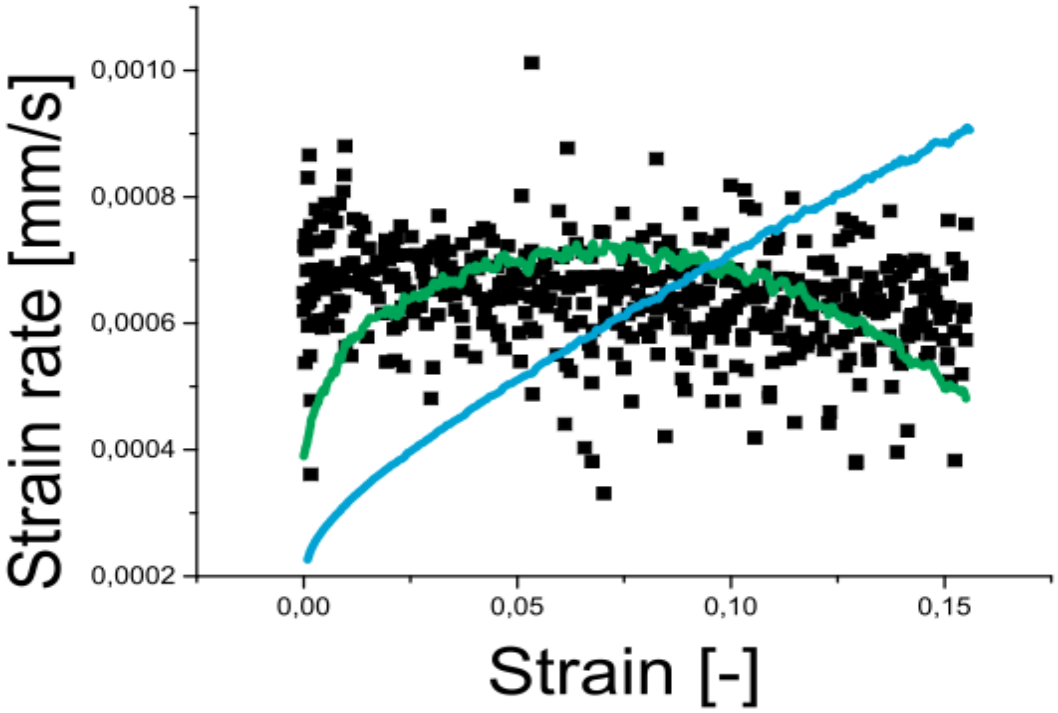

Fig. 145: 304-8980º-0p0001-Fitting II

	Time hardening		Strain hardening		Modified strain h.	
	Value	error	Value	error	Value	error
m	1,2933	0,00316	1,22875	0,01052	0,000179	2,339E-06
k					-0,00077	2,195E-05

Fig. 146: 304-980º-0p0001-parameters

- **0p00005**

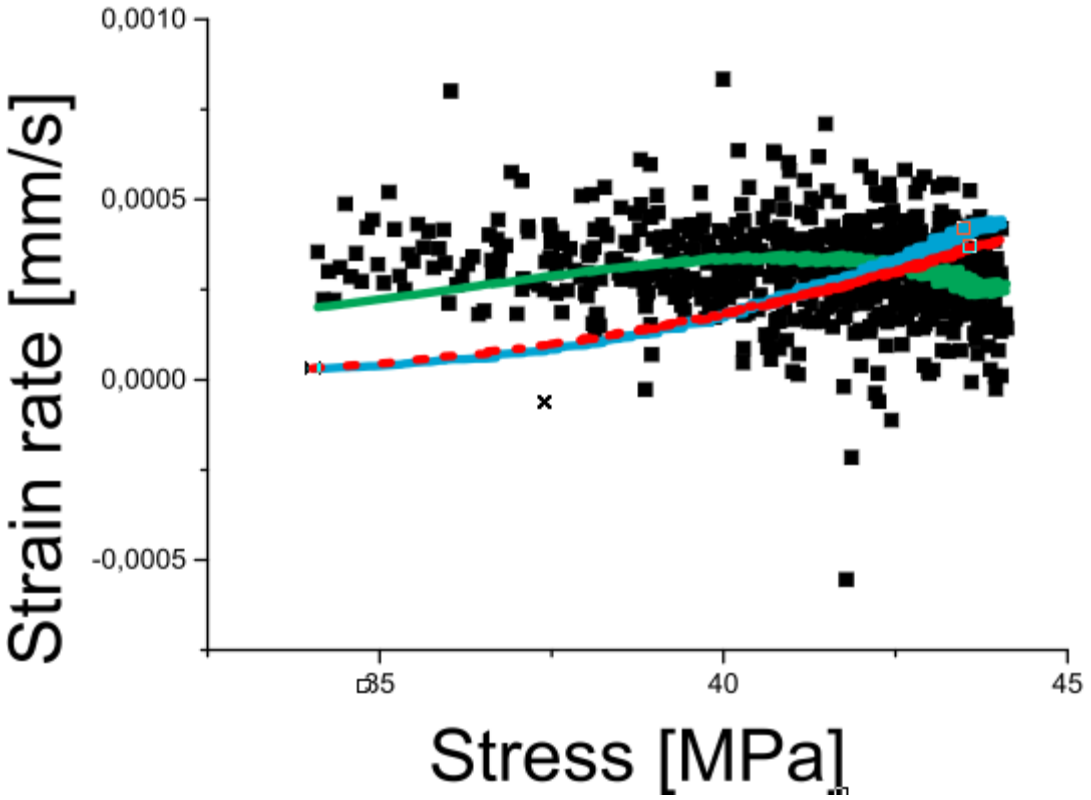

Fig. 147: 304-980º-0p00005-Fitting I

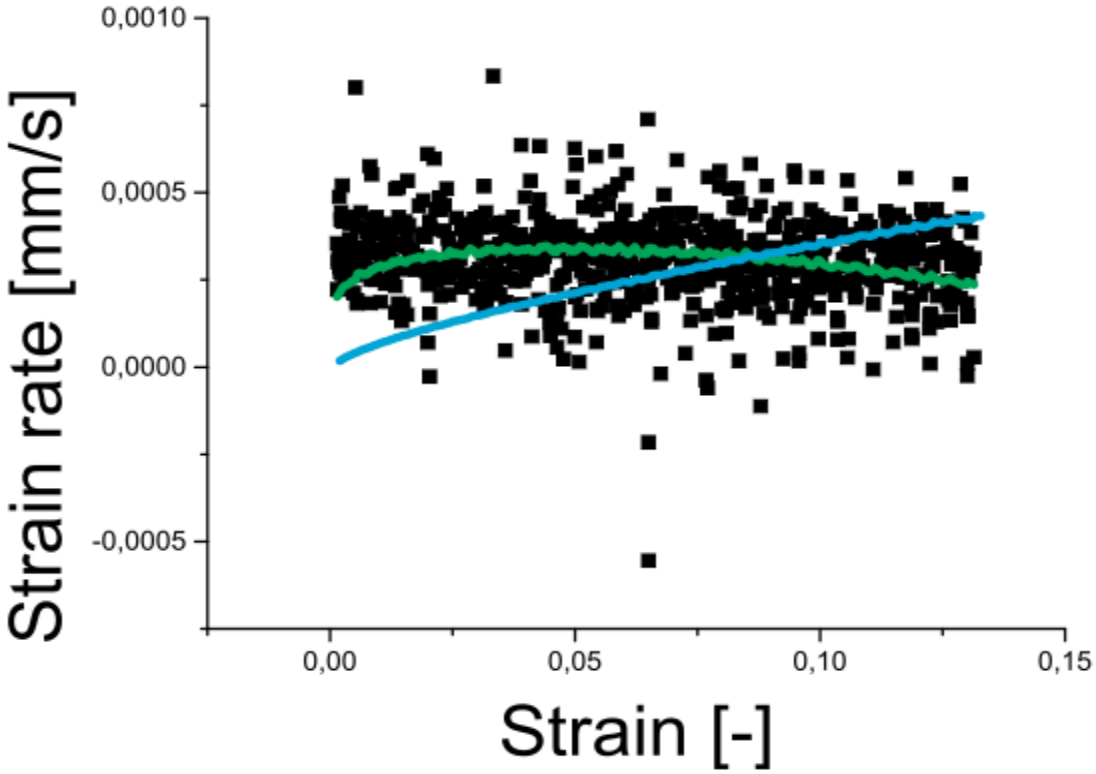

Fig. 148: 304-980º-0p00005-Fitting II

	Time hardening		Strain hardening		Modified strain h.	
	Value	error	Value	error	Value	error
m	1,23481	0,0027	1,48013	0,01673	0,000115	2,838E-06
k					-0,00052	3,251E-05

Fig. 149: 304-980º-0p00005-parameters

❖ **0p00001**

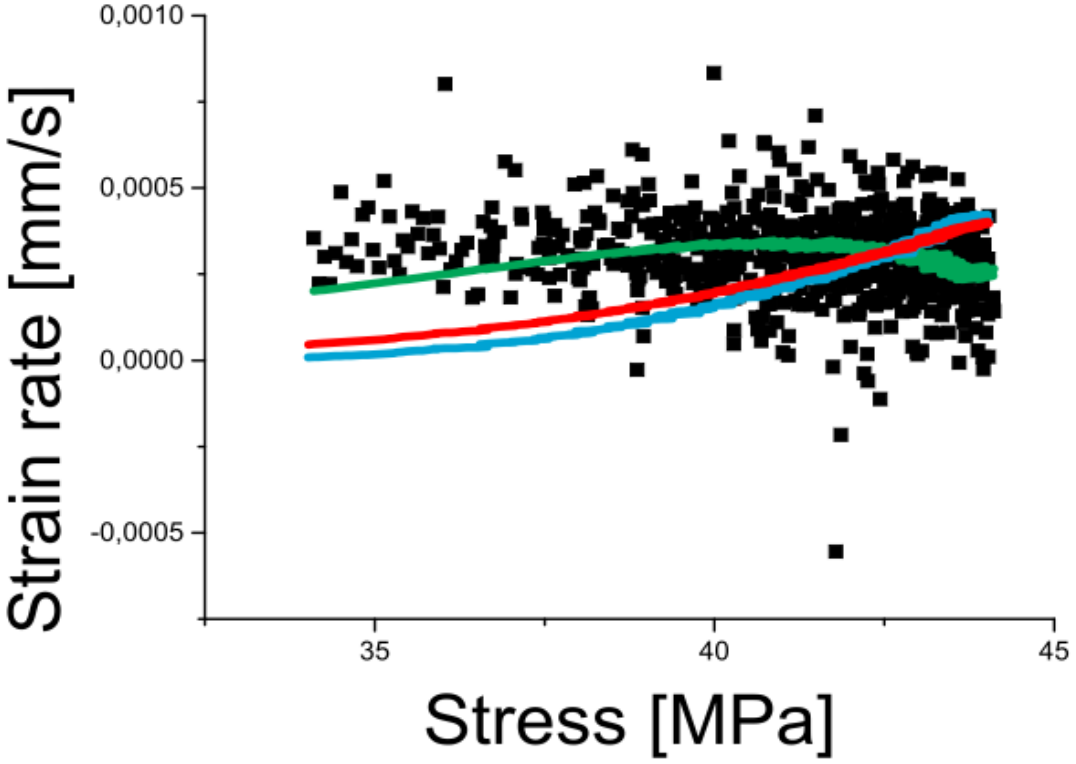

Fig. 150: 304-980º-0p00001-Fitting I

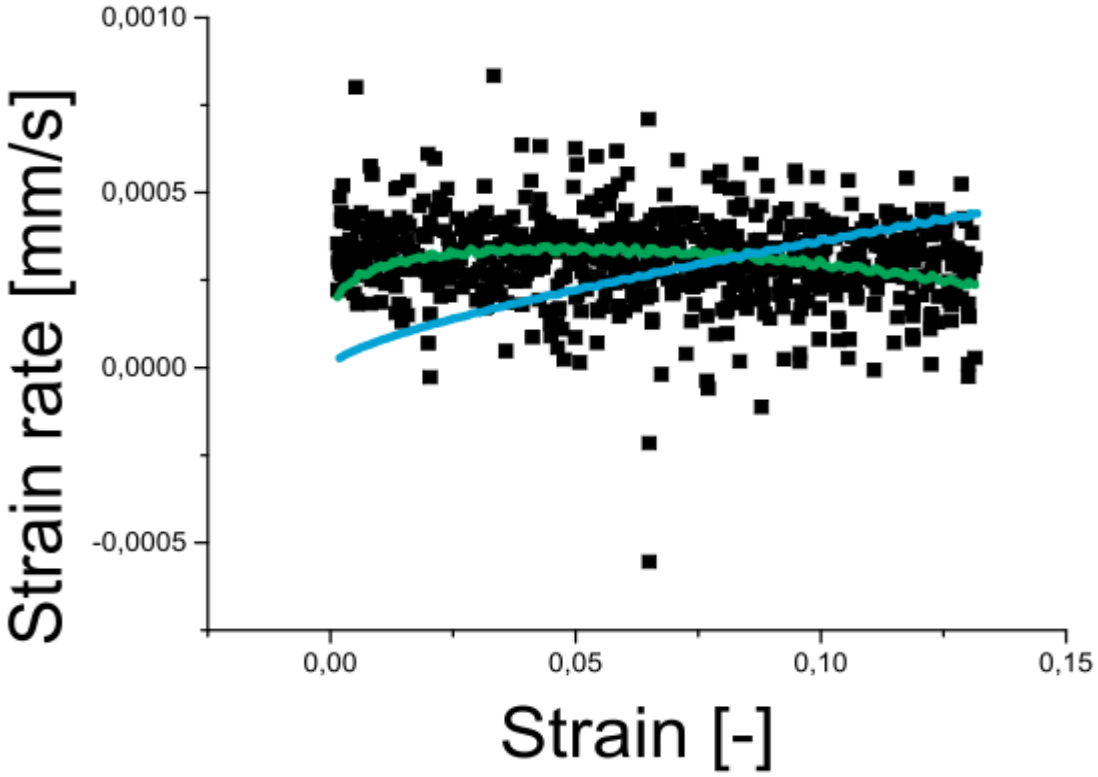

Fig. 151: 304-980º-0p00001-Fitting II

	Time hardening		Strain hardening		Modified strain h.	
	Value	error	Value	error	Value	error
m	1,33899	0,01106	1,01181	0,01907	1,08E-04	1,10E-05
k					-0,00444	0,0022

Fig. 152: 304-980º-0p00001-parameters

- **0p000005**

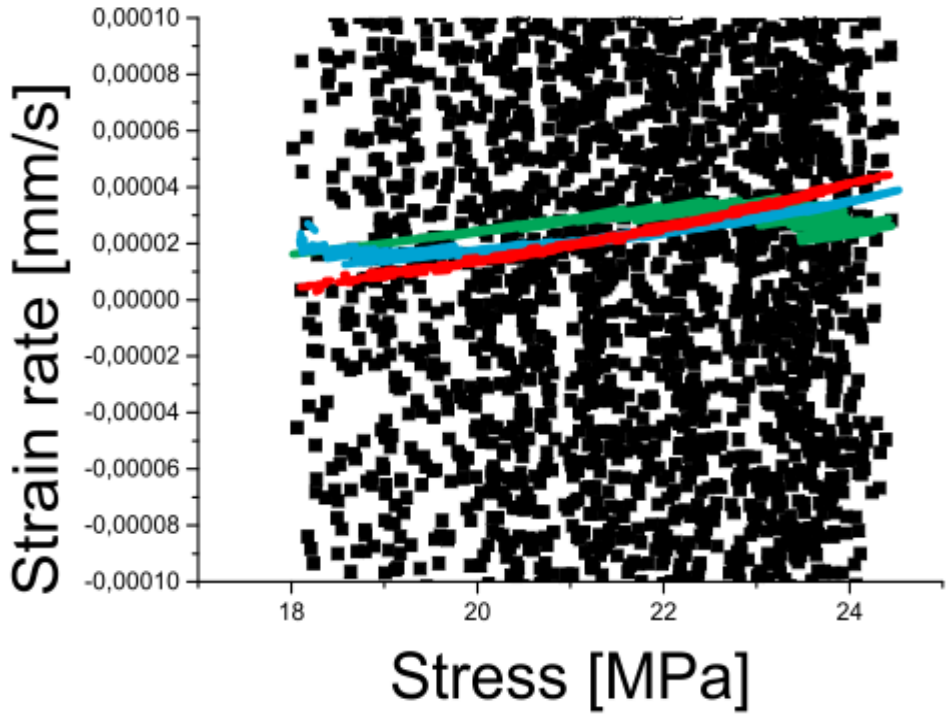

Fig. 153: 304-980º-0p00001-Fitting I

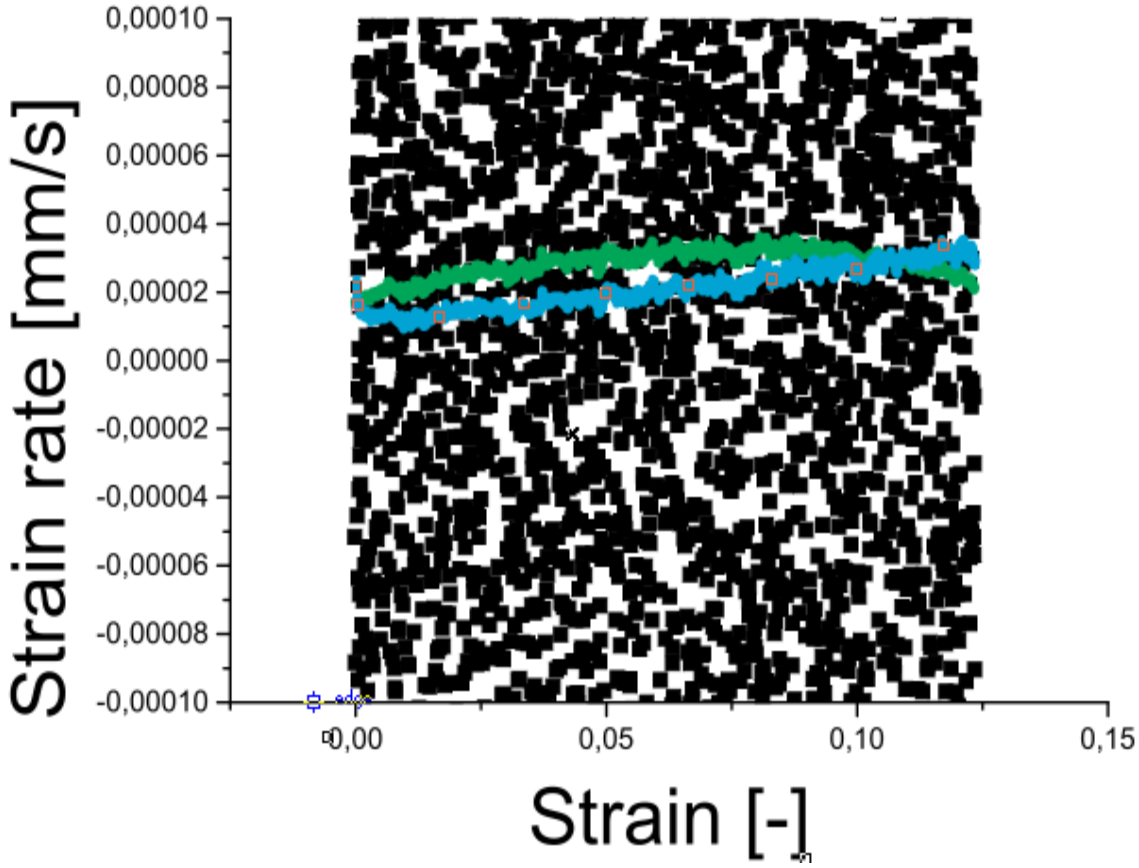

Fig. 154: 304-980º-0p00001-Fitting I

	Time hardening		Strain hardening		Modified strain h.	
	Value	error	Value	error	Value	error
m	1,21079	0,01072	-0,12636	0,0051	13,56465	1,84148

k					-17,7116	3,39305

Fig. 155: 304-980º-0p0001-parameters

- **1125ºC**
  - **0p00005**

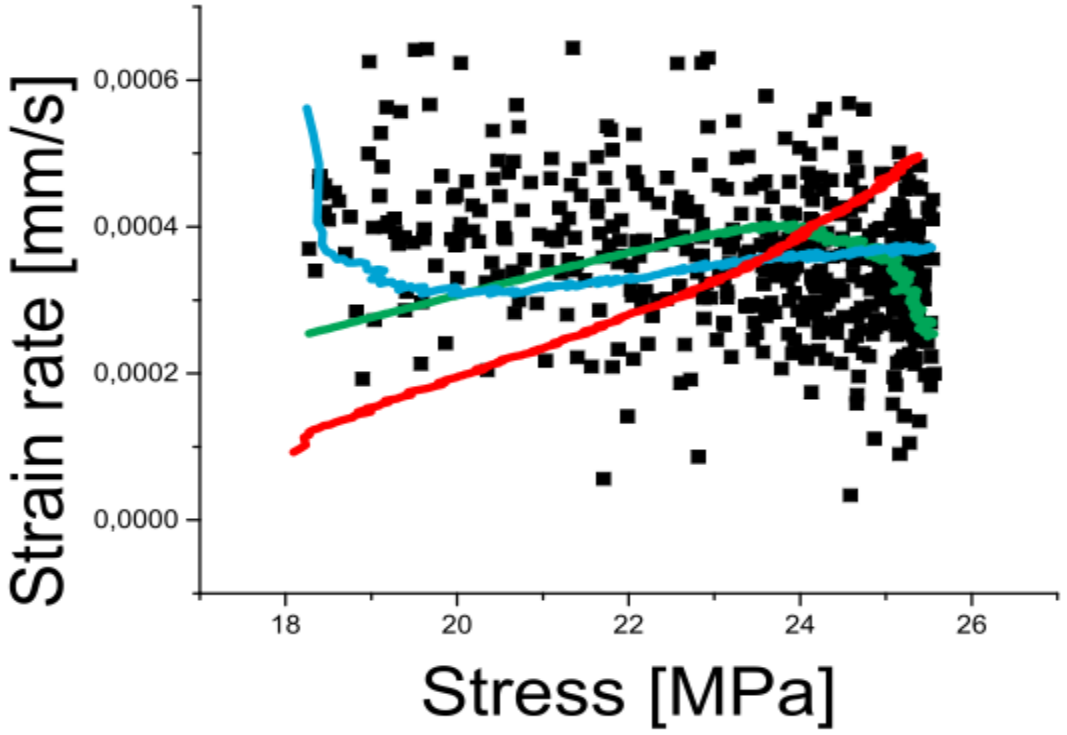

Fig. 156: 304-1125º-0p00005-Fitting I

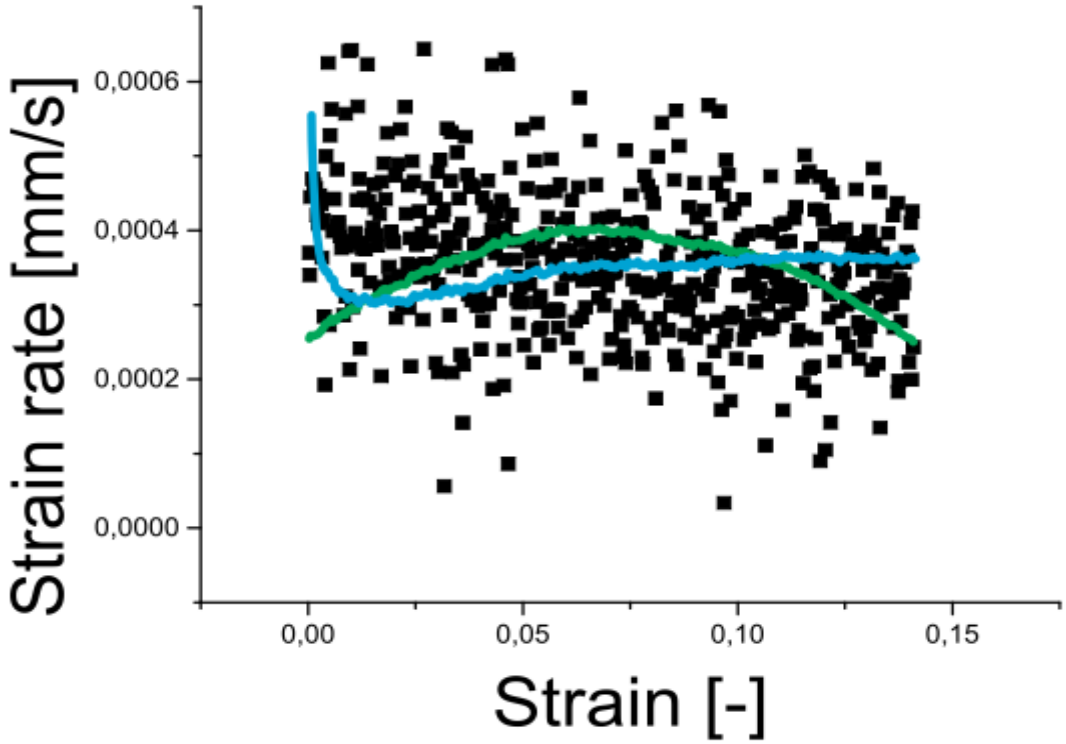

Fig. 157: 304-1125º-0p00005-Fitting II

	Time hardening		Strain hardening		Modified strain h.	
	Value	error	Value	error	Value	error
m	1,25894	0,00294	-0,17798	8,44E-04	11,19583	0,19566
k					-13,8221	0,42703

Fig. 158: 304-1125º-0p00005-parameters

- **0p00001**

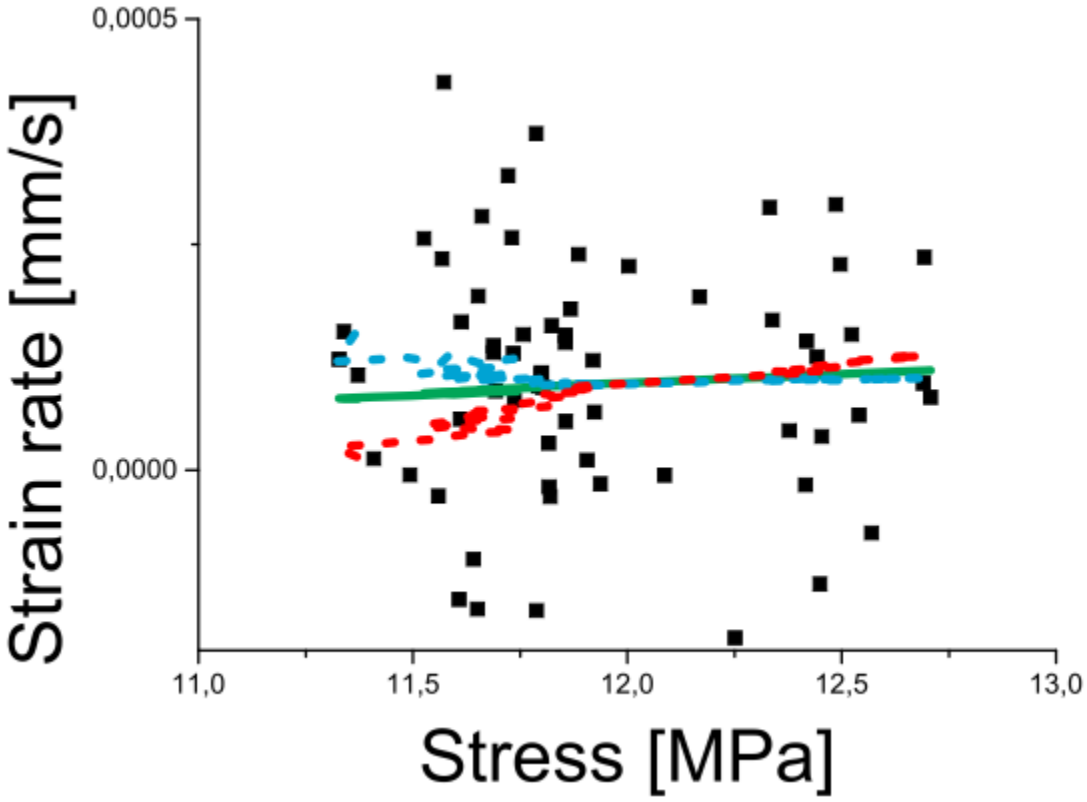

Fig. 159: 304-1125º-0p00001-Fitting I

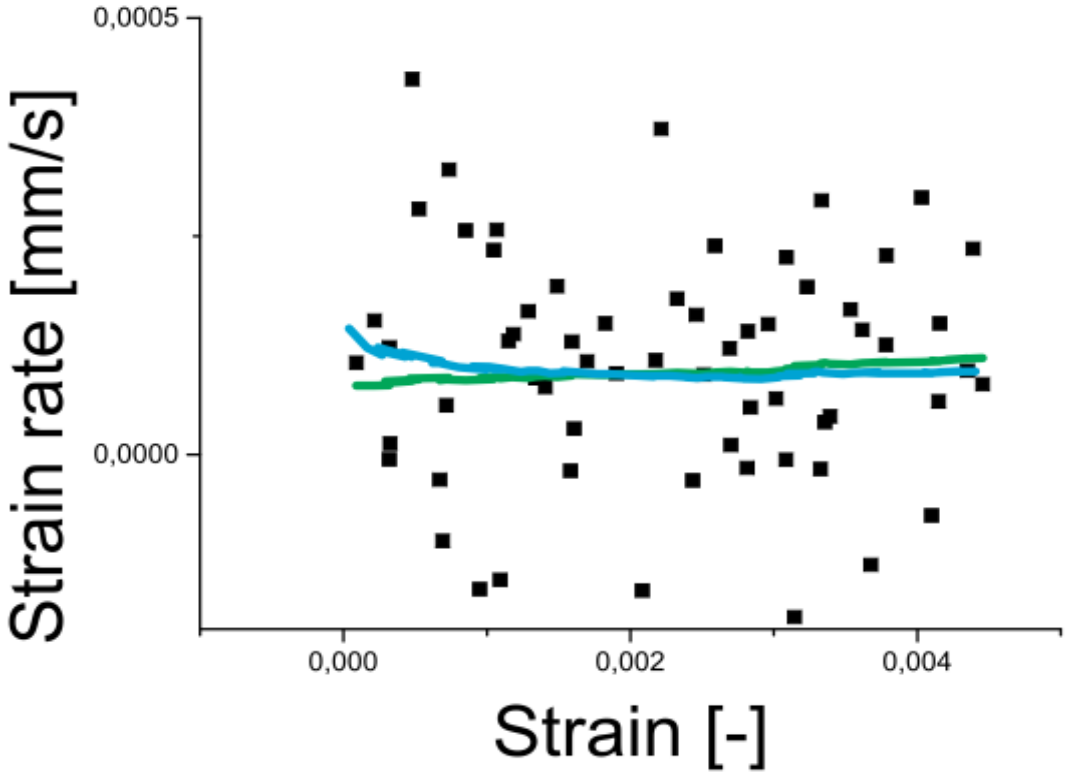

Fig. 160: 304-1125º-0p00001-Fitting II

	Time hardening		Strain hardening		Modified strain h.	
	Value	error	Value	error	Value	error
m	1,40197	0,0382	-0,16022	0,01339	10,04737	5,53105
k					920,4389	21578,107

Fig. 161: 304-1125º-0p00001-parameters

- **0p000005**

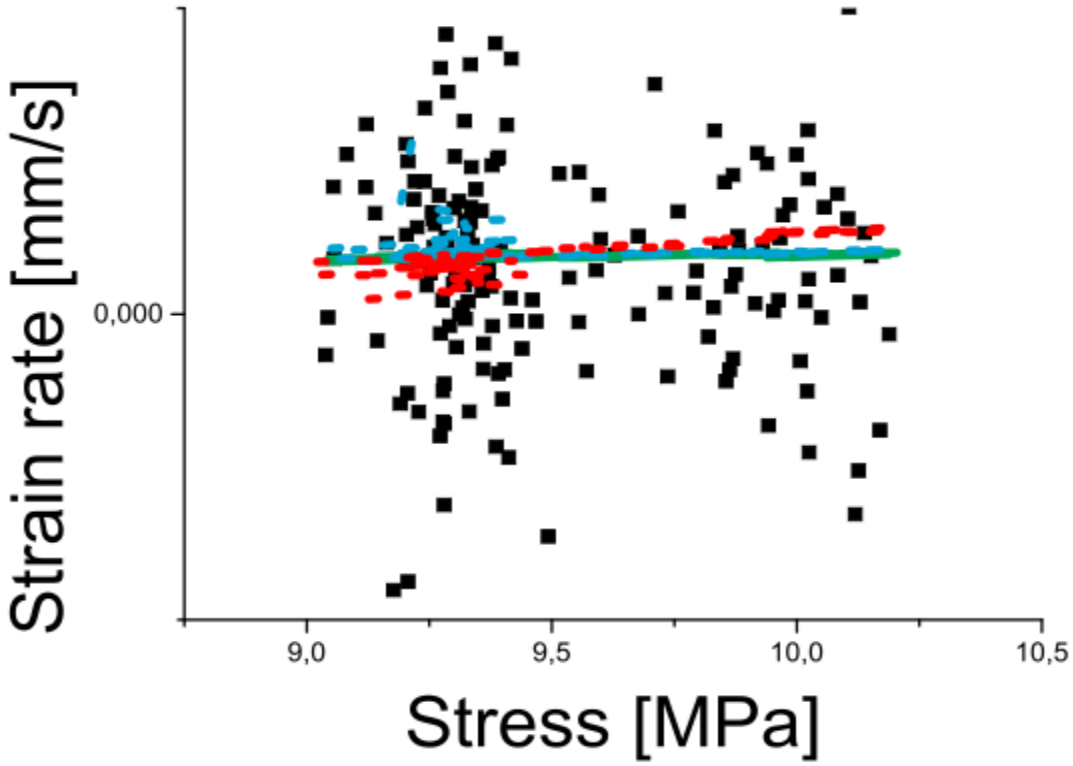

Fig. 162: 304-1125º-0p000005-Fitting I

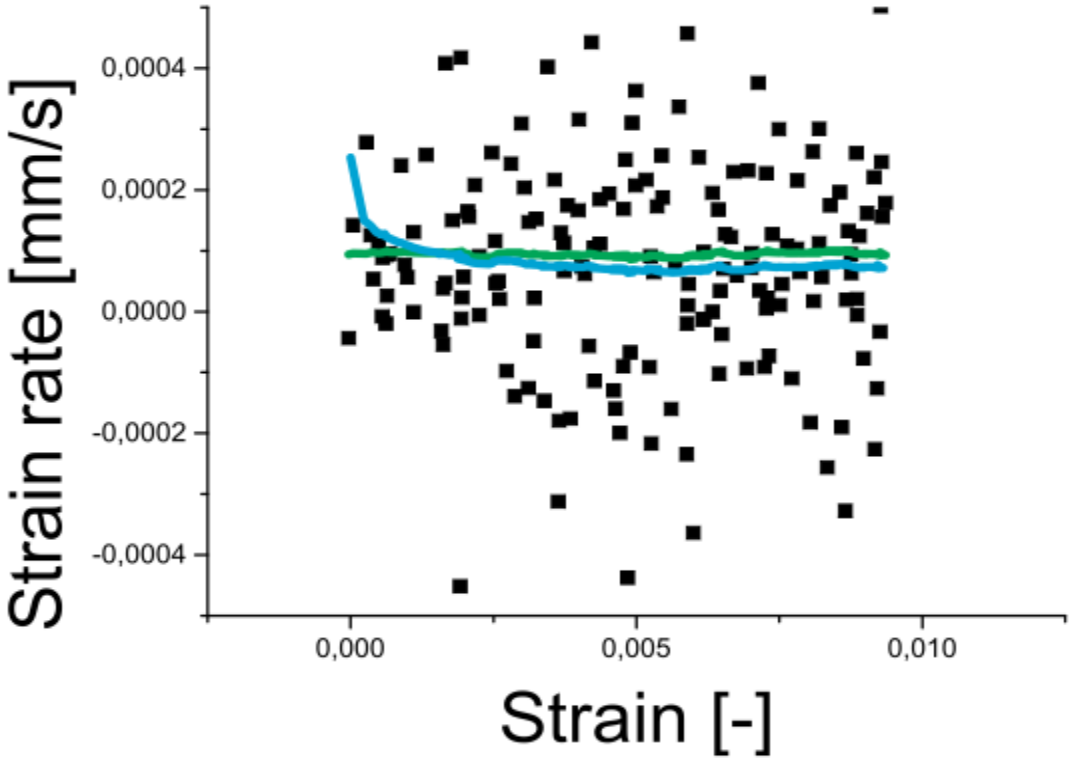

Fig. 163: 304-1125º-0p000005-Fitting II

	Time hardening		Strain hardening		Modified strain h.	
	Value	error	Value	error	Value	error
m	1,41393	0,03132	-0,2065	0,01152	19,72728	5,87925

k					-166,673	266,57151

Fig. 164: 304-700º-0p000005-parameters

6.2.2. 316L stainless steel

- **600ºC**
  - **0p0001**

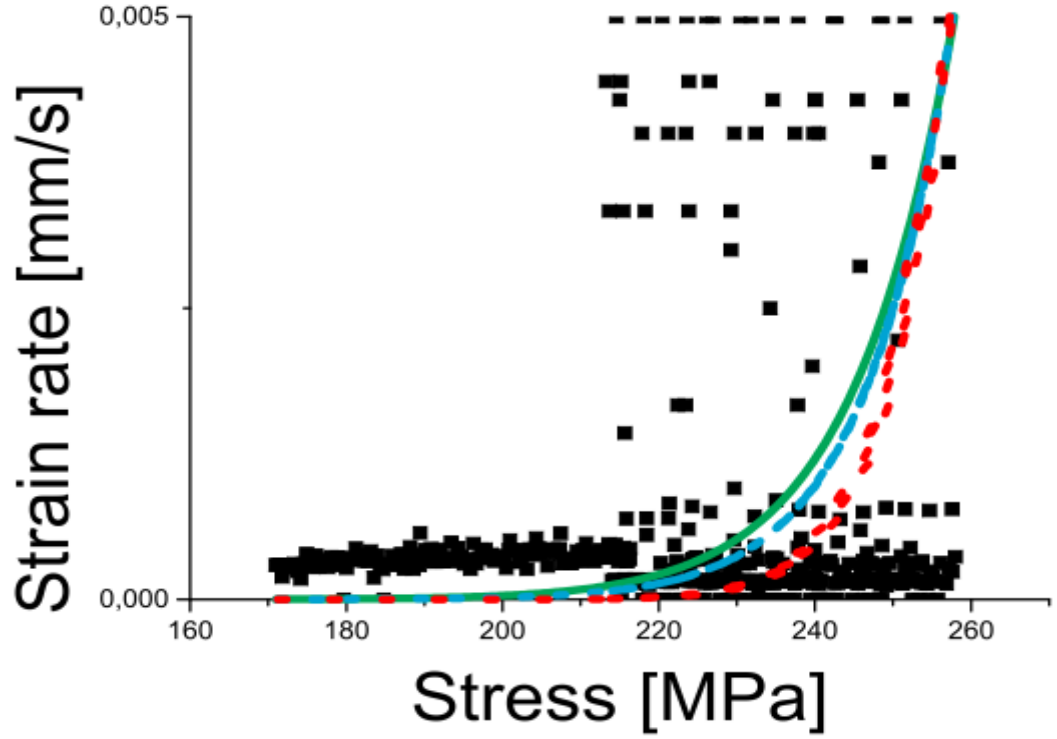

Fig. 165: 316L-600º-0p0001-Fitting I

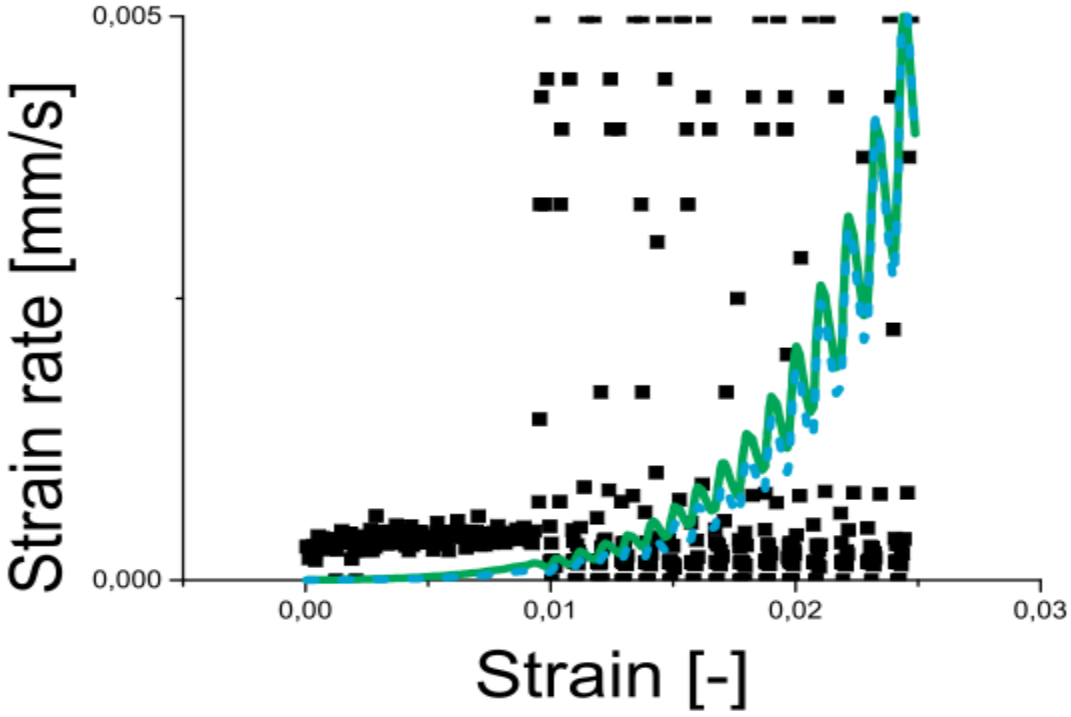

Fig. 166: 316L-600º-0p0001-Fitting II

	Time hardening		Strain hardening		Modified strain h.	
	Value	error	Value	error	Value	error
m	4,52437	0,01628	-0,16339	6,08E-04	4,61E+09	4,01E+08
k					4,42E+10	7,01038

Fig. 167: 316L-600º-0p0001-parameters

- **0p00005**

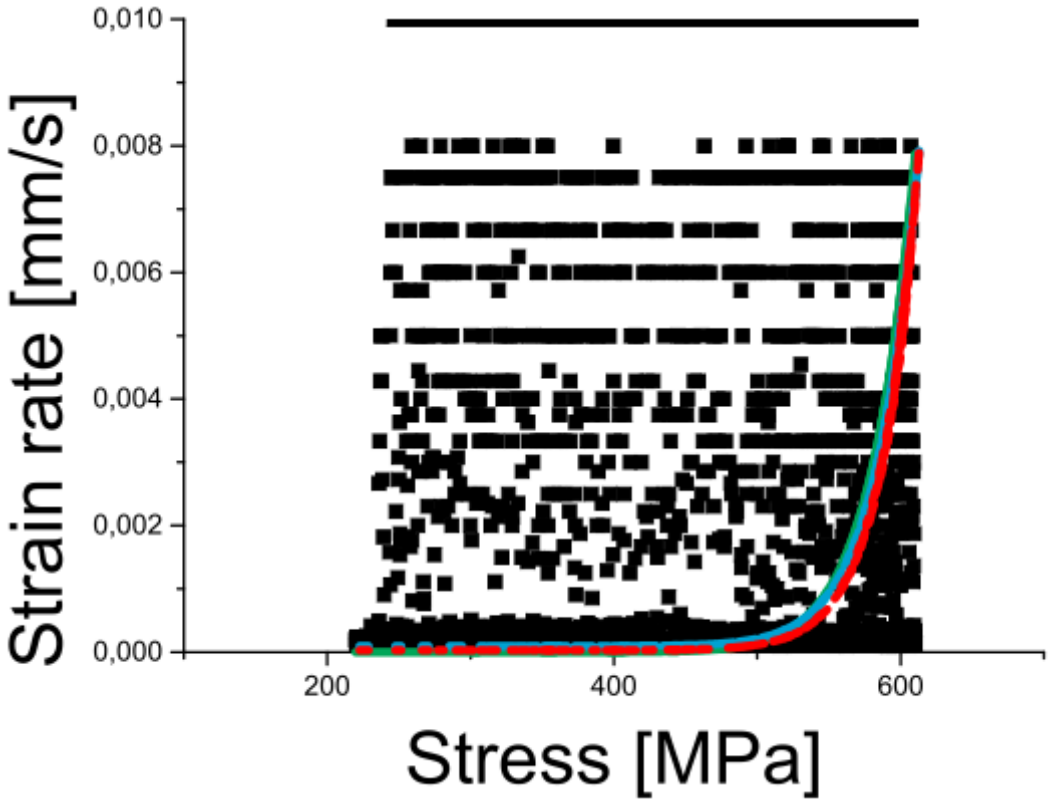

Fig. 168: 316L-600º-0p00005-Fitting I

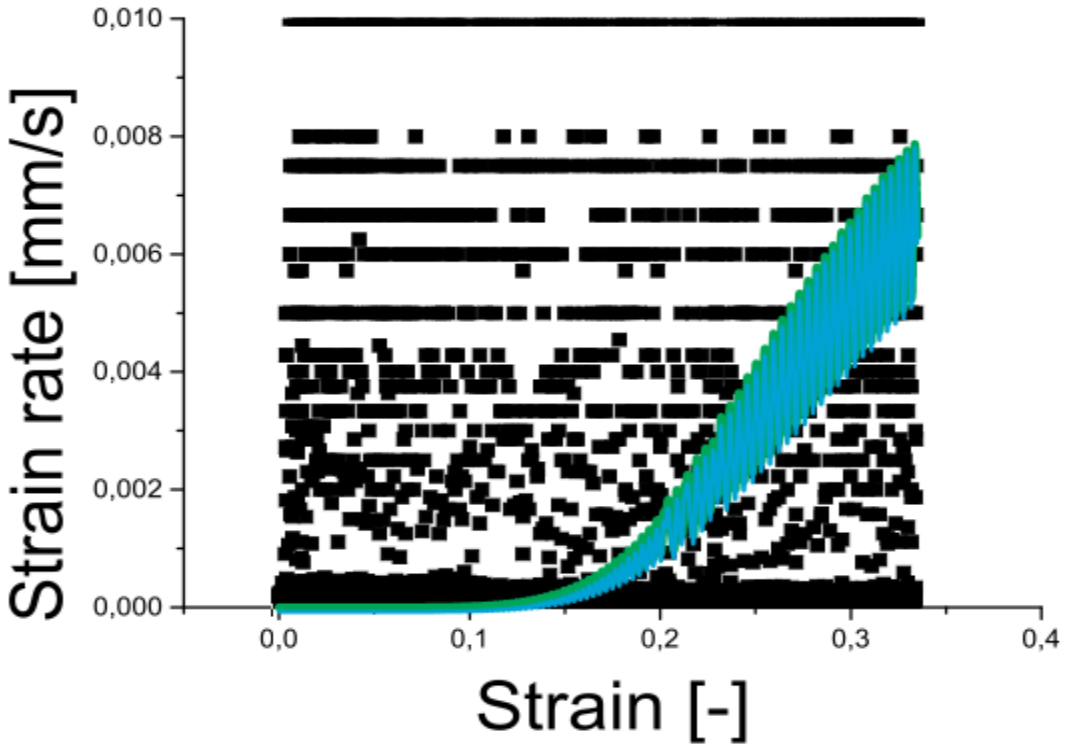

Fig. 169: 316L-600º-0p00005-Fitting II

	Time hardening		Strain hardening		Modified strain h.	
	Value	error	Value	error	Value	error
m	1,57915	4,11E-03	-0,04173	2,80E-04	267,9009	10,20282
k					6,32E+11	6,45308

Fig. 170: 316L-600º-0p00005-parameters

- **0p00001**

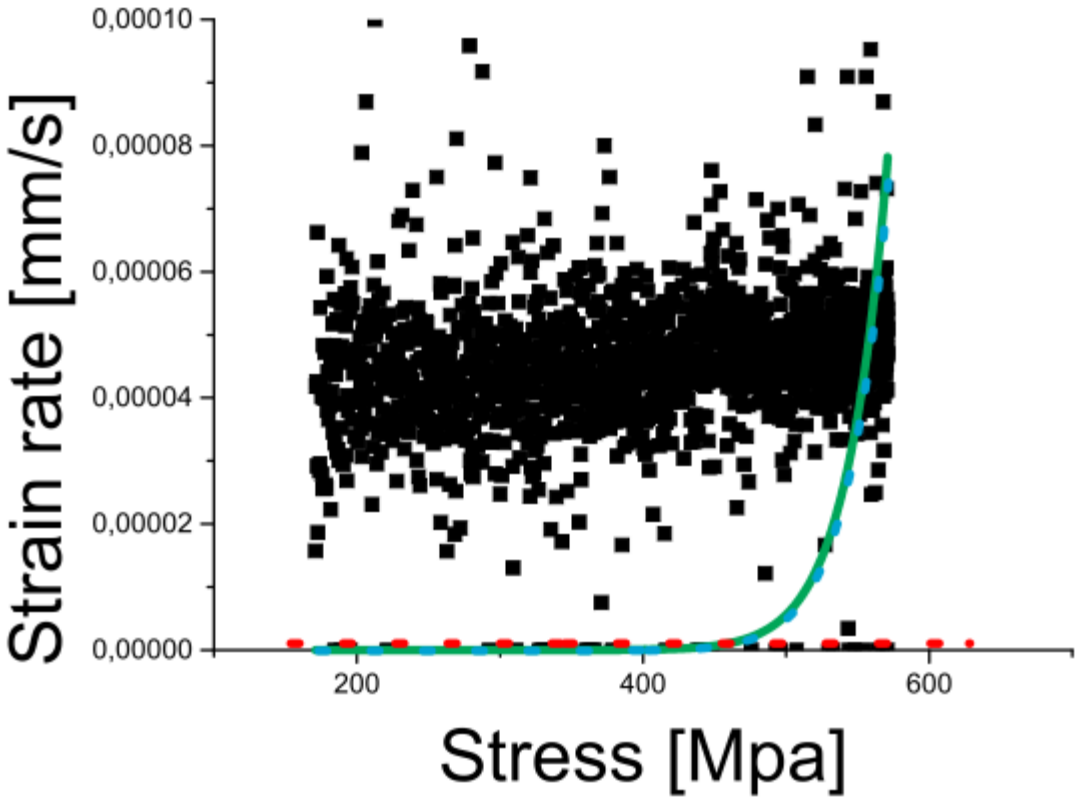

Fig. 171: 316L-600º-0p00001-Fitting I

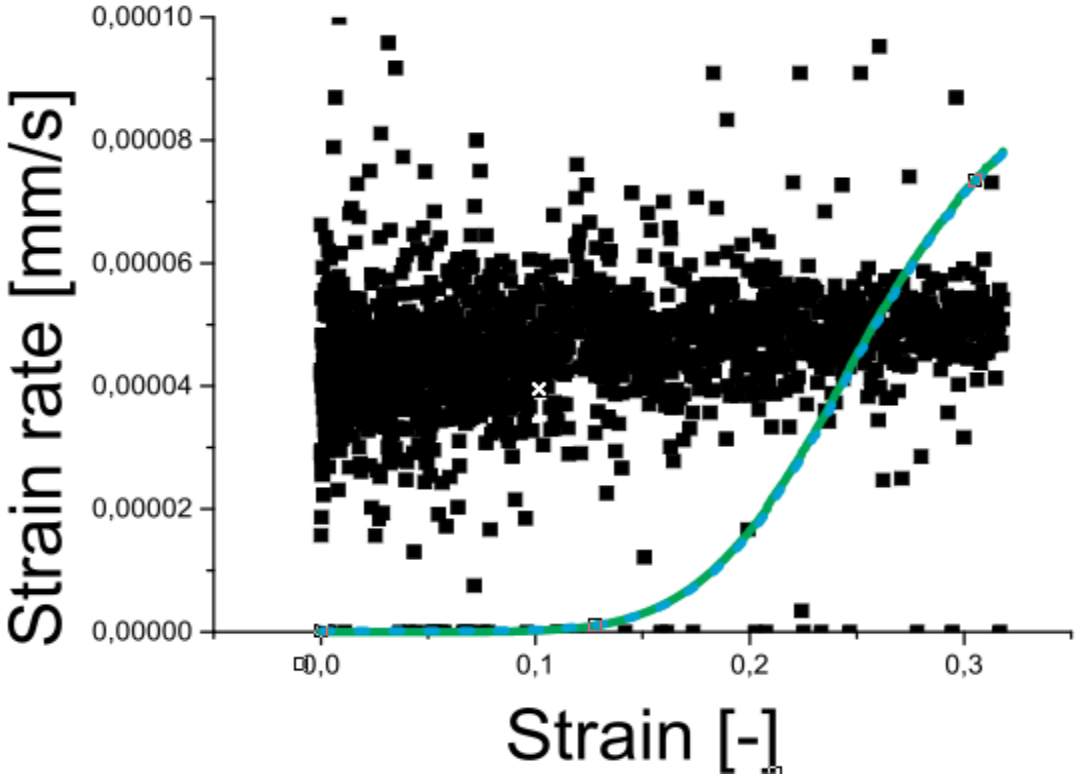

Fig. 172: 316L-600º-0p00001-Fitting II

	Time hardening		Strain hardening		Modified strain h.	
	Value	error	Value	error	Value	error
m	1	4,83E+63	-0,01776	3,31E-04	9,00222	0,43084
k					6,52E+15	11,67828

Fig. 173: 316L-600º-0p00001-parameters

- **0p000005**

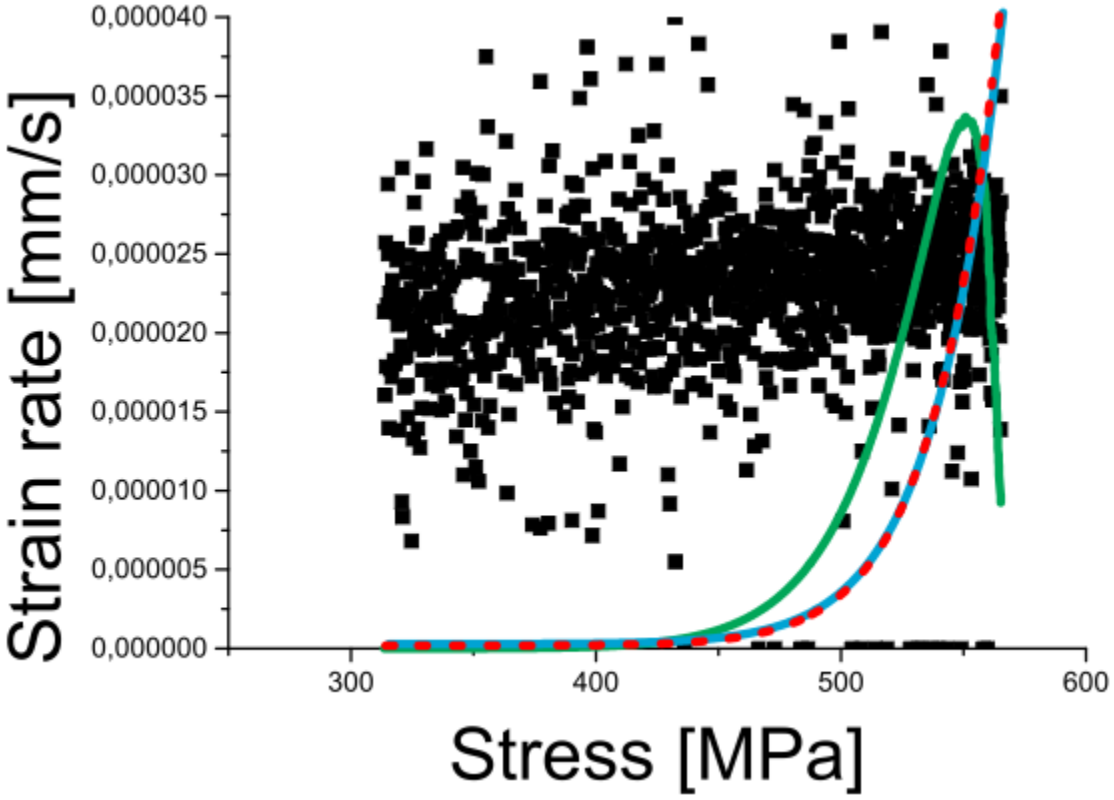

Fig. 174: 316L-600º-0p000005-Fitting I

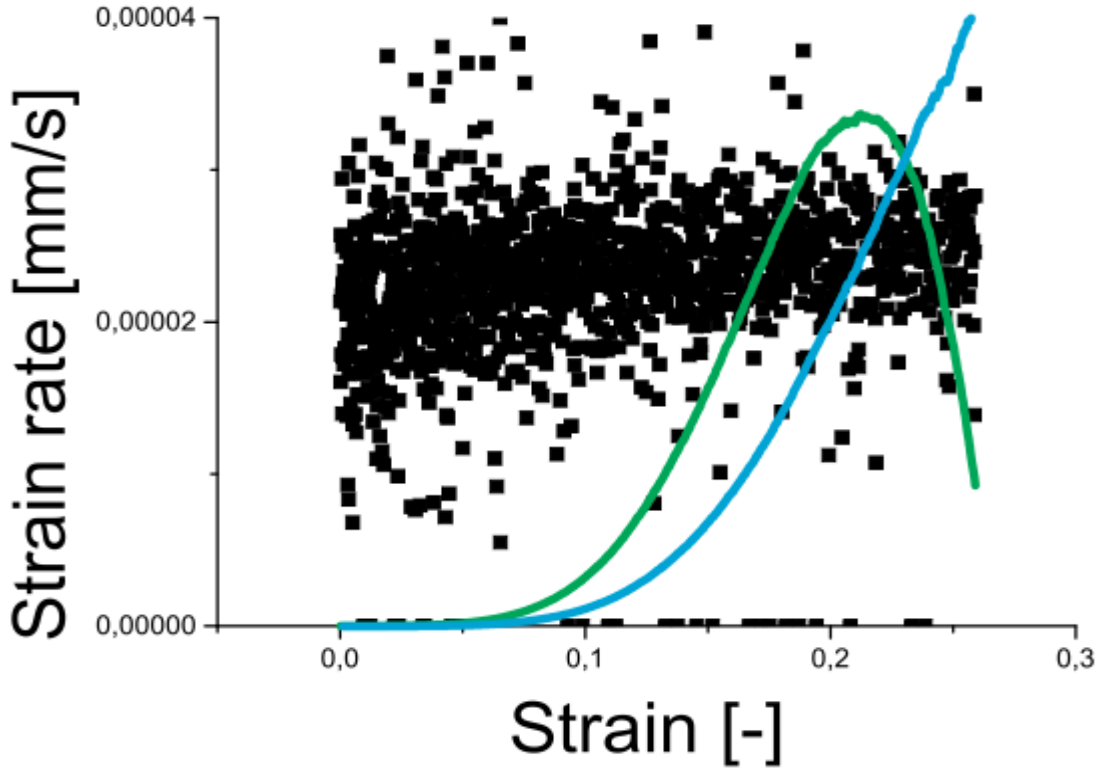

Fig. 175: 316L-600º-0p000005-Fitting II

	Time hardening		Strain hardening		Modified strain h.	
	Value	error	Value	error	Value	error
m	1,15798	0,00658	-0,01451	6,01E-04	18,5218	1,49705
k					-1,12E+01	0,46929

Fig. 176: 316L-600º-0p000005-parameters

- **700ºC**
  - **0p0001**

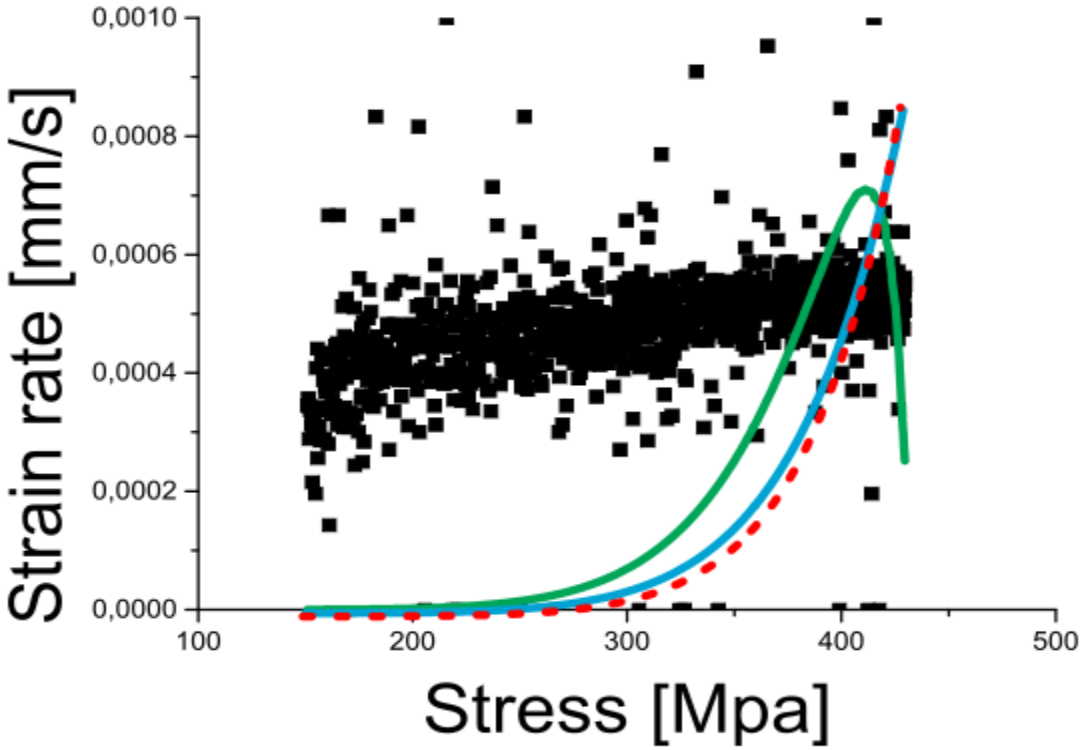

Fig. 177: 316L-700º-0p0001-Fitting I

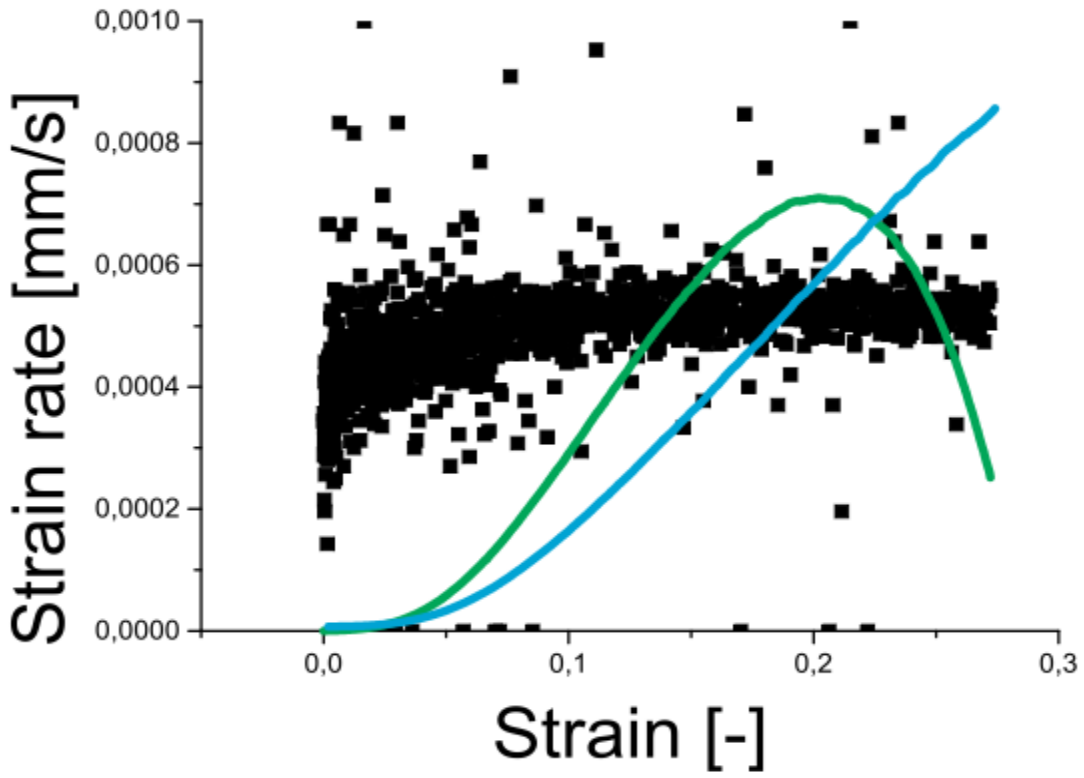

Fig. 178: 316L-700º-0p0001-Fitting II

	Time hardening		Strain hardening		Modified strain h.	
	Value	error	Value	error	Value	error
m	1,31569	0,00579	-0,04919	8,12E-04	29,89142	1,50419
k					-1,20E+01	0,38312

Fig. 179: 316L-700º-0p0001-parameters

- **0p00005**

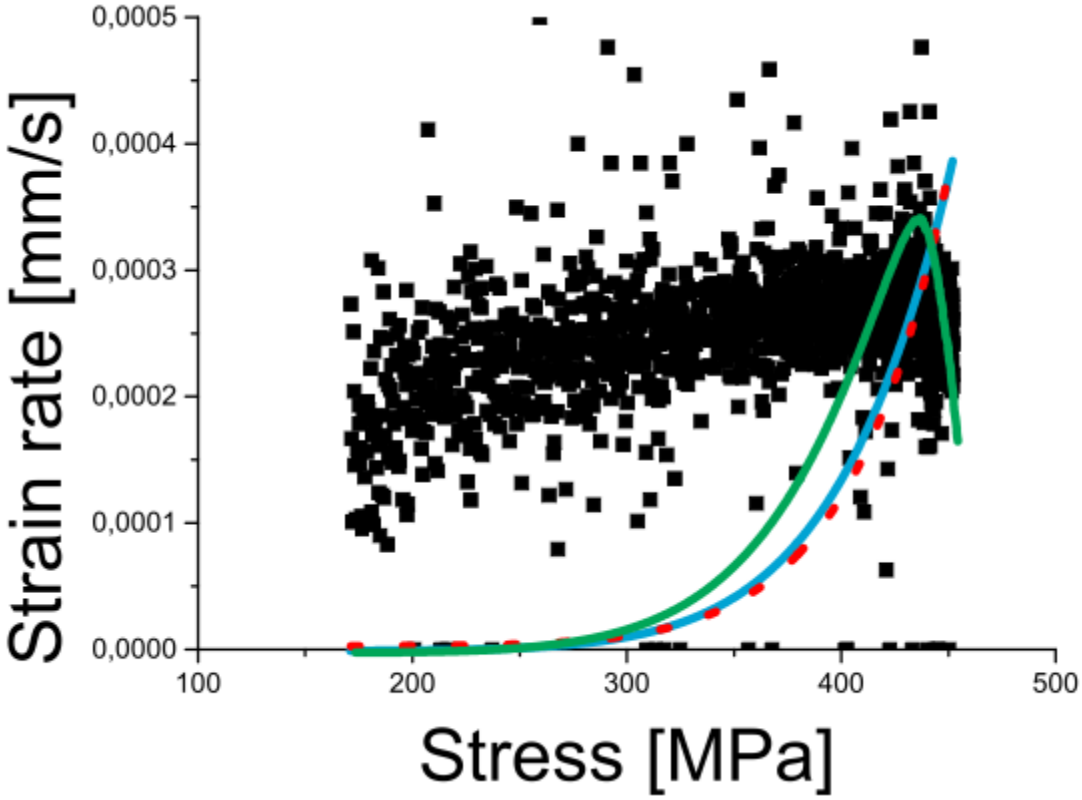

Fig. 180: 316L-700º-0p00005-Fitting I

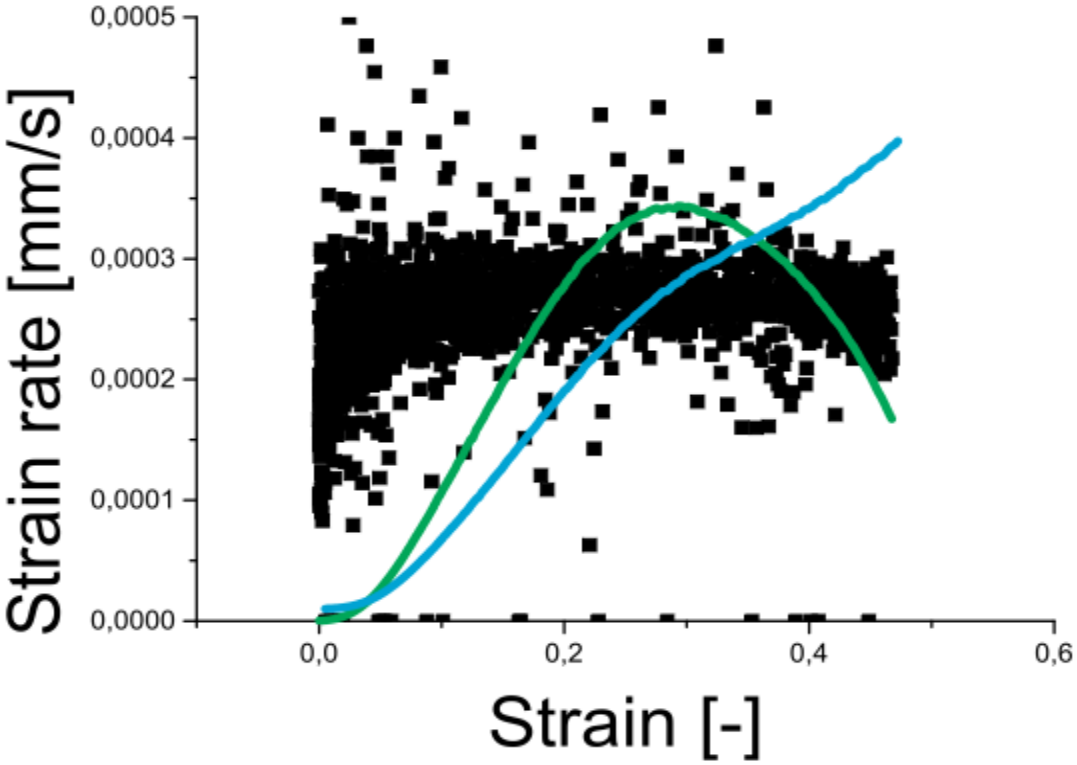

Fig. 181: 316L-700º-0p00005-Fitting II

	Time hardening		Strain hardening		Modified strain h.	
	Value	error	Value	error	Value	error
m	1,15558	2,39E-03	-0,02813	3,99E-04	8,40784	0,20807
k					-4,27439	0,10469

Fig. 182: 316L-700º-0p0001-parameters

- **0p00001**

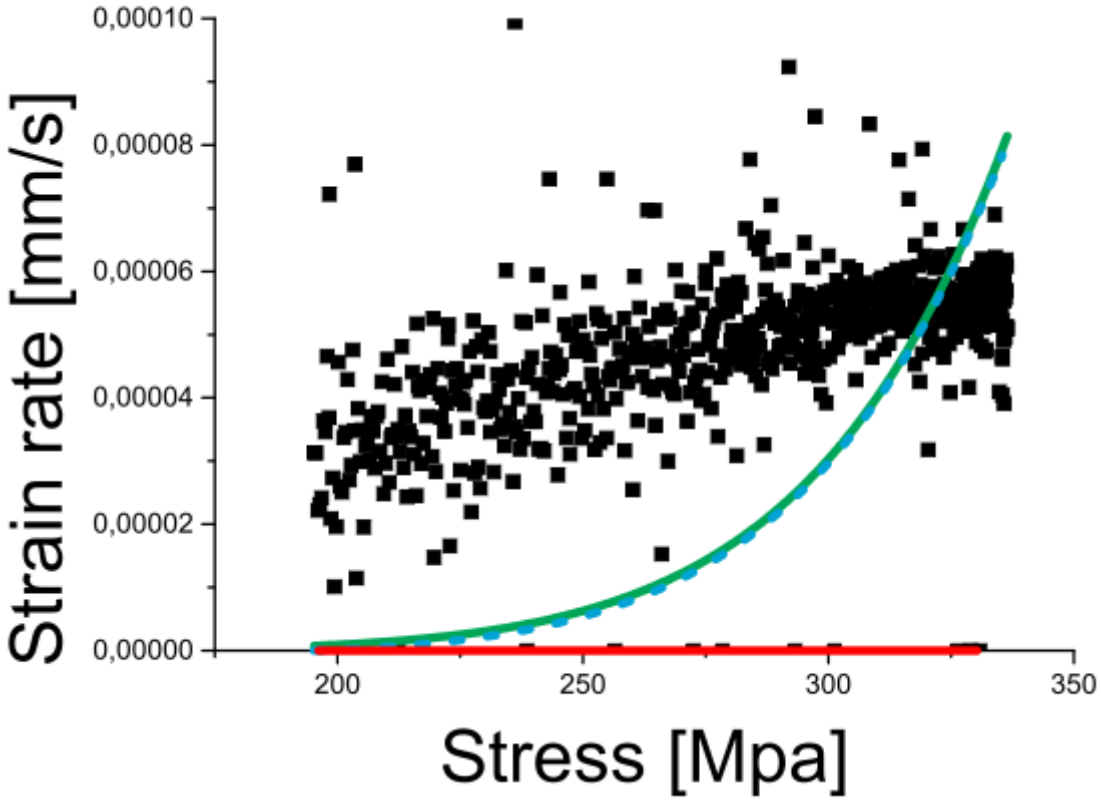

Fig. 183: 316L-700º-0p00001-Fitting I

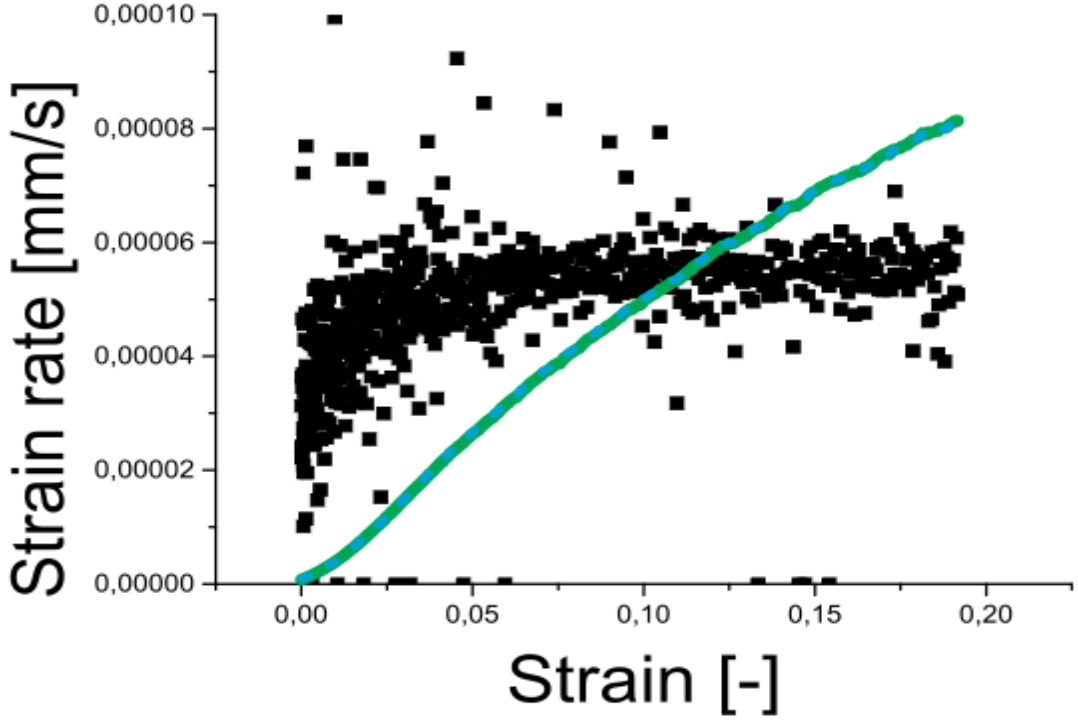

Fig. 184: 316L-700º-0p00001-Fitting II

	Time hardening		Strain hardening		Modified strain h.	
	Value	error	Value	error	Value	error
m	1	1,58E+27	-0,04662	5,67E-04	11,70043	0,41058
k					1,49E+06	476,04769

Fig. 185: 316L-700º-0p00001-parameters

- **0p000005**

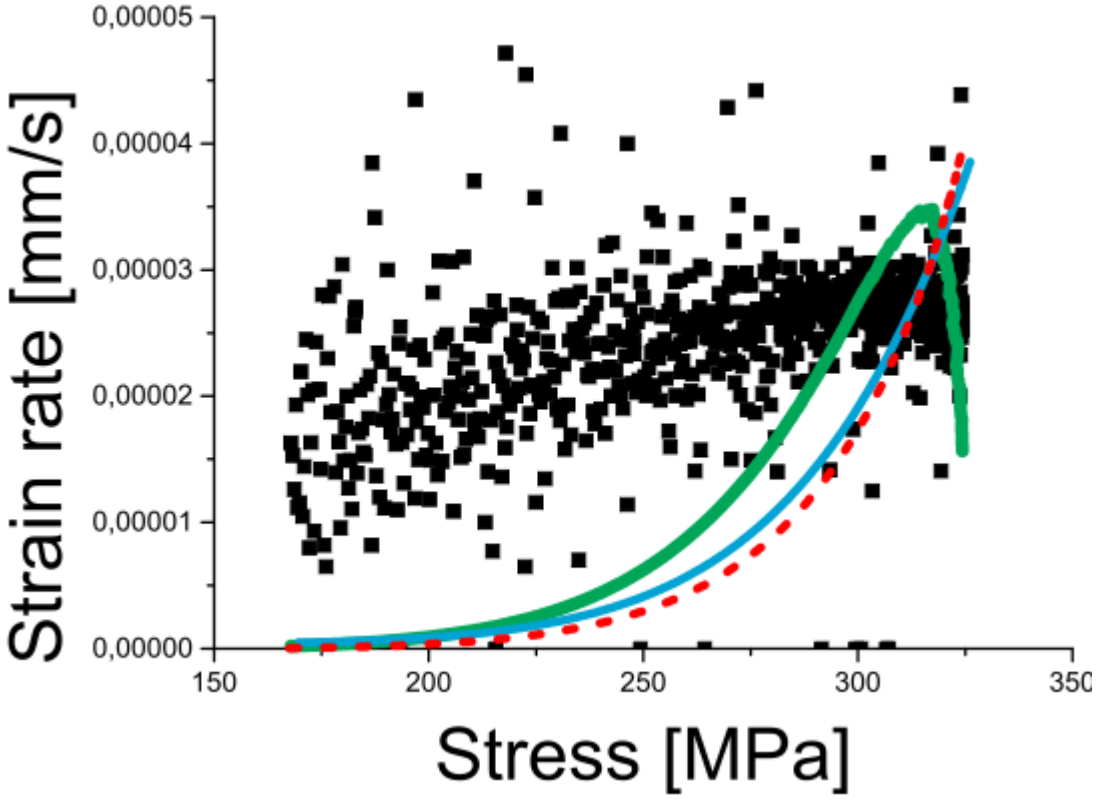

Fig. 186: 316L-700º-0p00005-Fitting I

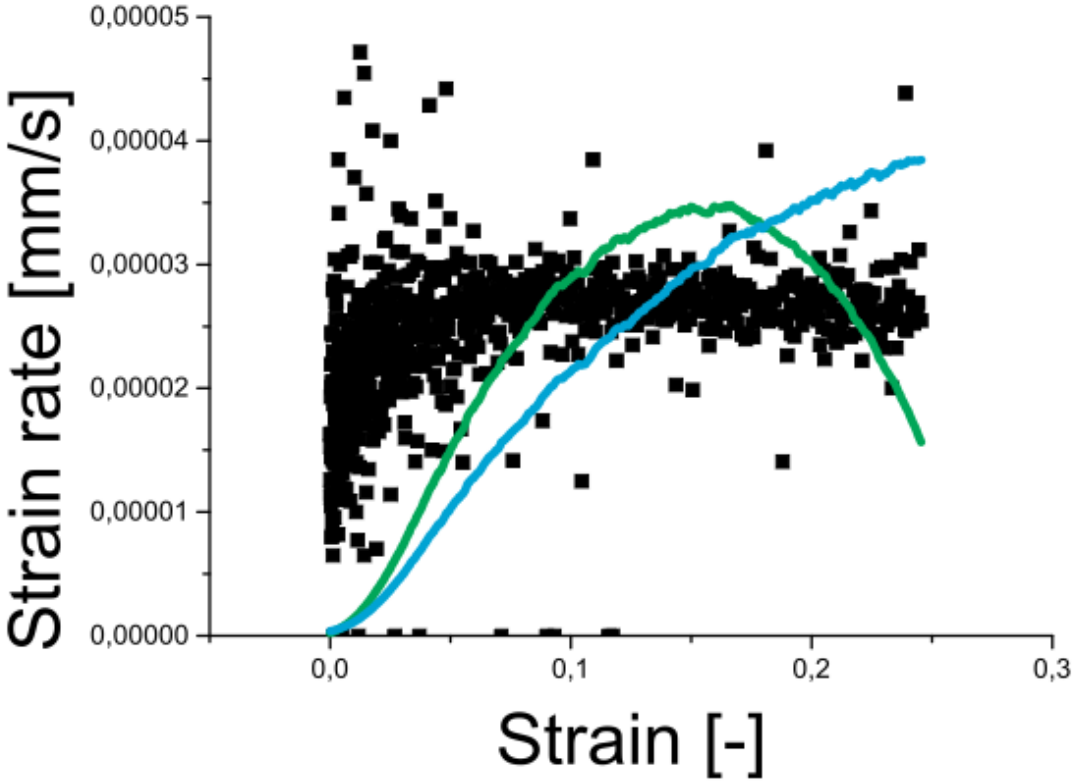

Fig. 187: 316L-700º-0p00005-Fitting II

	Time hardening		Strain hardening		Modified strain h.	
	Value	error	Value	error	Value	error
m	1,18041	0,00379	-0,03931	7,48E-04	12,91035	0,59741
k					-9,60E+00	0,45928

Fig. 188: 316L-700º-0p000005-parameters

- **800ºC**
  - **0p0001**

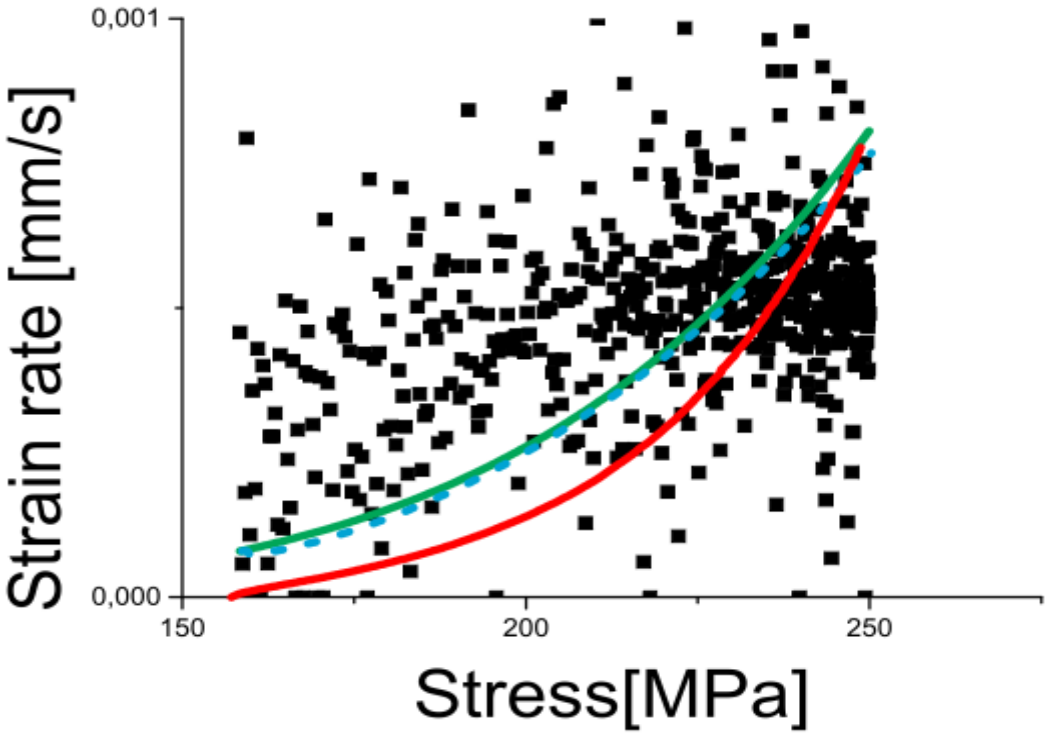

Fig. 189: 316L-800º-0p0001-Fitting I

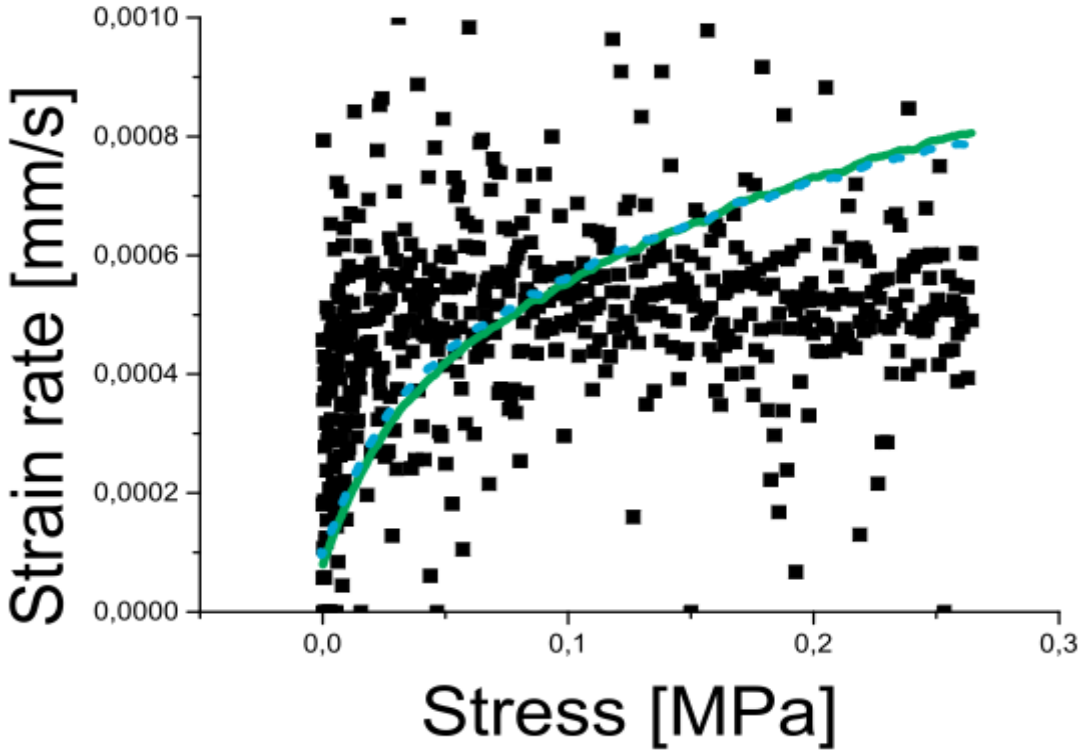

Fig. 190: 316L-800º-0p0001-Fitting II

	Time hardening		Strain hardening		Modified strain h.	
	Value	error	Value	error	Value	error
m	1,24901	0,04077	-0,06998	0,00836	8,16331	2,72908
k					274271	0

Fig. 191: 316L-800º-0p0001-parameters

- **0p00005**

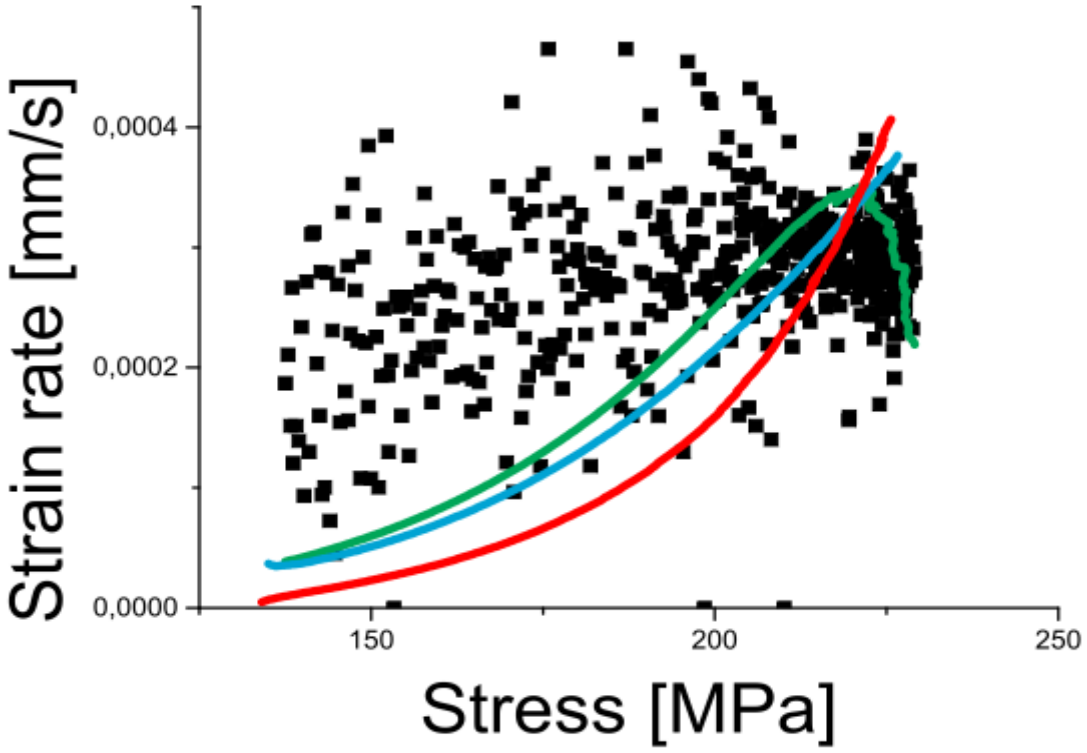

Fig. 192: 316L-800º-0p00005-Fitting I

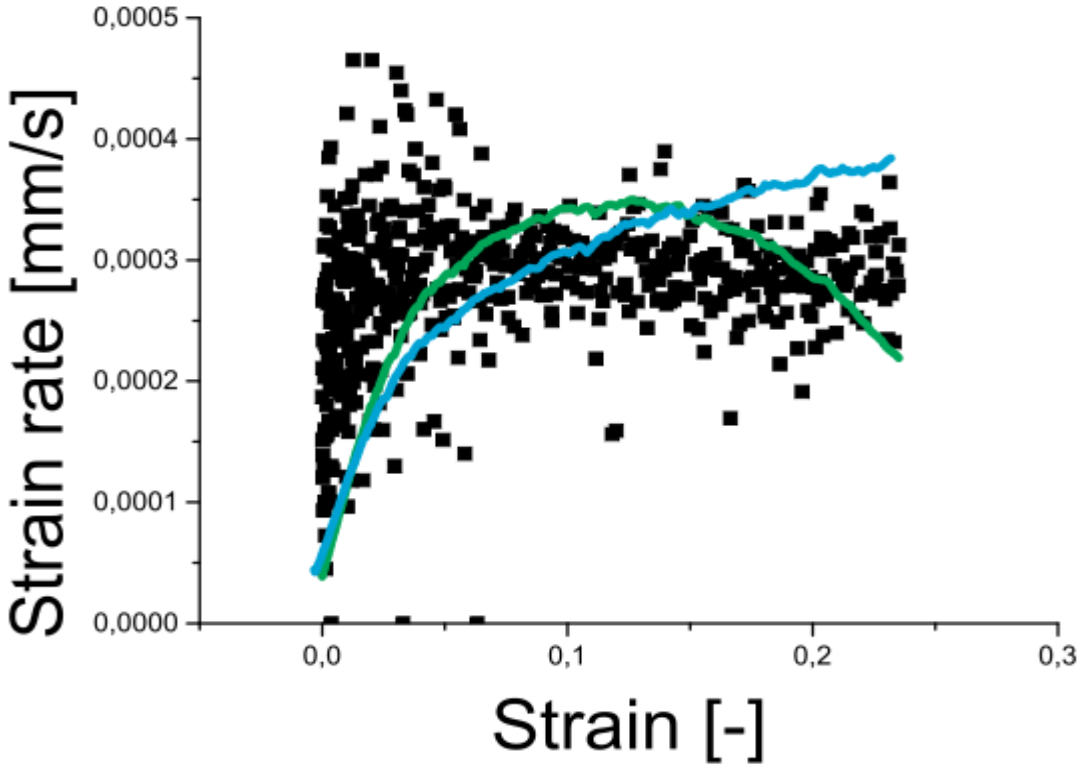

Fig. 193: 316L-800º-0p00005-Fitting II

	Time hardening		Strain hardening		Modified strain h.	
	Value	error	Value	error	Value	error
m	1,21215	0,00931	-0,0615	0,00225	9,11137	0,8382
k					-7,78237	1,22631

Fig. 194: 316L-800º-0p00005-parameters

- **0p00001**

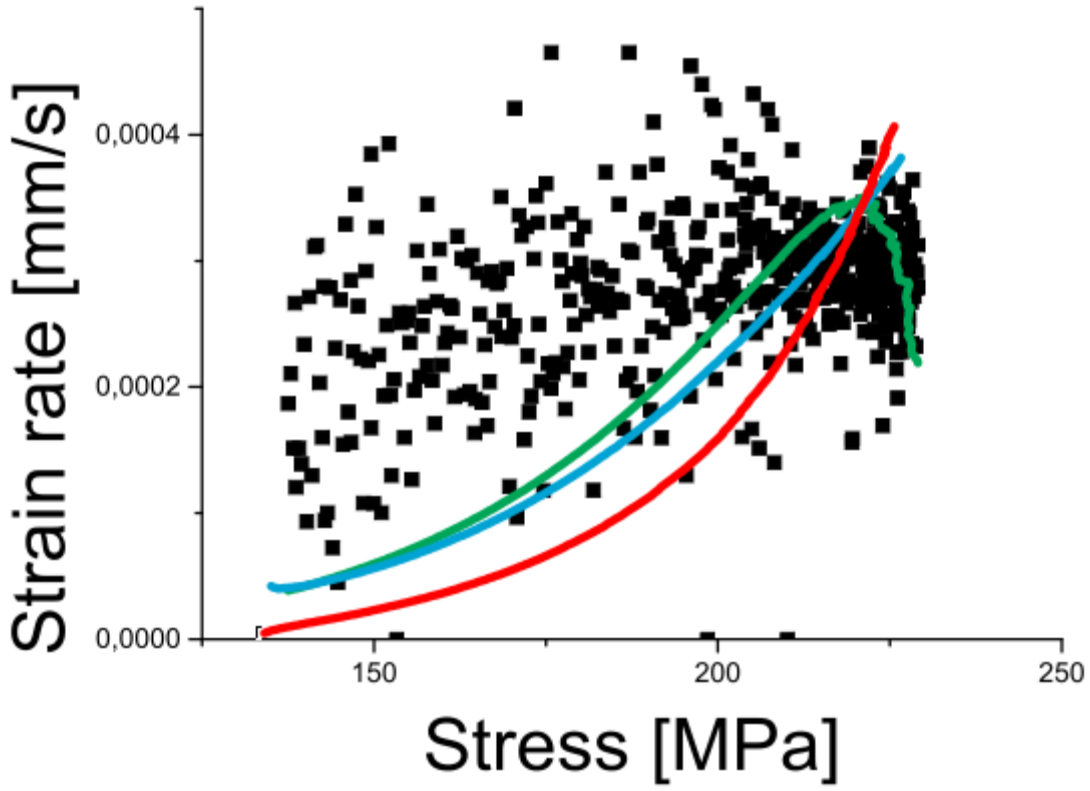

Fig. 195: 316L-800º-0p00001-Fitting I

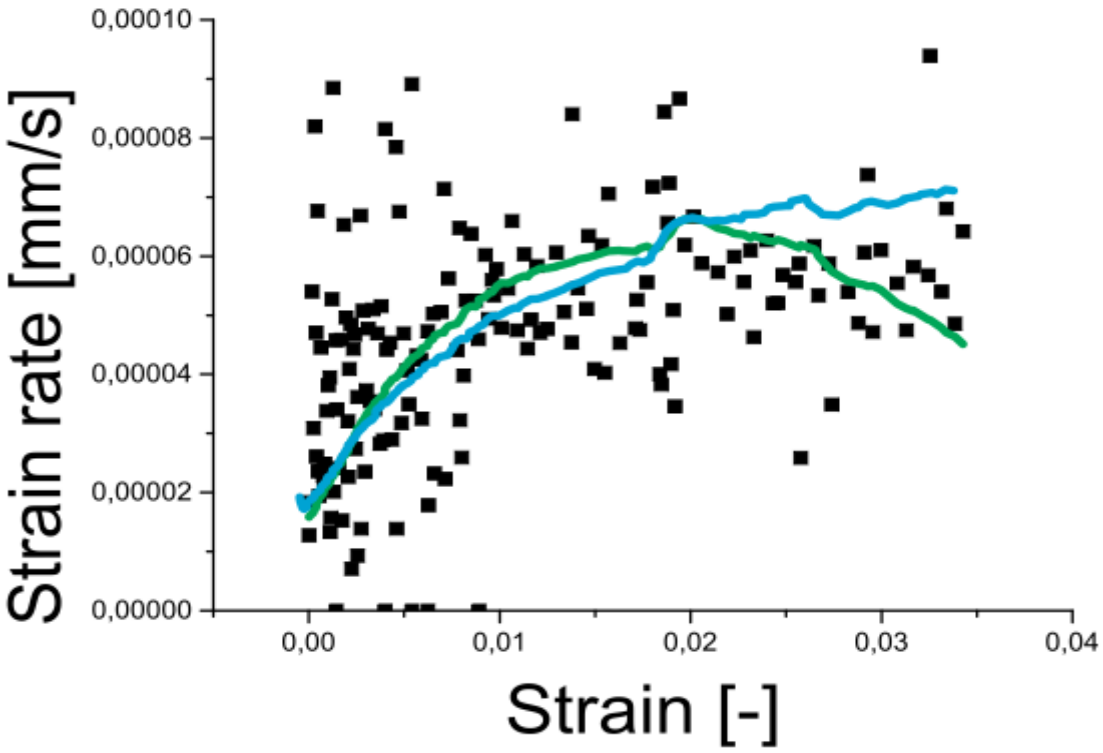

Fig. 196: 316L-800º-0p00001-Fitting II

	Time hardening		Strain hardening		Modified strain h.	
	Value	error	Value	error	Value	error
m	1,23665	0,00869	-0,06612	0,00203	10,16619	0,87453
k					-52,7235	9,6551

Fig. 197: 316L-800º-0p00001-parameters

- **0p000005**

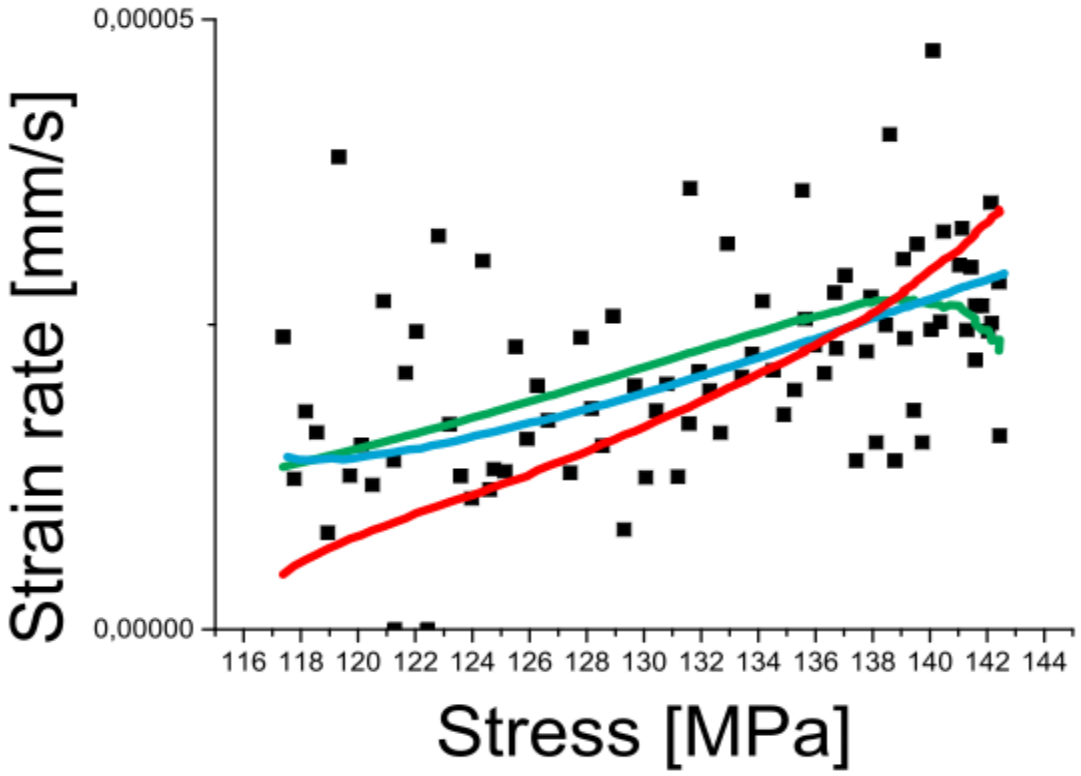

Fig. 198: 316L-800º-0p00005-Fitting I

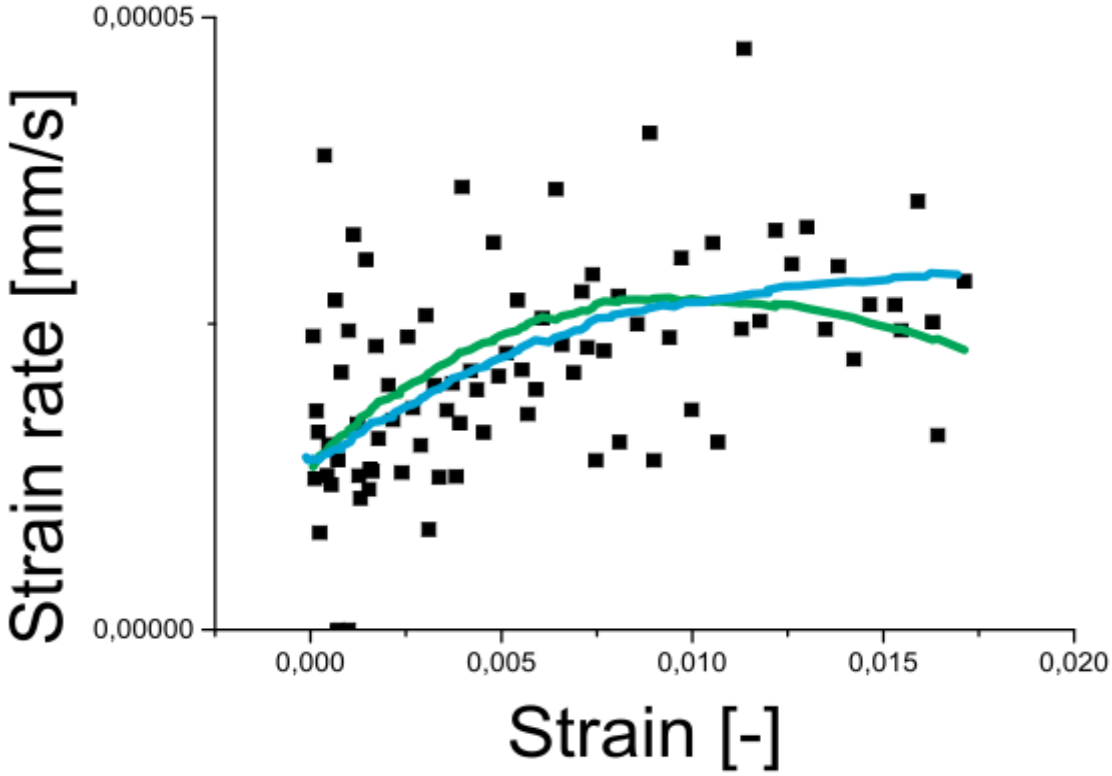

Fig. 199: 316L-800º-0p00005-Fitting II

	Time hardening		Strain hardening		Modified strain h.	
	Value	error	Value	error	Value	error
m	1,20407	0,00867	-0,05678	0,00196	7,04187	0,6218

k					-73,5162	24,11309

Fig. 200: 316L-800º-0p000005-parameters

- **980ºC**
  - **0p0001**

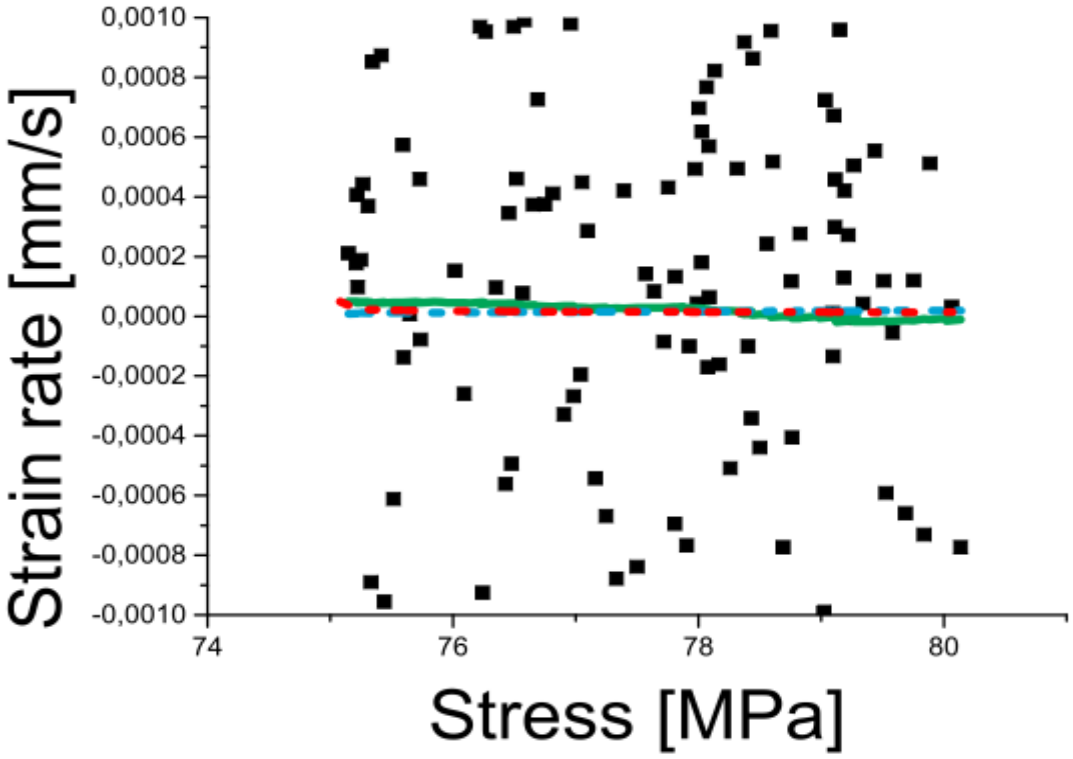

Fig. 201: 316L-980º-0p0001-Fitting I

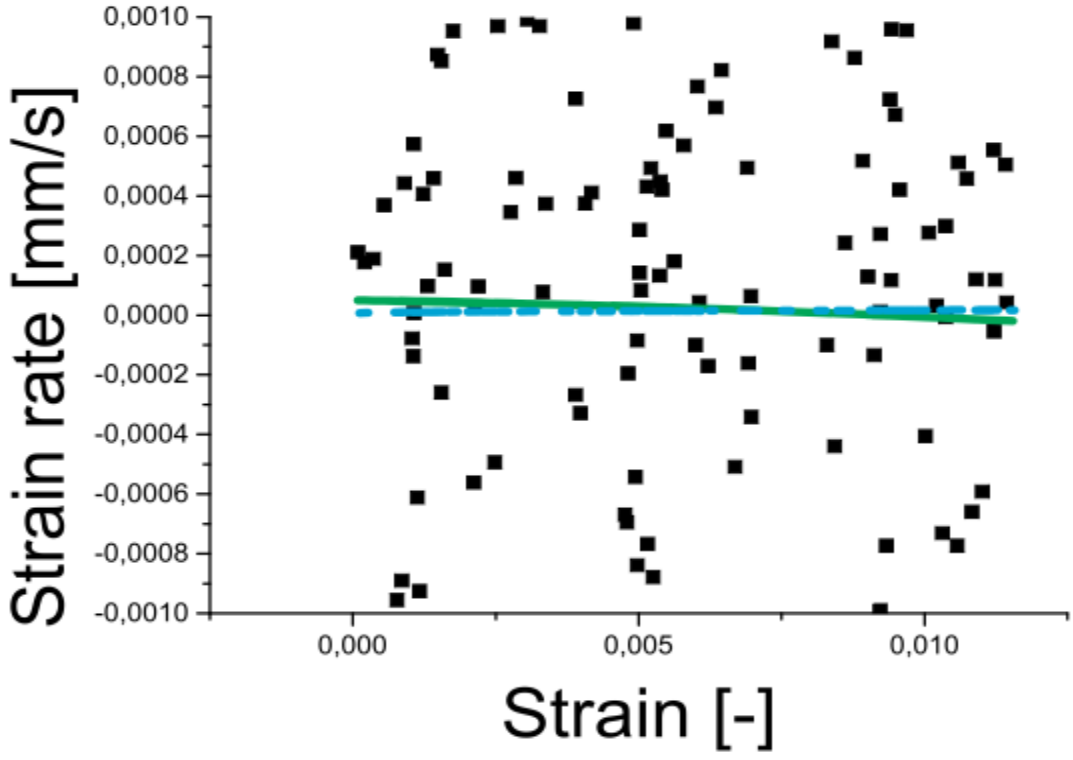

Fig. 202: 316L-980º-0p0001-Fitting II

	Time hardening		Strain hardening		Modified strain h.	
	Value	error	Value	error	Value	error
m	0,74992	0,81475	0,08684	0,3223	5,53E-01	1,99E+00
k					-4,76E+01	1,78E+02

Fig. 203: 316L-980º-0p0001-parameters

- **0p00005**

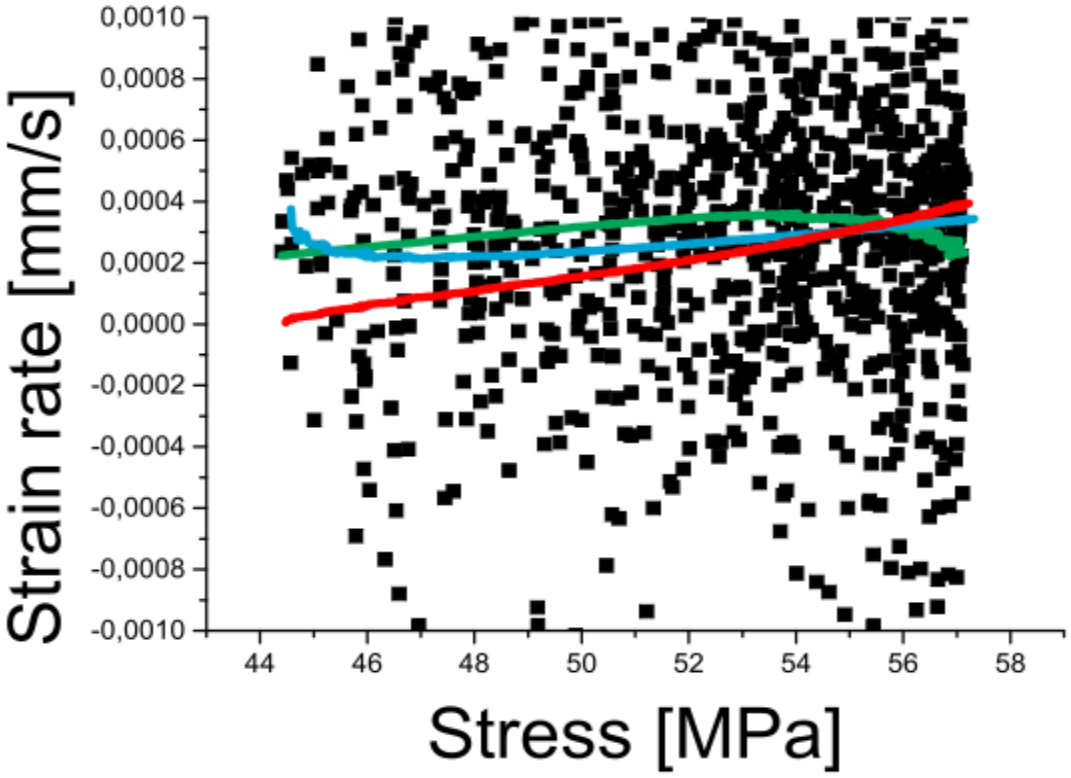

Fig. 204: 316L-980º-0p00005-Fitting I

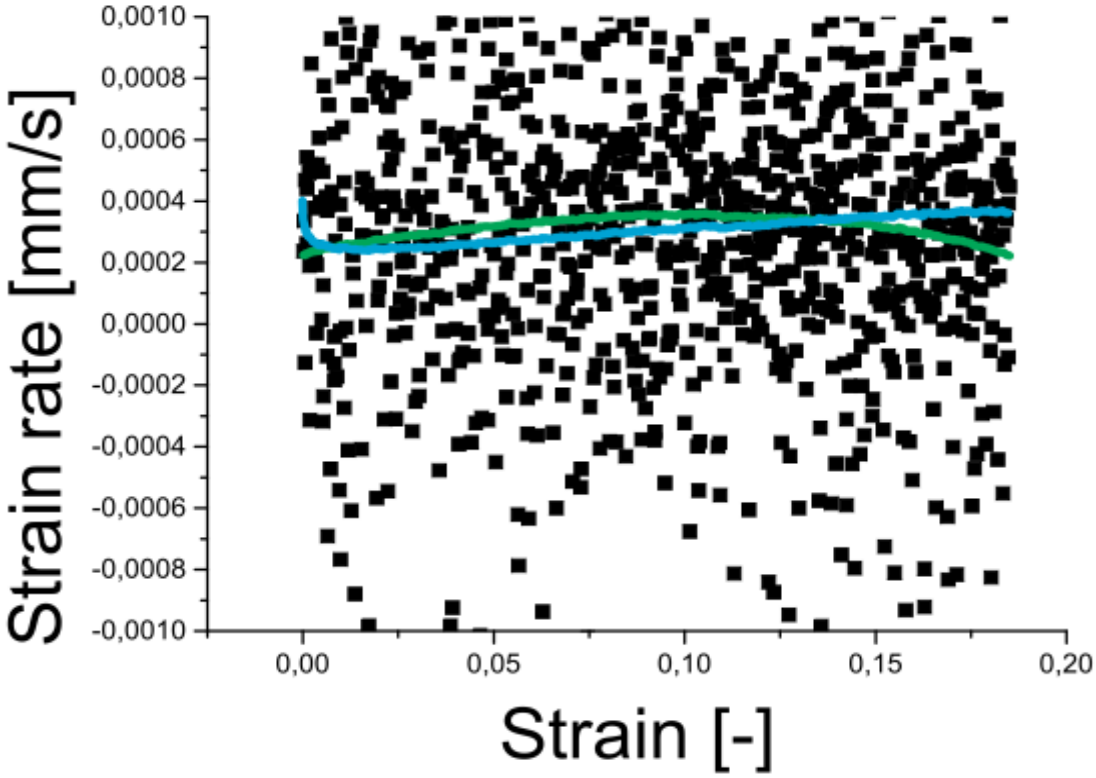

Fig. 205: 316L-980º-0p00005-Fitting II

	Time hardening		Strain hardening		Modified strain h.	
	Value	error	Value	error	Value	error
m	1,26878	0,00785	-0,13024	0,0029	1,49E+01	1,16E+00
k					-1,22E+01	1,36E+00

Fig. 206: 316L-980º-0p00005-parameters

- **0p00001**

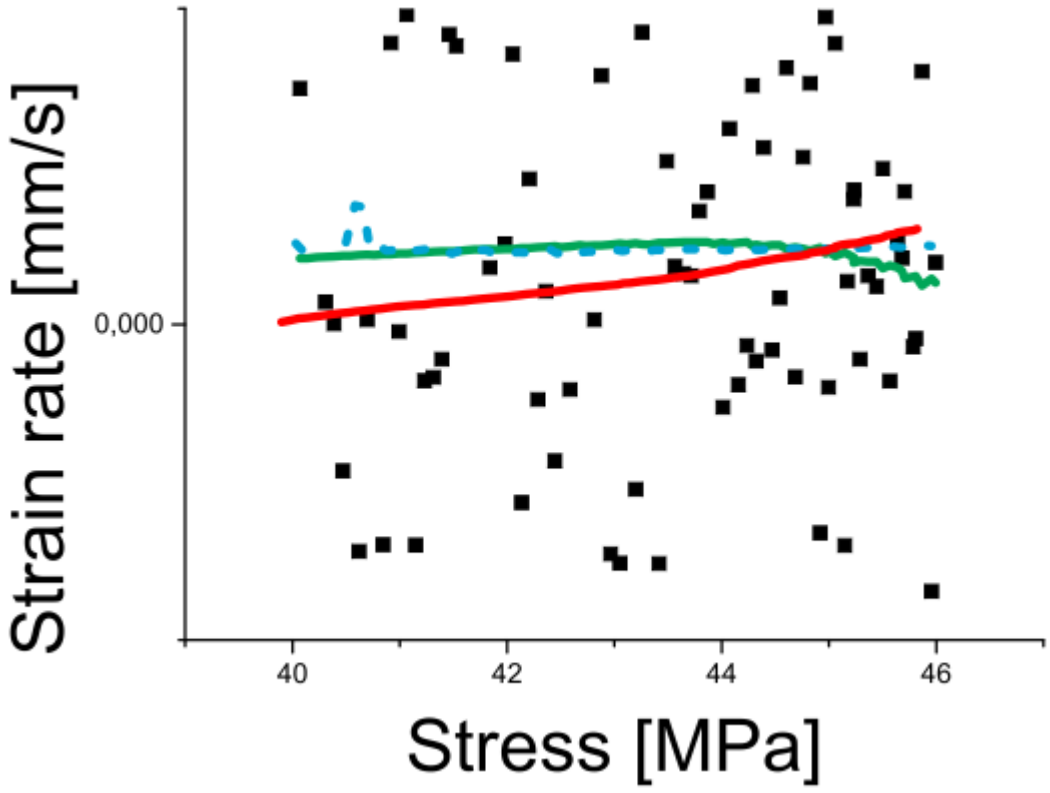

Fig. 207: 316L-980º-0p00001-Fitting I

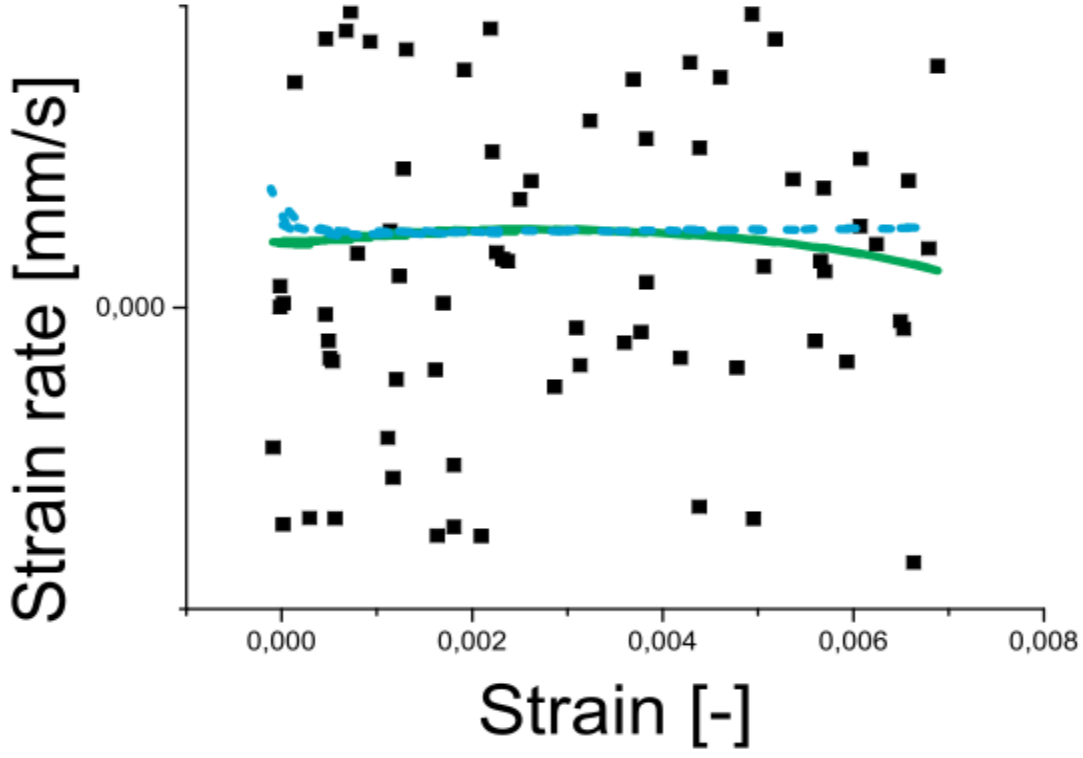

Fig. 208: 316L-980º-0p00001-Fitting II

	Time hardening		Strain hardening		Modified strain h.	
	Value	error	Value	error	Value	error
m	1,47363	0,08696	-0,12832	0,01375	1,97E+01	7,87E+00

k					-377,032	225,34559

Fig. 209: 316L-980º-0p00001-parameters

- **0p000005**

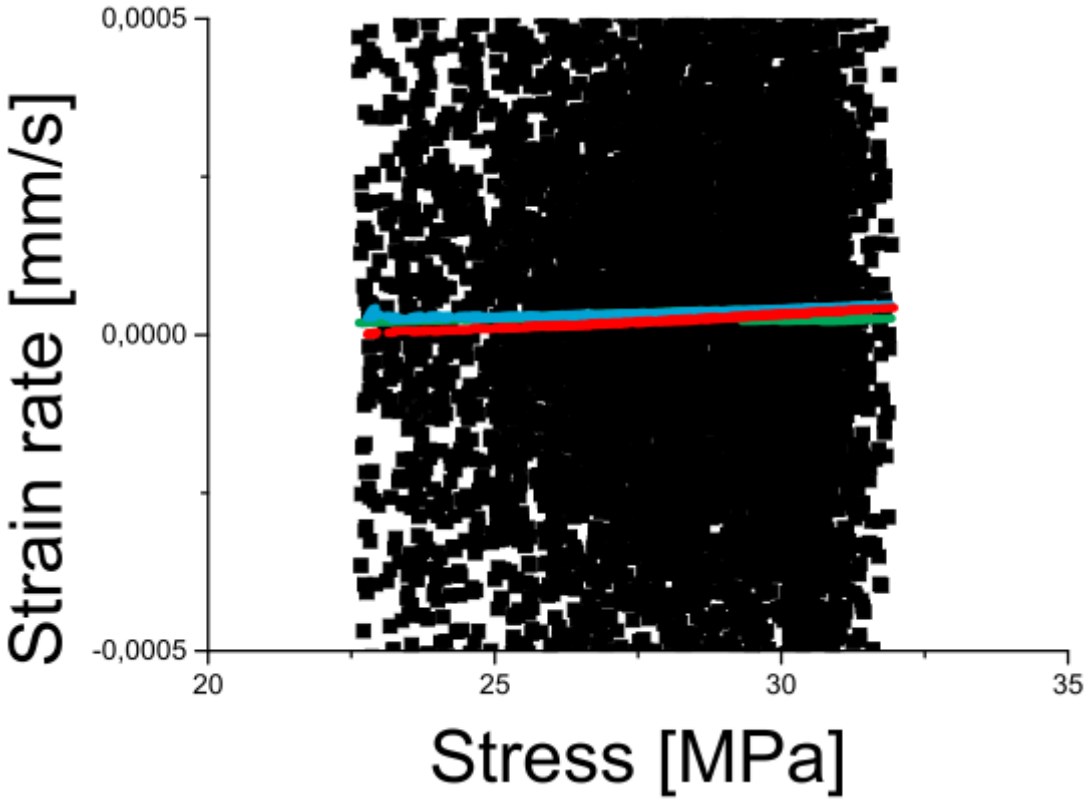

Fig. 210: 316L-980º-0p000005-Fitting I

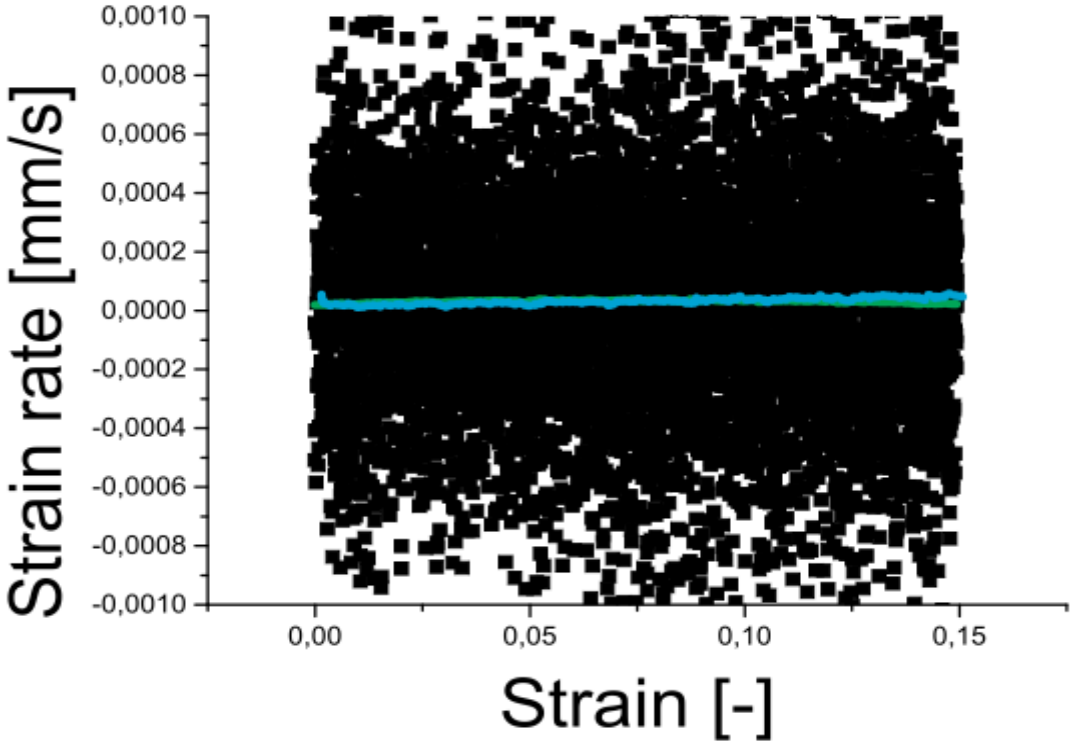

Fig. 211: 316L-980º-0p000005-Fitting II

	Time hardening		Strain hardening		Modified strain h.	
	Value	error	Value	error	Value	error
m	1,19761	0,01975	-0,1351	0,01062	12,60477	3,16403
k					-14,4773	4,91841

Fig. 212: 316L-980º-0p00005-parameters

- **1125ºC**
  - **0p0001**

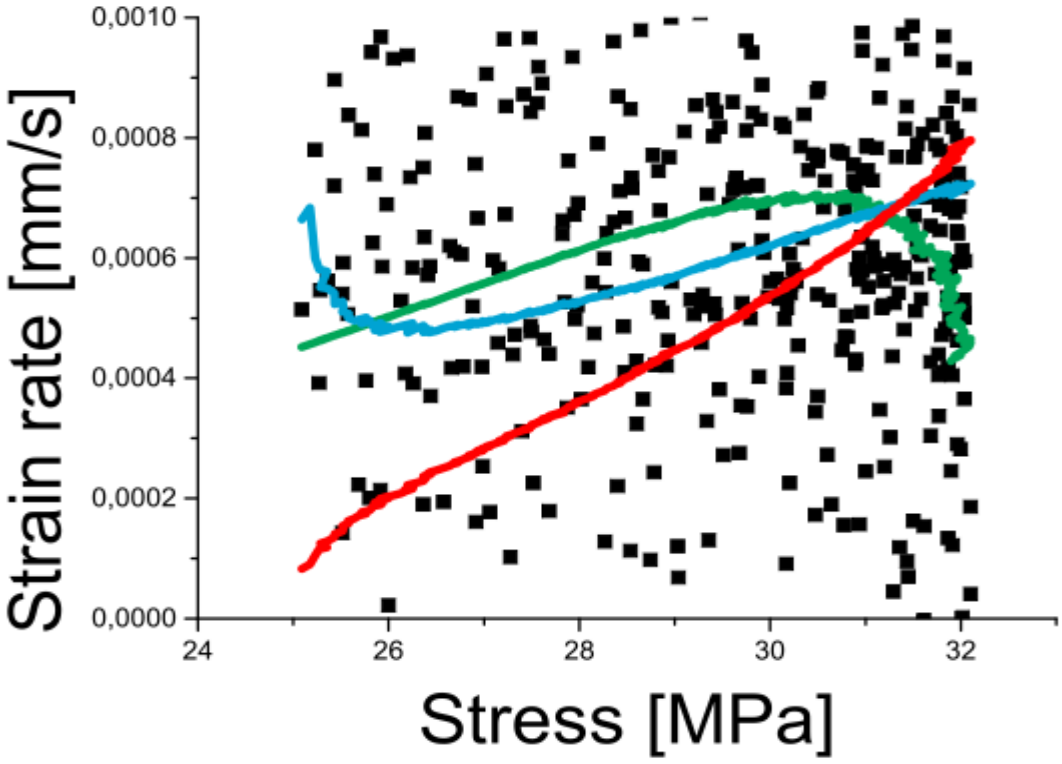

Fig. 213: 316L-1125º-0p0001-Fitting I

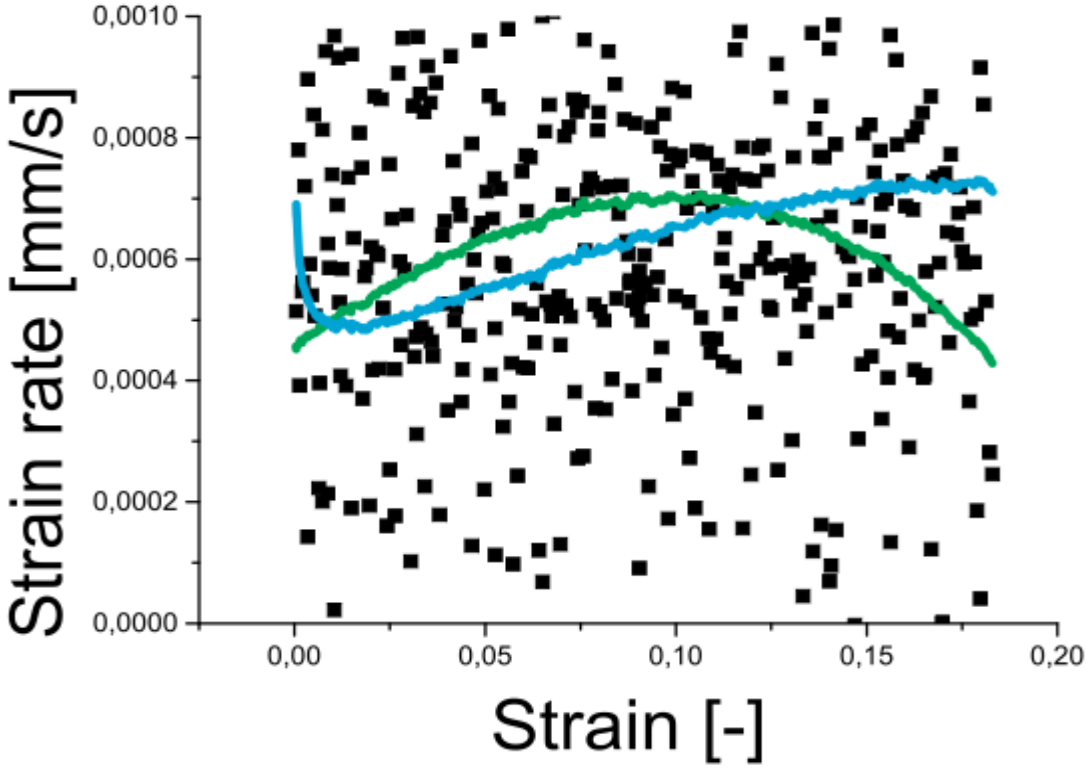

Fig. 214: 316L-1125º-0p0001-Fitting II

	Time hardening		Strain hardening		Modified strain h.	
	Value	error	Value	error	Value	error
m	1,23996	0,00543	-0,12328	0,00194	9,27265	0,41048
k					-10,0685	0,74993

Fig. 215: 316L-1125º-0p0001-parameters

- **0p00005**

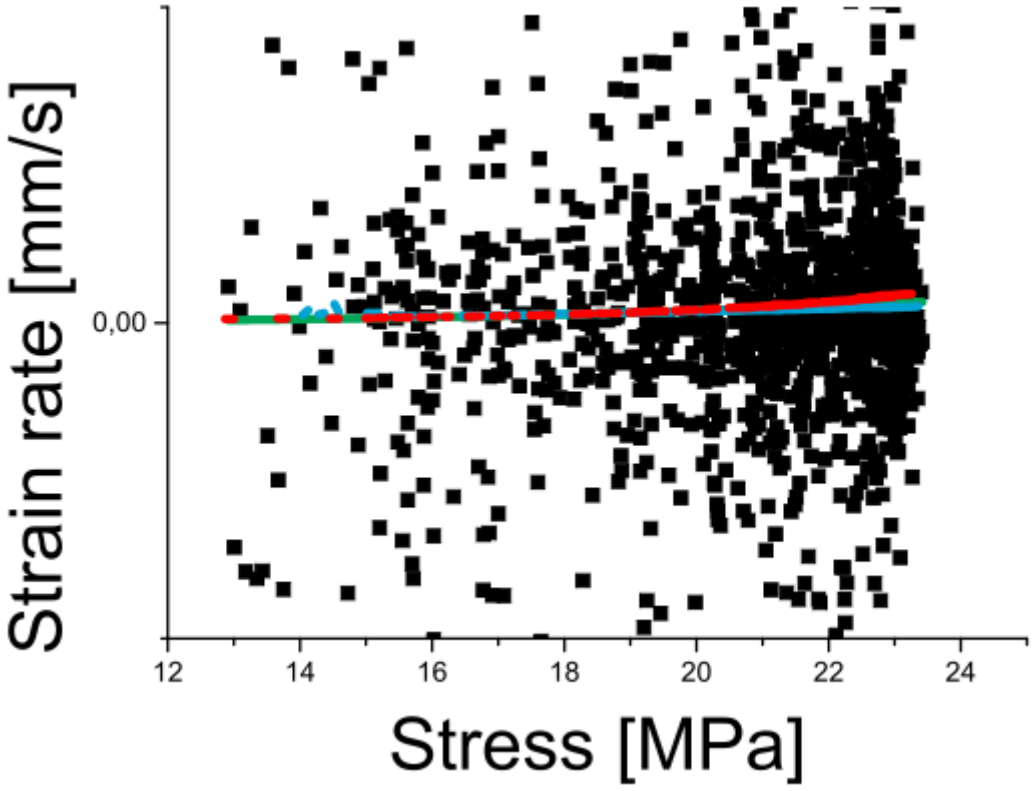

Fig. 216: 316L-1125º-0p00005-Fitting I

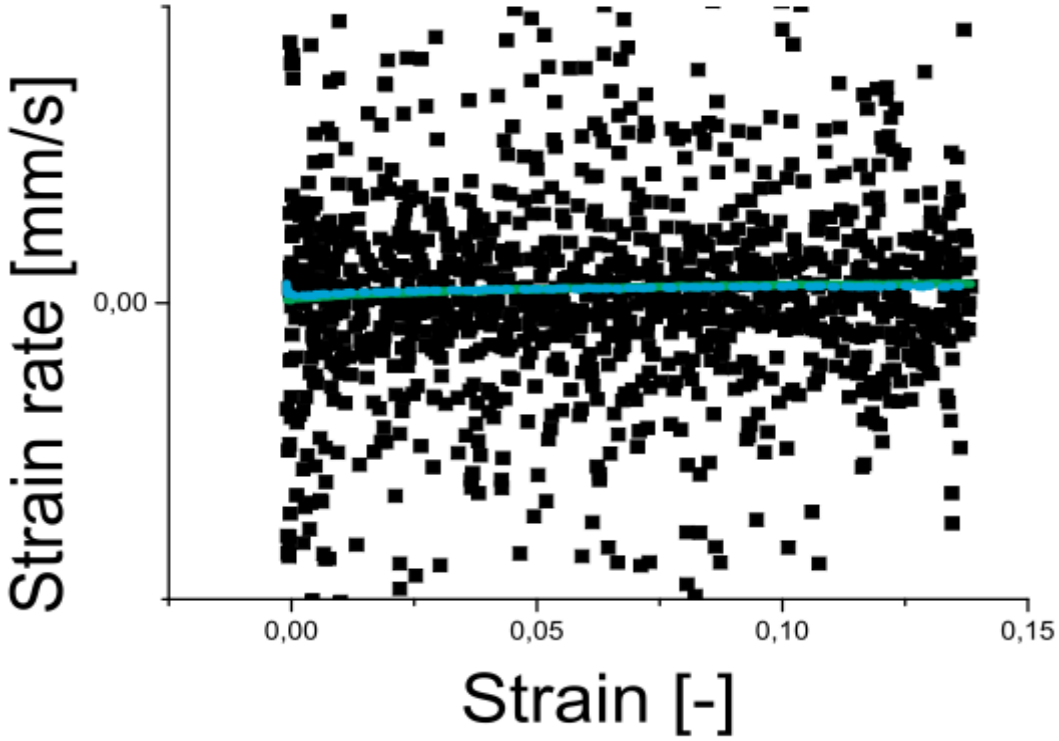

Fig. 217: 316L-1125º-0p00005-Fitting II

	Time hardening		Strain hardening		Modified strain h.	
	Value	error	Value	error	Value	error

m	1,35538	0,02439	-0,17761	1,10E-02	16,22295	10,67746
k					24,73199	1048,2882

Fig. 218: 316L-1125º-0p00005-parameters

- **0p00001**

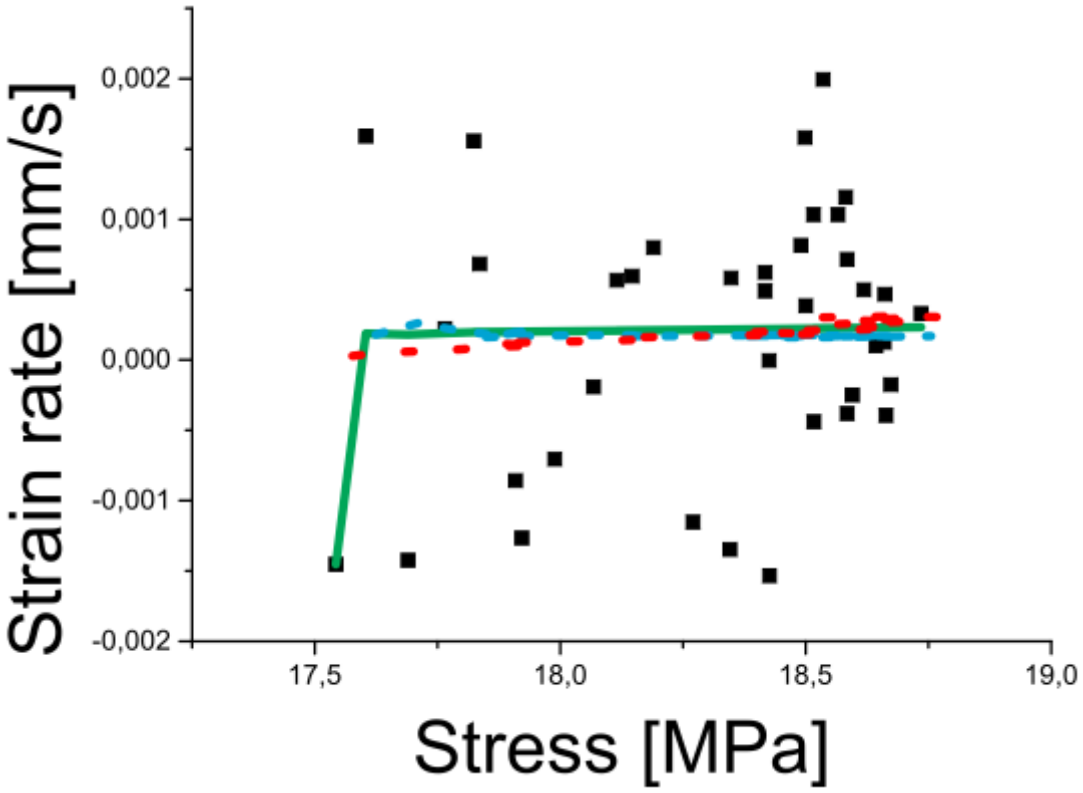

Fig. 219: 316L-1125º-0p00001-Fitting I

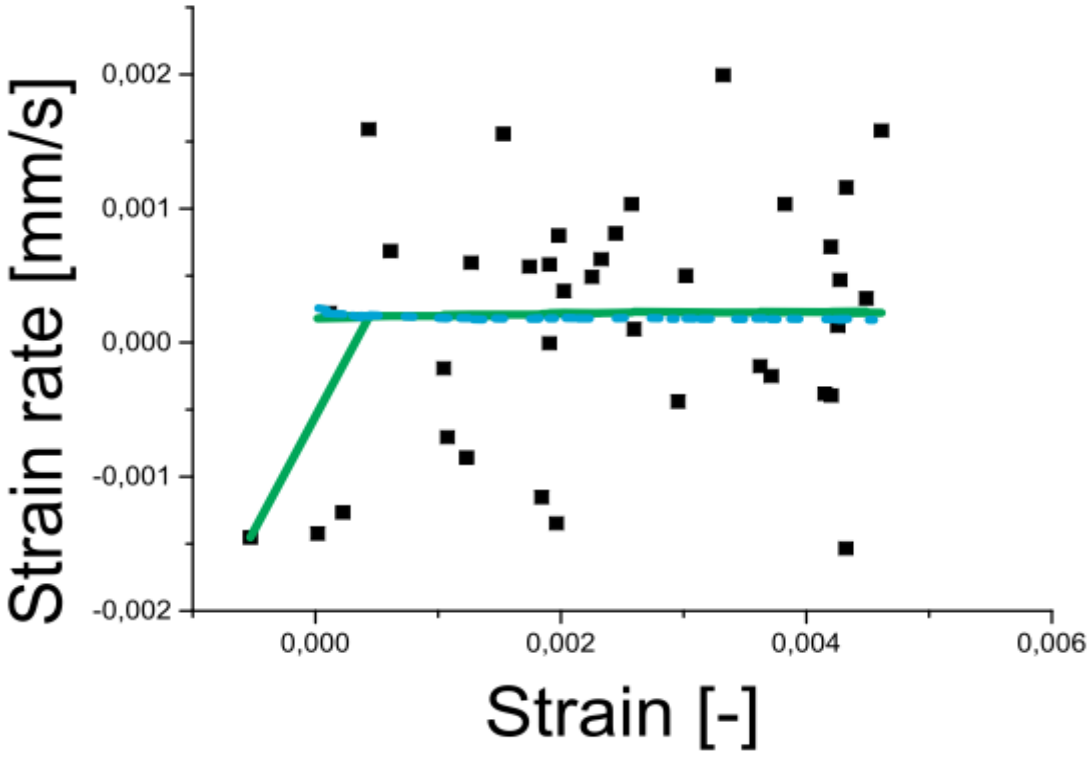

Fig. 220: 316L-1125º-0p00001-Fitting II

	Time hardening		Strain hardening		Modified strain h.	
	Value	error	Value	error	Value	error
m	1,53776	0,13927	-0,11731	0,04884	11,61652	8,53214
k					8856,581	1026,2484

Fig. 221: 316L-1125º-0p00001-parameters

- **0p000005**

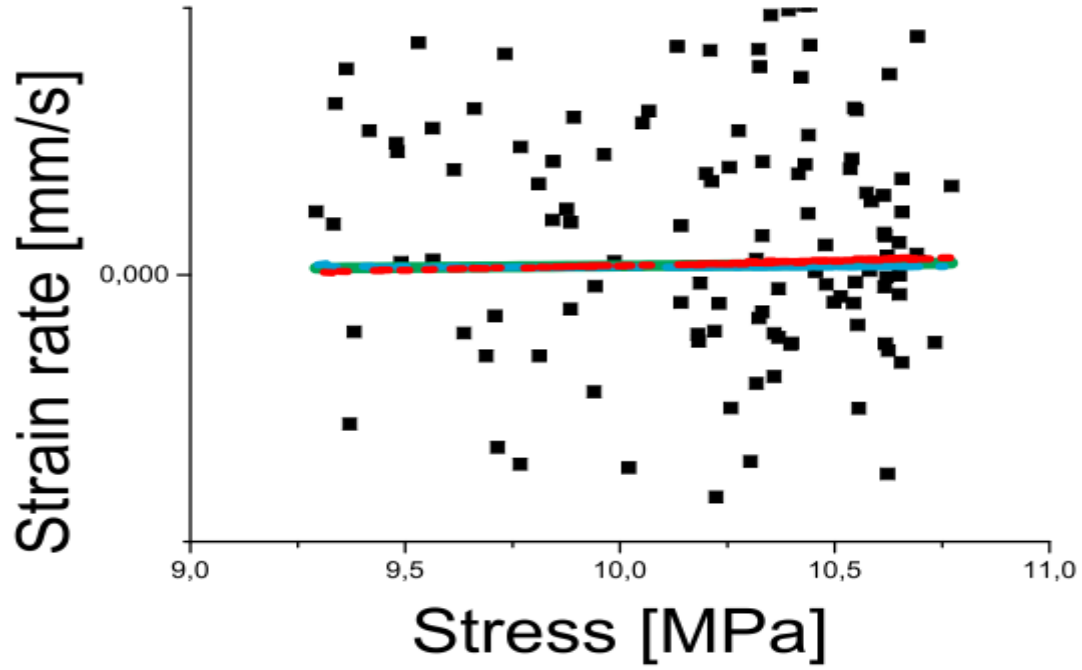

Fig. 222: 316L-1125º-0p000005-Fitting I

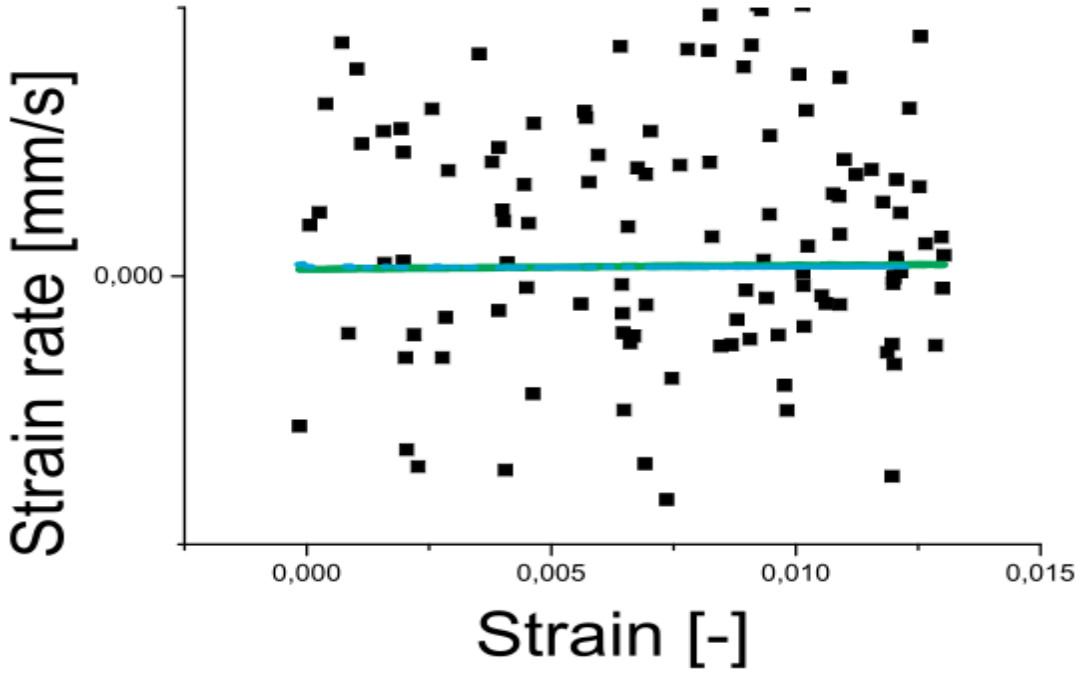

Fig. 223: 316L-1125º-0p00005-Fitting II

	Time hardening		Strain hardening		Modified strain h.	
	Value	error	Value	error	Value	error
m	1,42776	0,33166	-0,1475	0,21421	13,79267	130,53212
k					224,6177	109931,11

Fig. 224: 316L-1125º-0p000005-parameters

Given the graphical approach and the relationship between the values and their errors is considered that, for most cases, the model that best adjusts the behavior of secondary creep to such materials is the proposed as **Modified strain hardening**.

7. Problems in the experiments

29/07/2013

One hardening test with strain rate 0.0001 (s^{-1}) at 1125°C was tested (Instron/Zwick 1362 machine). The furnace supported by DFG can work until 2000°C. The obtained results were wrong. Some problems have observed during and after the test as described below:

- The initial force was set 40N, but it increased when the furnace´s temperature increased (*the initial force should be constant if the machine work correctly*).

- The lower punch was moved automatically to the limit positions (145mm) (*it should move down to control the initial force to be constant – not move down too much*).
- The green light of extensometer was off during the test. It turned on again after Withold Hildebrandt adjusted it (*the green light of extensometer should on during the test to show a good contact between extensometer and the ceramic punch*).
- The stress-strain curve was very unusual.
- The glue between Al_2O_3 punch and SiC part (Press reception) was not homogenous, and did not glue well. There was uneven gab between two ceramic parts.
- There were some crack appear in Al_2O_3 punch.
- The sample geometry did change, even though the applied force signal was approximately 500N (*the two punches were not in touch when the furnace was opened).*

ZWICK/ROELL Z020 machine, which is intended to do the experiment at low temperature (<900°C), is occupied by Sascha Buthmann. Thus hardening experiments with strain rate control could not start.

Actions:

- Glass cloud was put inside the ceramic pipe to avoid heat transfer from furnace to the Force gate.

- One ventilator was used to cool the force gate.

- One test to check the sensitive of the force signal to the temperature of force gate (connect to the furnace temperature).

Conclusion:

The problem of wrong signal comes from the high temperature of force gate. Test can be done as soon as the signal is stable.

- One more test in the real condition will continue. One ceramic tube need to be changed.
- Order a couple of longer ceramic tube (taking care to the parallel plan and coaxial of the tube when ordering).

20/09/2013

The experiments on Instron/Zwick 1362 machine were started. After several of them can be observed that the surface in contact with the sample is melted due the high temperature.

Actions:

There were introduced two metals elements between the sample and the press receptions.

11/10/2013

Appeared a message in display related to the furnace´s below part. The message was as follows:

S.br

Consulting with furnace´s manual, can be seen it means that the sensor of the related furnace part is broken.

Actions:

A new sensor was ordered to the manufacture company, and tests were interrupted until the new sensor arrived three weeks later (04/11/2013).

08/11/2013

The same message (*S.br*) appeared but this time in the display related to the middle part. Withold Hildebrandt checked it and discovered that in this occasion the problem was with the wire which connects the furnace with the display.

Actions:

A new wire should be placed in place of the old one. The tests were interrupted until the new wire is ready.

7. Conclusion and further works

Determine rheological and creep parameters of stainless steels is absolutely essential to know the behavior of these materials when they are under stress at high temperatures.

As explained in this thesis, is necessary to determine these parameters by empirical methods, ie, by testing on real samples of these stainless steels. Once the experiments have been realized, some aspects can be analyzed to improve or reduce the time of the experiments on these materials in the future.

First, after the experiments were performed, one has a better understanding of the ranges of temperatures at which the creep stages for different materials are produced. This makes that the total time of completion of the tests decreases. In the experiments would be conducted for this thesis were repeated several tests for this reason.

Another key to achieve good results in the carried out experiments, is to choose an appropriate time for each test, taking into account the remaining specific conditions of test (temperature, strain rate , relative density , and so on) . Sometimes a too short time affects to do not reach the desired results. At other times, a very long time conducts to break the sample.

Before and during the performance of the tests is very important to check that the cooling system is working correctly, otherwise the results will not be correct, and in addition, the team used will be exposed to deterioration.

One measure which allows obtain more reliable results, would be to carry out a greater number of experiments at different strain rates. Thus, it will be more data available for the regression.

For analysis of primary creep, in many cases, be performing the regression on a cloud of very sparse data. A measure to improve this analysis in the future may be taking data with higher time interval between shows. Thus greater data homogenization is achieved.

As for possible future work related to this area, other approaches to creep behavioral models that are contained in the relevant literature could be achieved. Further analysis can be completer doing more studies with data.

This is the case of carry on HIP test to calculate c and f values. Moreover, the analysis of the value A * from the obtained values of the parameter A in this thesis and specific constants of the material and develop an expression depending on the strain rate and temperature that will fit all the data obtained.

References

1: http://en.wikipedia.org/wiki/Creep_(deformation)

2: http://en.wikipedia.org/wiki/Rheology

3: HIP 2005 proceedings of the international conference on hot isostatic pressing paris may 2005. SF2M www.sf2m.asso.fr. John C. Hebeisen HIP technology the state of the art after 50 years pp.3-13. Victor Samarov, Charles Barre, Dmitry Seliverstov Net shape HIP for complex shape PM parts as a cost efficient industrial technology pp.48-52

4: Chritian Geindreau, Didier Bouvard & Pierre Doremus. Investigation of the constitutive behavior of metal powder during hot isostatic pressing with a simulation material. Int. J. mech.Sci. A/Solids 18, 1999, pp.581-596.

5: L. Sanchez, E.Ouedraogo, L.Federzoni, and P.Stutz New viscoplastic model to simulate hot isostatic pressing. Powder Metallurgy 2002 Vol.45 No.4

6: E. ARZT, M.F.ASHBY, and K.E EASTERLING Practical applications of Hot Isostatic Pressing Diagram: Four case studies. Volume 14A, 211-221, February 1983

7: http://en.wikipedia.org/wiki/Viscoplasticity

8: M. Abouaf, J. L. Chenot, P. Bauduin and G. Raisson, 'Prediction of the deformation during the production of near net shape superalloy parts by hot isostatic pressing', 2nd Inc. Conf. on fsostatic Pressing, Stratford-on-Avon, England, Sept. 21-23, 1982.

9: Chritian Geindreau, Didier Bouvard & Pierre Doremus: Investigation of the constitutive behavior of metal powder during hot isostatic pressing with a simulation material, Int. J. mech.Sci. A/Solids 18 (1999) 581-596 Printed in Elsevier. Paris.

10: Creep Mechanics Josef Betten. ISBN 3-540-23204-4 Springer Berlin Heidelberg New York.

11: courses.washington.edu/me354a/chap8.pdf

12: H.A. Kuhn and C.L.Downey: Deformation characteristics and plasticity theory of sintered powder material, International Journal of Powder Metallurgy 7(I) 1971

13: http://sundoc.bibliothek.uni-halle.de/habil-online/06/06H055/t3.pdf

14: K. Sawada, M. Tabuchi, K. Kimura Mater. Sci. Eng. A, 510–511 (2009), pp.190–194

15: S.R. Holdsworth, M. Askins, A. Baker, E. Gariboldi, S. Holmstrom, A. Klenk,, M. Ringel, G. Merckling, R. Sandstrom, M. Schwienheer, S. Spigarelli. Int. J. Press. Ves. Pip., 85 (2008), pp. 80–88

16: J.T. Boyle, J. Spence. Stress analysis for creep. Butterworth & Co. Ltd. (1983) ISBN:0-408-01172-6

17: M. Abouaf, J.L. Chenot,G. Raisson,P. Bauduin: Finite element simulation of Hot isostatic pressing of metal powder, Int. Journal for Numerical Methods in Engineering, Vol.25, 191-212 (1988).

18: G. Aryanpour, M. Farzaneh. Analysis of axial strain in one-dimensional loading by different models. Acta Mech Sim (2010) 26: 745-753 DOI 10.1007/s10409-010-0371-2

19: Ales Svoboda, Hans-Ake Haggblad. Simulation of hot isostatic pressing of metal powder components to near net shape Engineering computations, Vol.13, No.5 1996, pp.13-37, MCB University Press, 0264-4401. (2)

20: Ales Svoboda, Hans-Ake Haggblad: Simulation of hot isostatic pressing of metal powder components to near net shape Engineering computations, Vol.13, No.5 1996, pp.13-37, MCB University Press, 0264-4401.

21: K.T. Kim, Y. S. Kwon and H. G. Kim Near net shape forming of Alumina powder under hot pressing and hot isostatic pressing Int. J. Mech. Sci. Vol.39. No.9, p. 820